

**Fabrication Technology of High Density Cu/Polyimide
Interconnection by Hybrid Imprinting with Selective Electroless
Plating**

(ハイブリッドインプリントと選択的無電解メッキを用いた銅／ポリイミド
高密度配線作製技術)

朴 相 天

Copyright
by
Sang-Cheon Park
2014

**The Dissertation Committee for Sang-Cheon Park Certifies
that this is the approved version of the following dissertation:**

**Fabrication Technology of High Density Cu/Polyimide
Interconnection by Hybrid Imprinting with Selective Electroless
Plating**

(ハイブリッドインプリントと選択的無電解メッキを用いた銅／ポリイミド
高密度配線作製技術)

Committee:

Takahisa Kato, Professor

Junho Choi, Associate Professor

Hideki Takagi, Dr of Engineering

Shinichi Warisawa, Associate Professor

Reo Kometani, Lecturer

The University of Tokyo
Department of Mechanical Engineering

Thesis

**Fabrication Technology of High Density Cu/Polyimide
Interconnection by Hybrid Imprinting with Selective Electroless
Plating**

(ハイブリッドインプリントと選択的無電解メッキを用いた銅／ポリイミド
高密度配線作製技術)

by

Sang-Cheon Park

Presented in partial fulfillment of the
requirements for the degree of
Doctor of Engineering

2014

**Fabrication Technology of High Density Cu/Polyimide
Interconnection by Hybrid Imprinting with Selective Electroless
Plating**

(ハイブリッドインプリントと選択的無電解メッキを用いた銅／ポリイミド
高密度配線作製技術)

Sang-Cheon Park

The University of Tokyo, Department of Mechanical Engineering, 2013

ABSTRACT

This thesis describes the application of thermal/ultraviolet (UV) hybrid imprint and selective electroless copper plating using vacuum ultraviolet (VUV) light induced surfactant masking concepts to fabrication process of high density interconnection (HDI) interposer.

Transistors have been integrated to one chip, since the transistor was developed in 1947. The integrated circuit (IC) chips speed up invention of computing devices such as a handheld calculator and computer. In semiconductor industry, the number of transistors on IC doubles approximately every two years following Moor's Law. However, interconnections in a system board such as printed circuit board (PCB) and large scale integrated (LSI) circuits are failing to follow the integration speed of IC. The interconnection gap between IC and system board is widening more. As one of the solutions to make up interconnection gap between IC and system board, an interposer have been proposed in packaging industry. In addition, demand for miniaturization of a system board in the electronic devices such as a smart-phone and a tablet personal computer (PC) is increasing. Therefore, heterogeneous integration

system or three dimensional (3D) integration systems using interposer has been studied to meet the demand for the system integration. The interposer consists of HDI on dielectric layer. Copper plating on polyimide (PI) technology has been widely used for fabricating interconnections of microelectronic devices such as flexible printed circuit board (FPCB). Copper patterns are conventionally fabricated on PI film by lamination technology or electroplating. However, these conventional methods have some problems such as poor fine pattern formation capability, high-cost and low electrical properties. Recently, electroless Cu plating has an attraction as an alternative to conventional metallization technology because of its low cost and high purity Cu deposition. In addition, the electroless plating technology permits to deposit a metal selectively on a substrate. Many selective metallization approaches using screen printing, ink jet printing, micro-contact printing or selective surface modification by vacuum ultraviolet irradiation have been attempted to simplify the metal interconnect formation process without lithography patterning technology.

This thesis aims to simplify the fabrication process of HDI which can be applied to interposers. To achieve this, thermal/UV hybrid imprint (TUHI) using soluble block copolymer polyimide (SBC-PI) resin is invented for high precision and low temperature patterning process. Even though the imprint process is performed at temperatures lower than 120 °C, precise replication of SBC-PI with shape error less than 4% was achieved by TUHI after optimizing process parameters. In addition, very small patterns of 150 nm line-and-spaces was also successfully replicated

Adhesion between Cu and SBC-PI is enhanced by surface modification using VUV irradiation with wavelength of 184.9 nm and 253.7nm. The influence of VUV irradiation on surface properties of soluble block copolymer polyimide (SBC-PI) was investigated. The changes of topological and chemical properties of SBC-PI were investigated through water droplets test, dynamic force microscope (DFM) measurement, and X-ray photoelectron spectroscopy (XPS) analysis. Analysis results

revealed that the surface properties of VUV irradiated SBC-PI film changed from hydrophobic to hydrophilic without the increase of surface roughness, as a result of the generation of hydrophilic group. The Cu layer was deposited on modified SBC-PI film by electroless plating. Then it was also revealed that the adhesion of electroplated Cu to SBC-PI substrate can be controlled by varying VUV irradiation dose. The VUV induced surfactant masking (VISM) process is proposed to simplify selective copper metallization process using electroless plating. This selective electroless Cu plating using VUV treatment is based on the following two essentials. One is that most surfactants used as a pretreatment process for electroless plating composed of organics. The other is that the organics can be decomposed by VUV treatment. Firstly, hydrophobic PI film surface was modified to hydrophilic by VUV irradiation. Then surfactant layer absorbed on whole hydrophilic PI surface was selectively removed by VUV irradiation using a photo mask. After palladium (Pd) catalyzing process, Cu patterns with ranging from 10 to 150 μm in width were fabricated on residual surfactant layers by electroless plating.

Finally, fabrication of Cu/PI interconnection is demonstrated by TUHI and VISM processes. The Cu/PI interconnections with 50 μm line width and various lengths were fabricated. The electric resistance of the fabricated Cu interconnections with 300 nm thickness was evaluated.

Table of Contents

| | |
|---|----|
| Abstract..... | v |
| List of Tables | x |
| List of Figures | xi |
| | |
| Chapter 1. Introduction | 1 |
| 1.1 Background | 2 |
| 1.2 Motivation for study | 8 |
| 1.3 Purpose..... | 10 |
| | |
| Chapter 2. Previous study | 11 |
| 2.1 Polyimide patterning process | 12 |
| 2.1.1 Polyimide synthesis | 12 |
| 2.1.2 Polyimide patterning by lithography | 15 |
| 2.1.3 Polyimide patterning by thermal imprint..... | 17 |
| 2.2 Electroless copper plating | 19 |
| 2.2.1 Surface treatment for electroless plating..... | 20 |
| 2.2.2 Surface modification using VUV irradiation..... | 23 |
| 2.2.3 Selective electroless copper plating using VUV irradiation | 25 |
| | |
| Chapter 3. Polyimide patterning process by Thermal/UV hybrid imprint (TUHI) | 26 |
| 3.1 Soluble block copolymer polyimide (SBC-PI) | 27 |
| 3.2 Experimental system..... | 31 |
| 3.3 Thermal imprint of non-photosensitive SBC-PI | 36 |
| 3.4 Thermal/UV hybrid imprint of photosensitive SBC-PI | 38 |
| 3.5 Summary | 53 |

| | |
|--|----|
| Chapter 4. Adhesion enhancement by VUV irradiation surface modification | 54 |
| 4.1 VUV irradiation surface modification | 55 |
| 4.1.1 Adhesion problem between Cu and SBC-PI..... | 55 |
| 4.1.2 Surface modification system..... | 56 |
| 4.1.3 Modified SBC-PI surface VUV irradiation | 58 |
| 4.2 Electroless Cu plating using VUV irradiation surface modification | 61 |
| 4.3 Adhesion between Cu and modified SBC-PI..... | 64 |
| 4.4 Analysis of modified SBC-PI surface..... | 66 |
| 4.5 Summary | 73 |
| | |
| Chapter 5. Selective electroless Cu plating by VUV Induced Surface Masking (VISM)..... | 74 |
| 5.1 Application of Honma method to selective fabrication of Cu interconnection on SBC-PI..... | 75 |
| 5.2 Selective electroless Cu plating by VISM | 78 |
| 5.2.1 Mechanism of organic removal by VUV..... | 78 |
| 5.2.2 Application of VISM to electroless Cu plating..... | 82 |
| 5.2.3 Electric resistivity of fabricated interconnection | 84 |
| 5.3 Selective electroless Cu plating in PI pattern | 87 |
| 5.3.1 Application of THUI and VSIM to fabrication process of Cu/PI interconnection..... | 87 |
| 5.3.2 Fabricated Cu interconnection in PI pattern | 88 |
| 5.4 Summary | 89 |
| | |
| Chapter 6. Conclusion..... | 90 |
| | |
| Reference | 93 |
| Research achievement..... | 96 |

List of Tables

| | | |
|------------|--|----|
| Table 1-1: | Ideal properties of interposer dielectric material | 5 |
| Table 3-1: | Specification of Imprint system..... | 32 |
| Table 4-1: | VUV dose at 10 cm distance from lamp..... | 59 |
| Table 4-2: | Procedure of electroless plating | 62 |
| Table 4-3: | Composition of electroless Cu plating bath..... | 63 |
| Table 4-4: | Binding energy of each bond groups | 68 |

List of Figures

| | |
|--|----|
| Figure 1-1: Interconnection gap between IC and PCB scaling | 2 |
| Figure 1-2: Trends of system integration utilizing interposer | 3 |
| Figure 1-3: Roadmap of package transitions to address memory bandwidth challenge | 3 |
| Figure 1-4: High density interconnection and dielectric material in Interposer..... | 4 |
| Figure 1-5: Typical fabrication processes of interconnection | 7 |
| Figure 1-6: Fabrication process of via interconnection | 9 |
| Figure 2-1: Conventional polyimide (Kapton) synthesis process..... | 13 |
| Figure 2-2: Shrinkage ratio of PI film thickness (PAA)..... | 14 |
| Figure 2-3: Patterning process comparison of non photosensitive with photosensitive PI..... | 16 |
| Figure 2-4: PI patterning process using thermal imprint technology | 18 |
| Figure 2-5: Electroless plating using mechanical interlocking..... | 22 |
| Figure 2-6: Mechanism of Vacuum Ultraviolet (VUV) irradiation surface modification | 24 |
| Figure 2-7: Electroless copper plating process applying VUV irradiation surface modification..... | 25 |
| Figure 3-1: Soluble block copolymer polyimide(SBC-PI)..... | 27 |
| Figure 3-2: Film thickness shrinkage ratio of PAA and SBC-PI..... | 28 |
| Figure 3-3: Load and displacement graph of SBC-PI and young`s modulus | 29 |
| Figure 3-4: Commercial SBC-PI patterning process using photolithography..... | 29 |
| Figure 3-5: Commercial PI pattern by photolithography process of SBC-PI..... | 30 |
| Figure 3-6: Imprint system and mechanism | 31 |
| Figure 3-7: Fabrication process of Si mask mold..... | 33 |
| Figure 3-8: Fabricated Si mask mold..... | 33 |

| | |
|--|----|
| Figure 3-9: Fabrication process of flexible polymer mold | 34 |
| Figure 3-10: Duplicated flexible polymer stamp | 34 |
| Figure 3-11: Pattern profiles of Si mast mold and flexible polymer mold | 35 |
| Figure 3-12: Thermal imprint process using non photosensitive SBC-PI | 36 |
| Figure 3-13: Pattern profiles before and after curing | 37 |
| Figure 3-14: Thermal/UV hybrid imprint process using photosensitive SBC-PI.. | 38 |
| Figure 3-15: Shrinkage ratio of pattern height non and photosensitive SBC-PI ... | 39 |
| Figure 3-16: Influence of UV dose on pattern height shrinkage of photosensitive SBC-PI | 40 |
| Figure 3-17: Various conditions of curing temperature..... | 41 |
| Figure 3-18: Shrinkage ratio of pattern height after various curing conditions.... | 42 |
| Figure 3-19: Schematic diagram of photo sensitizer chemical reaction by UV exposure and PEB | 43 |
| Figure 3-20: Displacement and load graph of SBC-PI film after prebake and exposure and PEB | 44 |
| Figure 3-21: Hardness of SBC-PI after prebake, exposure and PEB | 45 |
| Figure 3-22: Young`s modulus of SBC-PI after prebake, exposure and PEB..... | 46 |
| Figure 3-23: Curing temperature profile for economical process..... | 47 |
| Figure 3-24: Pattern height after curing conditions of starting temperature 25 °C and 100 °C..... | 48 |
| Figure 3-25: Shrinkage ratio–curing temperature curves of SBC-PI samples imprinted at 100 °C and 120 °C | 49 |
| Figure 3-26: Pattern profiles of mold and SBC-PI samples imprinted at different temperature after curing at the same condition..... | 50 |
| Figure 3-27: Pattern profiles of SBC-PI after heat treatment on hotplate of (1) 200 °C, (2) 225 °C and (3) 260 °C for 10min..... | 51 |
| Figure 3-28: SEM images of fabricated polyimide pattern | 52 |

| | |
|---|----|
| Figure 4-1: Chemical structure of SBC-PI | 55 |
| Figure 4-2: Contact angle of SBC-PI surface and adhesion between Cu and SBC-PI..... | 56 |
| Figure 4-3: VUV irradiation system | 57 |
| Figure 4-4: VUV light power density according to distances | 58 |
| Figure 4-5: Modified SBC-PI surface properties by VUV irradiation | 60 |
| Figure 4-6: Procedure of pre-treatment and electroless copper plating..... | 61 |
| Figure 4-7: Cross-section SEM image of Cu/polyimide | 63 |
| Figure 4-8: Schematic diagram of adhesion strength test..... | 64 |
| Figure 4-9: Measured adhesion strength Between Cu and SBC-PI..... | 65 |
| Figure 4-10: X-ray photoelectron spectroscopy (XPS) system | 66 |
| Figure 4-11: XPS spectra graphs of SBC-PI surface..... | 67 |
| Figure 4-12: Atomic concentrations of modified PI surface | 68 |
| Figure 4-13: Chemical structure of PI surface..... | 69 |
| Figure 4-14: Concentration of Carboxyl and hydroxyl group..... | 71 |
| Figure 4-15: Chemical structure of SBC-PI surface..... | 72 |
| Figure 5-1: Selective electroless copper plating process on SBC-PI surface by Honma method..... | 75 |
| Figure 5-2: Ni stencil mask..... | 76 |
| Figure 5-3: Fabricated Cu layer on SBC-PI surface by Honma method | 77 |
| Figure 5-4: Mechanism of VUV induced surfactant removal | 78 |
| Figure 5-5: Transmittance of (a) soda-lime glass and quartz glass with (b) 0.5 mm thickness and (c) 1 mm thickness with UV wavelength of (1) 184.9 nm and (2) 253.7 nm..... | 79 |

Figure 5-6: Surface contact angle of SBC-PI film with increase of UV irradiation dose; (a) after PI modification and (b) after surfactant absorption and schematic diagram of surface state of (1) original PI film, (2) modified PI film and (3) absorbed surfactant80

Figure 5-7: Surface contact angle after surfactant absorption with increase of UV/Ozone treatment time; (a) removing selection of surfactant and (b) surface modification selection of PI substrate.....81

Figure 5-8: Schematics diagram of Surfactant coating and removal.....82

Figure 5-9: Selective electroless copper plating process using VUV induced surfactant masking83

Figure 5-10: Selectively fabricated Cu/PI patterns.....83

Figure 5-11: Electric resistance measuring system.....84

Figure 5-12: Selectively fabricated Cu/PI interconnection using VUV induced surfactant masking85

Figure 5-13: Measured electric resistance86

Figure 5-14: Selective electroless copper plating process in imprinted SBC-PI pattern87

Figure 5-15: Selectively fabricated Cu interconnection in imprinted PI patterns .88

Chapter 1

Introduction

- 1.1 Background
- 1.2 Motivation for study
- 1.3 Purpose

1.1 Background

The transistor invented by William Shockley, John Bardeen and Walter Brattain have used to amplify and switch electronic signals and electrical power. The transistors were integrated to one chip by Jack St. Clair Kilby in 1958. The integrated circuit (IC) chips speed up invention of computing devices such as a handheld calculator and computer. In semiconductor industry, the number of transistors on IC doubles approximately every two years following Moor's Law. Recently, memory chips with less than 28 nm line-width have been manufactured. However, interconnections between a system board such as printed circuit board (PCB) and a large scale integrated (LSI) circuits chip are failing to follow the integration speed of IC. AS shown in [Figure 1-1](#), the interconnection gap between IC and system board is widening more [1-9].

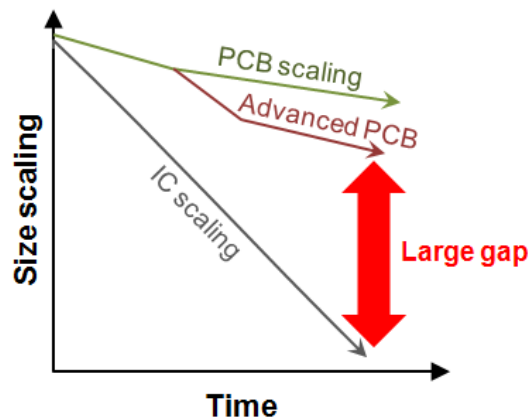


Figure 1-1. Interconnection gap between IC and PCB scaling

As one of the solutions to make up interconnection gap between IC chips and system board, an interposer has been suggested in the packaging industry ([Figure 1-2](#)). The interposer is an intermediate board placed between the chips and the system board. This interposer enables an interconnection of wider and narrow pitch and

reroutes simply the interconnections of system to a different chips as a protocol conversion device.

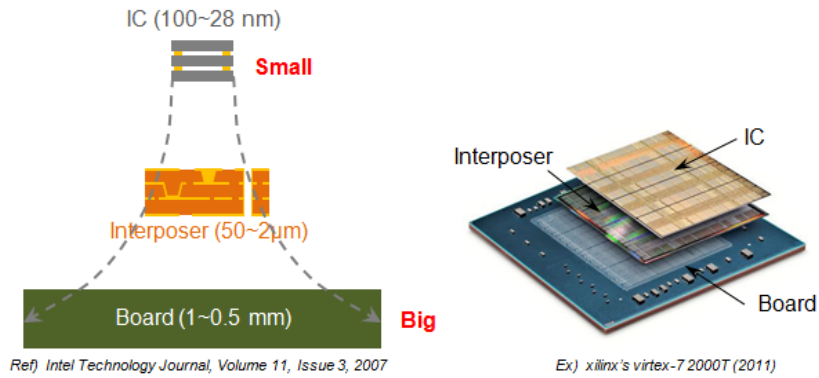


Figure 1-2. Trends of system integration utilizing an interposer

In addition, demand for miniaturization of system boards used in electronic devices such as a smart-phone and a tablet personal computer (PC) is increasing. Therefore, heterogeneous integrated system or three dimensional (3D) integrated systems using the interposer has been studied to meet the demand from a system integration as shown in Figure 1-3 [10-12].

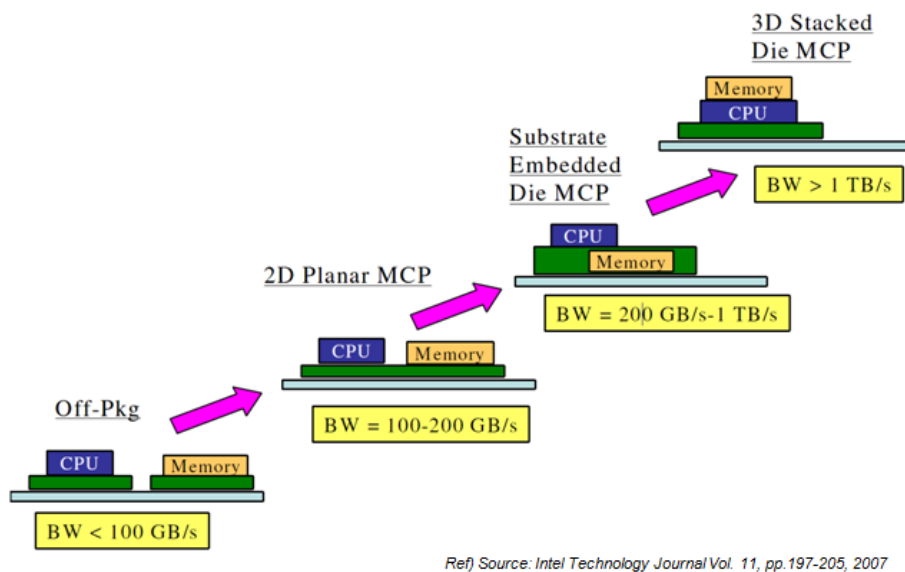


Figure 1-3. Roadmap of package transitions to address memory bandwidth challenge

The interposer consists of metal high density interconnection (HDI) on dielectric layer as shown in [Figure 1-4](#). The HDI in interposer is classified into two types such as plane interconnection and vertical interconnect access (via or through hole interconnection). The plane interconnections play important roles in redistributing wirings. Miniaturization of the plane interconnections has been also required according to miniaturization of the wirings in IC chip. Recently, interconnections with approximately 10 μm width are used. In the case of 2.5 D packaging technology, interconnections with 2 μm width are used. In the case of via or through hole interconnections for linking IC and board of system, there is also demand for miniaturization. Formation of uniform copper layer at side wall of via or through hole with high aspect ratio is another important technical task.

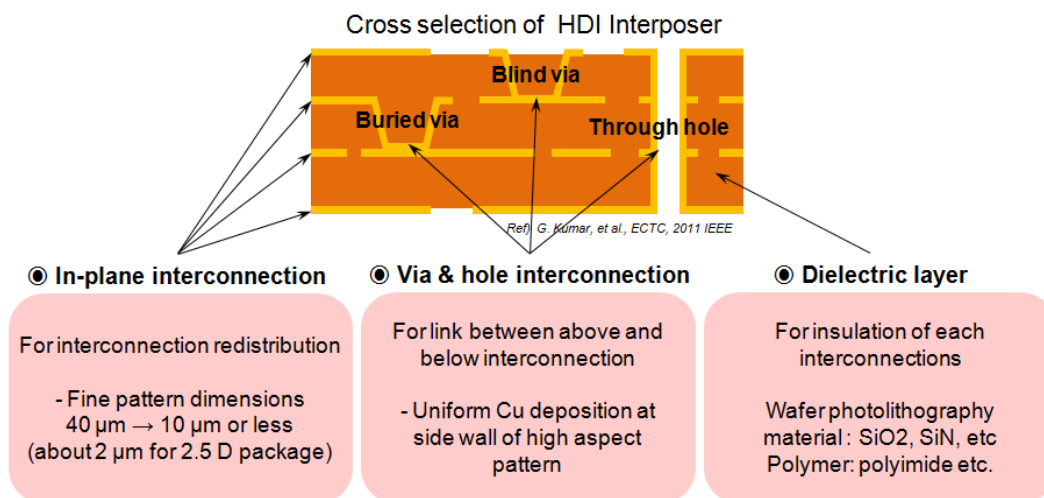


Figure 1-4. High density interconnection and dielectric material in Interposer

The HDI in interposer is electrically isolated by insulation layer [13-15]. The miniaturization of HDI deeply depends on insulation materials. [Table 1](#) shows properties of insulation materials. The patterning process using silicon (Si) substrates enables smallest patterns of interconnection. Inorganic layers such as SiO₂ and SiN is used as an insulation material. However, Si patterning process based on lithography and

etching technology have limits to application because of high fabrication cost. Interconnection patterning process using organic materials can largely reduce the fabrication cost. However organic materials have some problems such as poor chemical stability and heat resistance. On the other hand, polyimide (PI), one of the organic materials, have widely used as an insulation material of PCB and flexible printed circuit board (FPCB) because of its excellent chemical stability and thermal resistance. However, it is difficult to fabricate fine PI pattern less than 10 μm by photolithography process. Therefore, PI fine patterning technology has become a major issue in application to an insulation material of interposer [16-20].

Table 1-1. properties of interposer dielectric material

| Characteristic | Materials/ Process | | | |
|----------------|---------------------------------|-----------------------------------|-------------------|---------------------|
| | Ideal properties | Inorganic (SiO ₂ /SiN) | Organic (General) | Organic (Polyimide) |
| Electrical | High resistivity Low loss | Good | Good | Good |
| Physical | Smooth surface | Good | Good | Good |
| Thermal | High temperature limit | Good | Poor | Good |
| Chemical | Resistance to process chemicals | Fair | Poor | Good |
| Processability | Fine pattern formation | Good | Good | Poor |
| Cost | Low cost | Very High | Low | Low |

Figure 1-5 shows traditional fabrication processes of plane interconnections. They are subtractive, additive and semi-additive method. Subtractive method is shown in Figure 1-5(a). Firstly, seed layer is deposited on insulating substrate by sputtering technology and Cu layer is plated on seed layer by electro plating technology. Then, photo-resist is patterned by lithography process. Finally, Cu interconnection is fabricated by etching technology of Cu layer. It is difficult to fabricate fine Cu

interconnections by subtractive method because of undercut during the Cu etching . In the case of additive method shown in [Figure 1-5\(b\)](#), photo-resist patterns are fabricated and seed and Cu layer is sequentially formed on whole area of substrate. Finally, Cu interconnections are fabricated by lift-off process of photo-resist layer. The additive method has also a problem to fabricate fine interconnection because it is difficult to remove the photo-resist covered by seed and Cu layer. [Figure 1-5\(c\)](#) shows semi-additive method. The semi-additive method is used for fabrication both plane and via or through hole interconnection. In the process, a seed layer is deposited and photo-resist is patterned. Then, Cu is plated on seed layer unblocked with photo-resist. Finally, photo-resist is removed and seed layer is etched. This semi-additive method is compromised method between subtractive and additive method. Recently the semi-additive method is widely used in fabrication of fine interconnection. Abovementioned methods such as subtractive, additive and semi-additive method use the photo-resist patterning process. So the processes are complex and long. As shown in [Figure 1-5\(d\)](#), in damascene process, insulation layer with fine patterns is fabricated for via and through hole interconnections. Then seed layer is deposited on whole surface of the insulation layer with fine patterns and Cu layer is thickly plated on seed layer. Finally, the thick Cu layer is removed until top side of the insulation layer by chemical mechanical polishing (CMP). The miniaturization of interconnections depends mainly on insulation patterning technology [\[21-24\]](#).

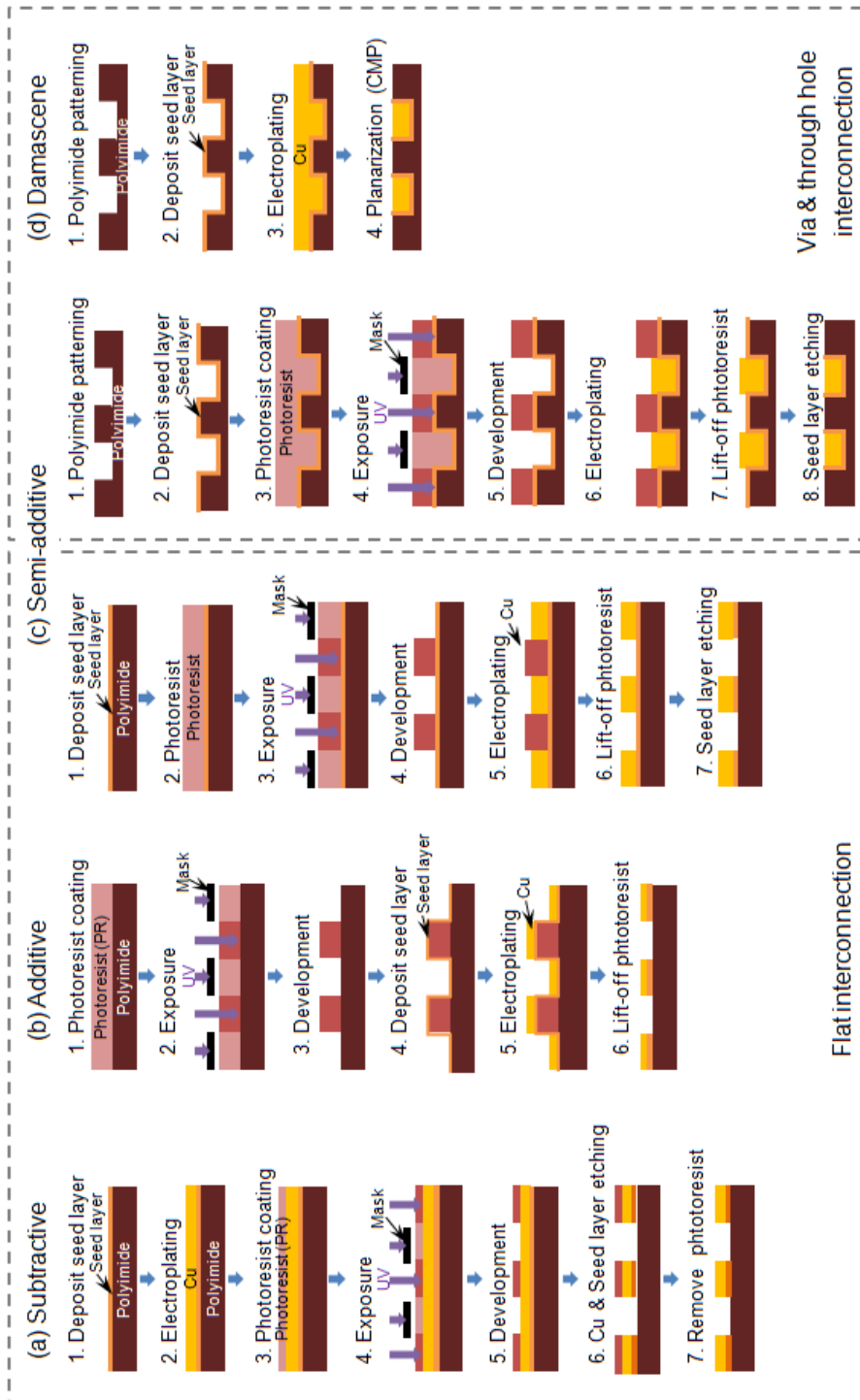


Figure 1-5. Typical fabrication processes of interconnection

1.2 Motivation for this study

Semi-additive or damascene method is one of the technologies which are able to fabricate the smallest metal interconnections at present.

In the case of fabrication of multilayer interconnections including via interconnections, via and plane patterns are fabricated by respective lithography processes. As shown in [Figure 1-6\(a\)](#), this via and plane patterning process using lithography technology is terribly complex. In addition, there are limits to miniaturization of via and plane patterns in polyimide by lithography process. On the other hand, it is possible that via and plane patterns are simultaneously fabricated by nanonimprint process utilizing multistage mold shown in [Figure 1-6\(b\)](#). In addition, fine via and plane patterns are expected by nanonimprint process. Therefore, this nanonimprint technology is expected to simplify via and plane patterning process.

Meanwhile, Cu is metalized in fabricated via and plane patterns by damascene process. In damascene process, seed layer deposition (Seed layers are generally deposited by sputtering process.) and CMP process are necessary. Seed layer deposition and CMP process lead to increase of process cost. Therefore, selective Cu plating process is expected as a simple and inexpensive Cu metallization process because seed layer deposition and CMP process is not necessary.

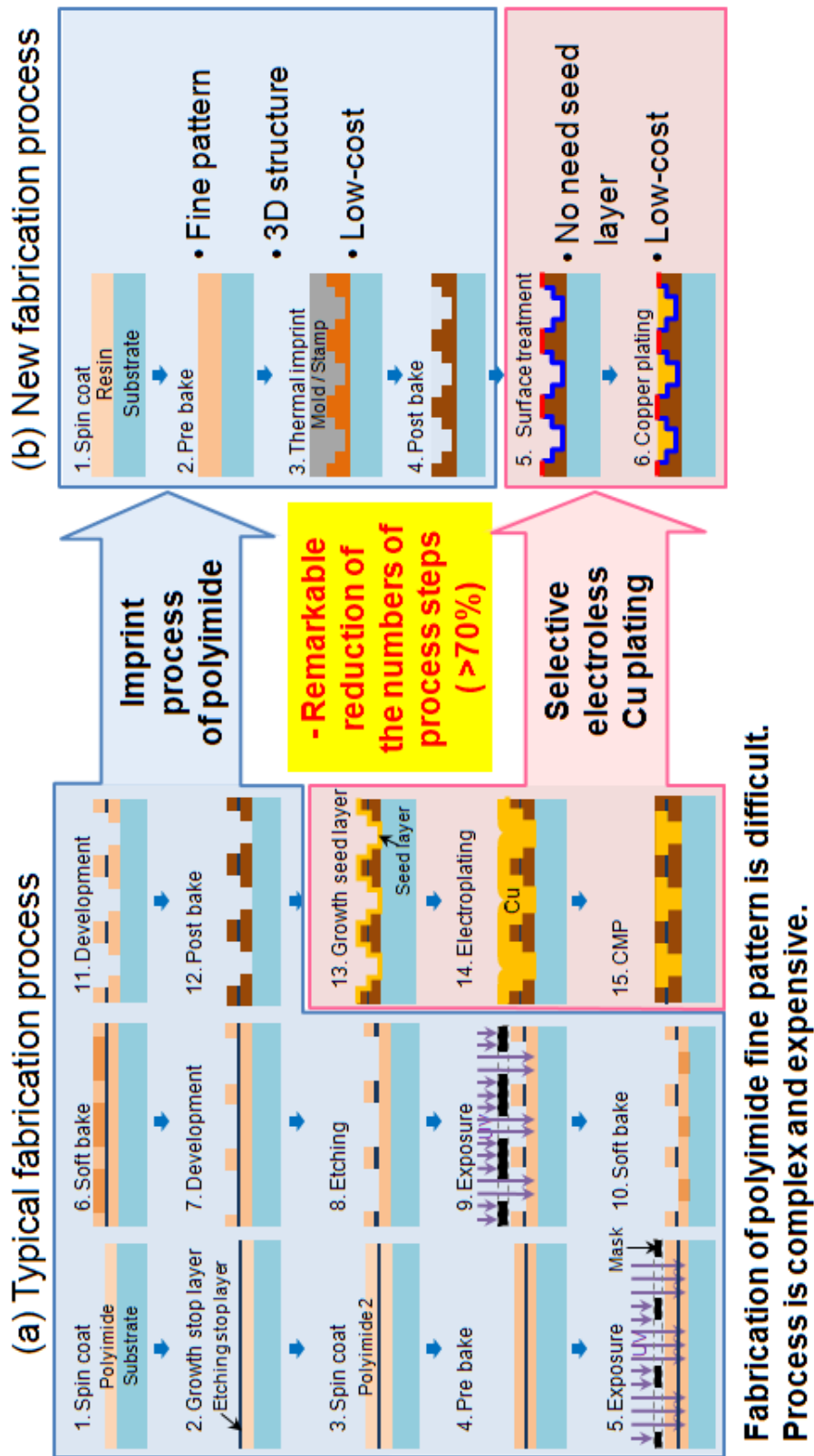


Figure 1-6. Fabrication process of via interconnection

1.3 Purpose

This thesis aims to develop a simplified fabrication process of HDI which can be applied to interposers.

To simplify Cu/PI interconnection fabrication process,

- 1) Thermal/UV Hybrid Imprint (TUHI) is applied to soluble block copolymer polyimide (SBC-PI) resin to fabricate fine PI patterns at low imprinting temperature.
- 2) Surface modification method for SBC-PI by vacuum ultraviolet (VUV) irradiation is developed to enhance adhesion between Cu and SBC-PI.
- 3) Selective electroless copper plating using VUV Induced Surfactant Masking (VISM) is developed to simplify Cu metallization process.
- 4) Fine Cu/PI interconnection is fabricated by TUHI and VISM processes.

Chapter 2

Previous study

2.1 Polyimide patterning process

2.1.1 Polyimide synthesis

2.1.2 Polyimide patterning by lithography

2.1.3 Polyimide patterning by thermal imprint

2.2 Electroless copper plating

2.2.1 Surface treatment for electroless plating

2.2.2 Surface modification using VUV irradiation

2.2.3 Selective electroless copper plating using VUV irradiation

2.1 Polyimide patterning process

Polyimides are a polymer of imide monomers that are mainly based on aromatic chemical structures. PIs are a class of thermally and chemically stable polymers. These PIs have desirable properties such as excellent mechanical properties, chemical resistance, good adhesion properties and low dielectric constant. In addition, they have a relatively low thermal expansion coefficient in organic materials. Therefore, the PIs have been used in a wide variety of applications such as high temperature adhesive, dielectric layer of microelectronics. Especially, PIs are widely used as an insulating and passivation layers in semiconductor industry. In addition, some polyimides can be used like a photoresist of both positive and negative types [25,26].

2.1.1 Polyimide synthesis

The PIs is fabricated by various synthesis methods. The most famous procedure in PIs synthesis methodologies is the two step process using polyamic acid (PAA). This PAA is a polymer precursor for PIs. These PIs synthesis process consist of two step chemical reactions of dianhydride and diamine in a dipolar aprotic solvent such as N,N-dimethylacetamide (DMAc) or N-methylpyrrolidinone(NMP). For example, [Figure 2-1](#) shows the PIs synthesis process of KaptonTM (DuPont). This process using a PI precursor was developed by DuPont in 1950's and has been used as a primary PIs synthesis method to this day. Most PIs are insoluble due to their planar aromatic structures and thus the PAA was synthesized by condensation reaction of dianhydride and diamine in a dipolar aprotic solvent. The KaptonTM PI is fabricated by dehydration reaction of synthesized PI precursor. Thermal imidization method is used for this dehydration reaction [27-33].

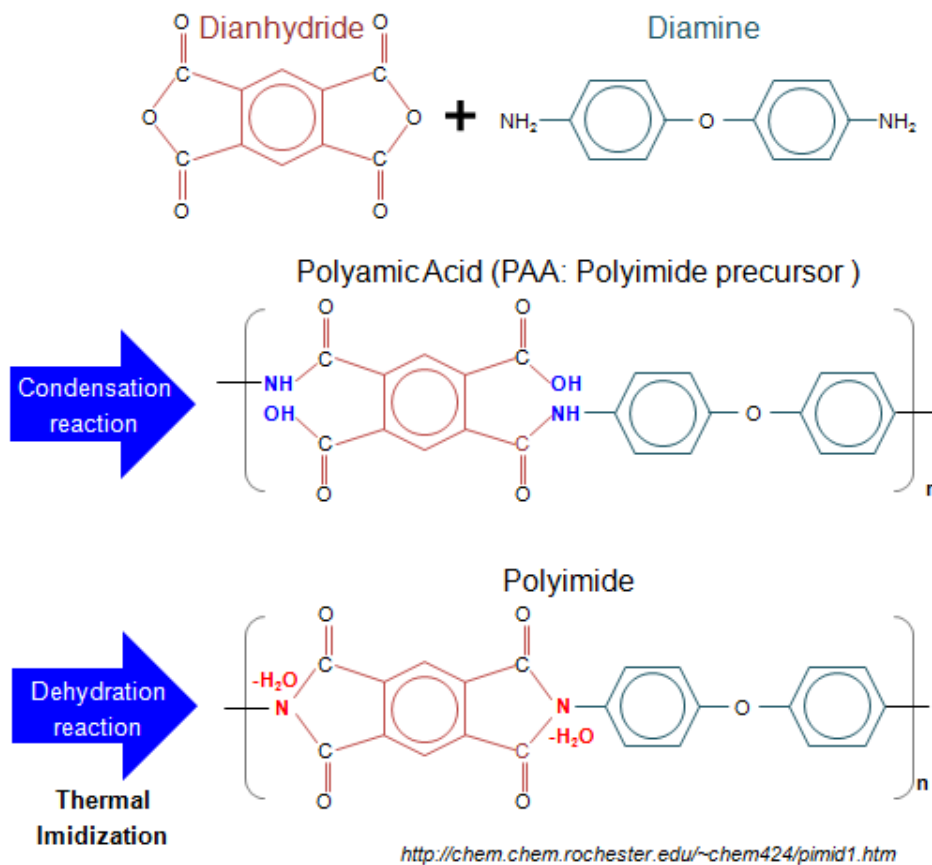


Figure 2-1. Conventional polyimide (Kapton) synthesis process

However, fabricated PI undergoes size deformation during dehydration reaction by thermal imidization. Figure 2-2 shows the thickness shrinkage of fabricated PI film using PAA resin (UR3100, Toray Inc). Fabricated PI film by thermal imidization shrunk to 48% thickness of PAA film because of dehydration reaction. This thickness shrinkage of PI film is a major obstacle in application of PI to semiconductor material [34- 40].

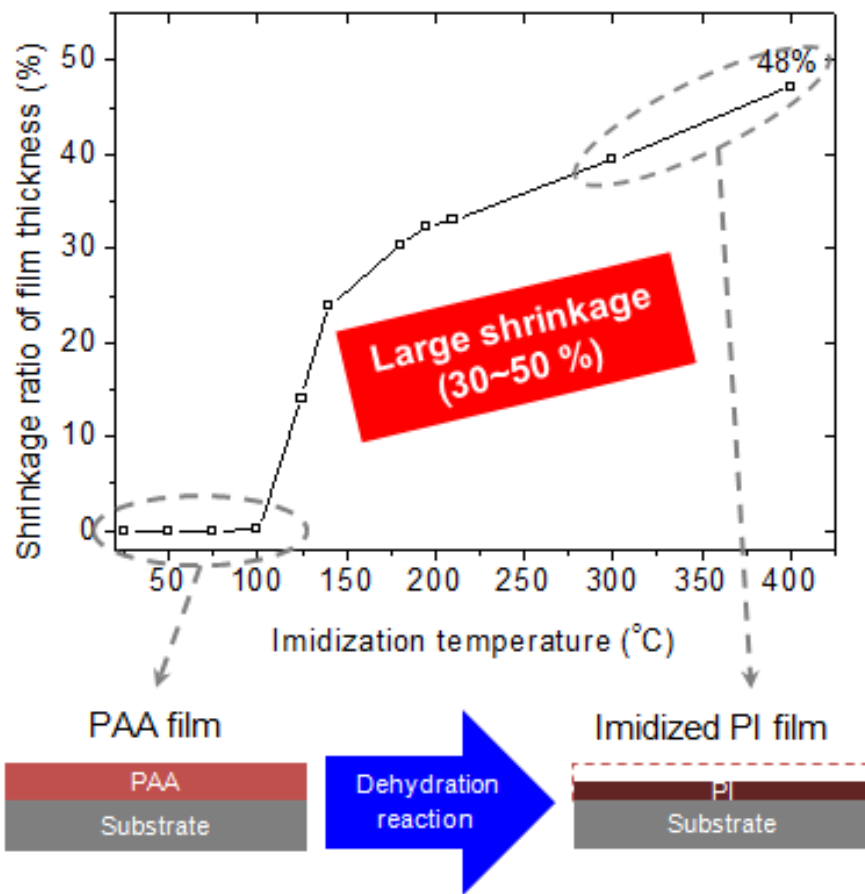


Figure 2-2. Shrinkage ratio of PI film thickness during imidization

2.1.2 Polyimide patterning by lithography

In microelectronics industry, PI is a material for the insulation layers. PI patterns have been fabricated by lithography process using PI precursor resin. The patterning processes are shown in [Figure 2-3](#). In the case of non-photosensitive PI precursor, PI precursor is coated by spin coater. Coated PI precursor is baked to evaporate solvent. Then photoresist is coated and baked on PI precursor film. This photoresist layer is patterned by lithography process consisting exposure and develop steps. PI precursor layer is etched by using photoresist patterns as a protective film. After formation of PI precursor patterns, the photoresist patterns are removed. Finally, PI precursor patterns are synthesized by thermal imidization and then PI patterns are fabricated. However, PI patterns shrink because of dehydration reaction. In addition, non-photosensitive PI pattern process is complex because of lithography process using photoresist. So, photosensitive PI precursor has been developed and widely used to fabricate micro PI patterns simply. The photosensitive PI precursor contains a photosensitive agent in its chemical structure. Photosensitive PI precursor is used in almost the same way as usual photoresist. Photosensitive PI precursor patterns are fabricated by lithography process without using photoresist. However, photosensitive PI patterns also shrink during thermal imidization step because of dehydration reaction of PI precursor [\[41-49\]](#).

PAA: Polyamic acid, PSPI: Photo Sensitive Polyimide

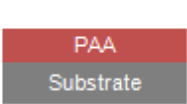
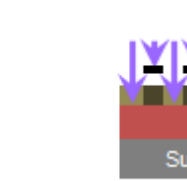
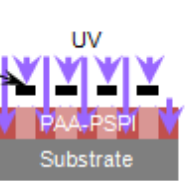
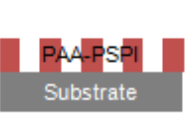
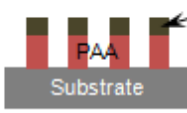
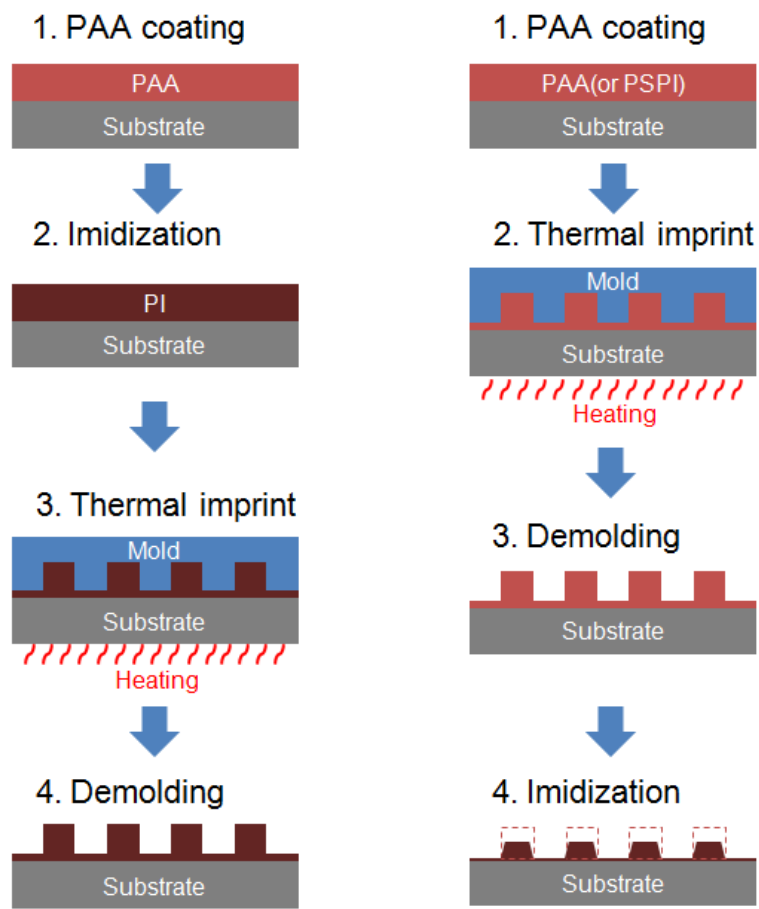
| Process | Photolithography + etching | | State |
|-------------------|---|--|---|
| | Non photosensitive PI | PSPI | |
| Coating & Prebake |  |  | Polyamic acid (PI precursor)  |
| Patterning |  |  | |
| Develop |  |  | |
| Etching & Removal |  | - | |
| Imidization |  |  | |

Figure 2-3. Patterning process comparison of non photosensitive and photosensitive PI

2.1.3 Polyimide patterning by thermal imprint

To resolve the problems of shrinkage of PI patterns caused by dehydration reaction of PI precursor, the PI patterning process by thermal imprint process using imidized PI film was reported. The thermal imprint process is shown in [Figures 2-4](#). In the process shown in figure 2-4(a), PI precursor is spun coated and thermally imidized before imprint. Therefore the shrinkage problem is no longer needed to be considered. Then a mold is pressed onto imidized PI film at an elevated temperature in a thermal imprint process. The size of imprinted PI patterns is basically determined by pattern size in the mold. The fabrication of fine PI patterns is possible by this thermal imprint process. However, the imprint temperature is too high. It is typically higher than 300 °C. This high temperature process causes high cost of imprint apparatus and short mold lifetime. Meanwhile, thermal imprint process using PI precursor film enables to fabricate PI patterns at low imprint temperature. However, a thermal imidization step is necessary after the imprint process. Therefore, the shrinkage problem occurs [\[50,-54\]](#).



(a) PI film thermal imprint

(b) PAA thermal imprint

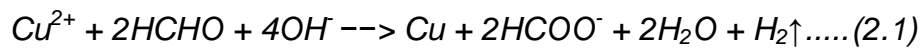
Figure 2-4. PI patterning process using thermal imprint technology

2.2 Electroless copper plating

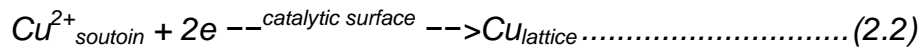
Cu has been widely used as an interconnection metal of PCB or large scale integration (LSI) because of its low resistivity and high electromigration resistance. The Cu interconnection has better electrical properties than aluminum (Al) conventionally used in semiconductor industry. This Cu is deposited on insulation layer by various technologies such as chemical vapor deposition (CVD), physical vapor deposition (PVD) and electro- or electroless-plating. It is difficult to deposit commercially cost-effective Cu by CVD or PVD technology. Therefore, Cu is typically deposited by electro- or electroless-plating technology. In the case of electroplating on insulating substrate, seed layers are necessary because it uses electrical current to reduce dissolved Cu cation. The seed layers are generally deposited by sputtering technology. It is difficult to deposit seed layers on side walls of high aspect ratio patterns and this deposition process of seed layers leads to increase of process cost. Meanwhile, electroless Cu plating is based on the reduction of Cu ions from solution onto substrate without electric current. Therefore, electroless Cu plating does not require deposition process of seed layer. In addition, the high purity Cu is uniformly plated on substrate. Therefore, the electroless Cu plating technology is expected as a major Cu deposition technology in packaging industry [55-57].

2.2.1 Surface treatment for electroless plating

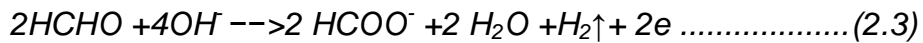
Electroless plating is based on the reduction of metallic ions from solution on catalyzed surface of substrate. Table. 2 shows general electroless plating process. The overall chemical reaction formula for electroless Cu plating with formaldehyde as the reduction agent is as Eqs. (2.1).



where formic acid ($HCOO^-$) is the oxidation product of the reduction agent. The cathodic partial reaction is as Equation (2.2)



and one oxidation reaction, the anodic partial reaction is as Equation (2.3)



Thus the overall reaction of Equation (2.1) is the result of the combination of two difference reaction of Equation (2.2) and Equation (2.3).

In electroless copper plating, surface treatment is necessary because of poor adhesion between Cu and insulating substrate. As shown in [Figure 2-5](#), chemical wet etching, plasma treatment and laser machining technology are widely used as the surface treatment technologies for electroless Cu plating. These surface treatment technologies enhance the adhesion by mechanical interlocking mechanism and anchoring effect. The mechanical interlocking mechanism uses the increase of surface roughness of substrate for enhancing adhesion between Cu and substrate. Therefore, the roughness of the interface between Cu and the insulating substrate is poor. This is a problem of surface treatment technology for electroless Cu plating. The fine patterns are damaged by increase of surface roughness caused by these surface treatment technologies. In addition, the poor surface roughness disturbs the electron transfer. Therefore, the insulation substrate interface should be as smooth as possible [\[58-60\]](#).

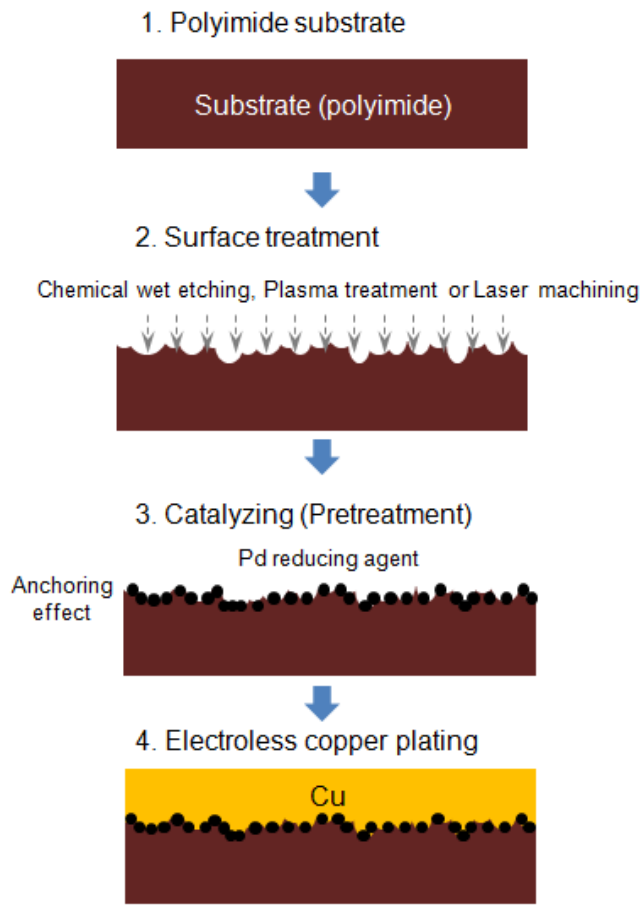


Figure 2-5. Electroless plating using mechanical interlocking

2.2.2 Surface modification using VUV irradiation

As a surface treatment technology without increase of surface roughness for electroless Cu plating, vacuum ultraviolet (VUV) irradiation has been attempted. It changes surface properties from hydrophobic to hydrophilic. The mechanism of the surface modification using VUV is shown in [Figure 2-6](#). Low pressure Hg lamp (LP Hg lamp) is widely used for irradiation of VUV. The LP Hg lamp irradiates two types of UVs with 185 nm and 254nm wavelength. First, Ozone is generated by 185 nm VUV. The ozone gas breaks multiple carbon and carbon bond. In addition, ozone gas is decomposed to active oxygen gas by 254nm UV. The broken carbon and carbon bonds are replaced by oxygen double bonds by active oxygen gas. The oxygen double bond forms the hydrophilic groups such as carboxyl and hydroxyl group. Therefore, hydrophobic surface of polymers is modified to hydrophilic surface by VUV irradiation. This modification technology utilizes the changes of chemical structures without increase of surface roughness. This modified hydrophilic surface is expected to exhibit enhanced adhesion between Cu and insulation substrate [\[61, 62\]](#).

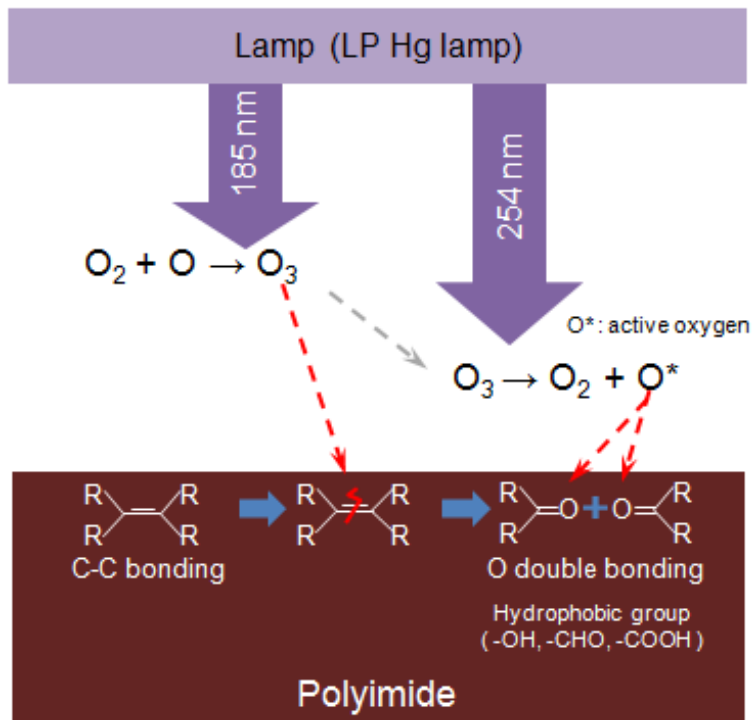
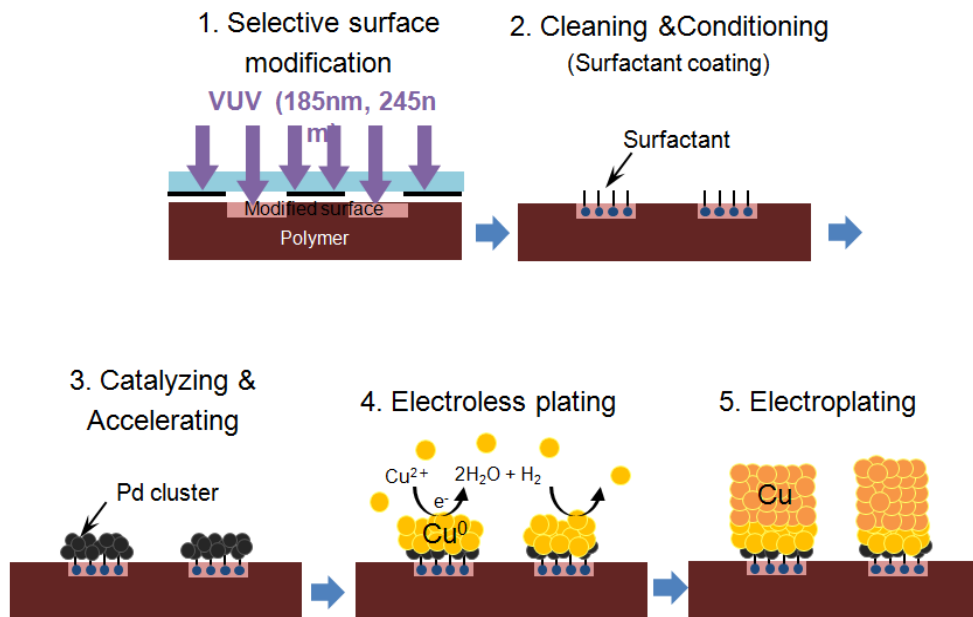


Figure 2-6. Mechanism of surface modification by Vacuum Ultraviolet (VUV) irradiation

2.2.3 Selective electroless copper plating

The VUV irradiation surface modification technology is expected as an enhancement technology of adhesion between Cu and insulation substrate. Furthermore, its application to selective electroless Cu plating process has been reported. As shown in Figure 2-6, a mask is used for selective surface modification of substrate. This is like to exposure technology of photolithography process. Only the light source is different. The Cu is then plated on selectively modified surface. This selective electroless Cu plating process enable to fabricate Cu interconnection simply.

[63-65]



Brief layout of process developed by Prof. Honma group (Kanto Gakuin univ.)

Figure 2-7 Selective electroless copper plating process applying VUV irradiation surface modification

Chapter 3

Polyimide patterning process by Thermal/UV hybrid imprint (TUHI)

- 3.1 Soluble block copolymer polyimide (SBC-PI)
- 3.2 Experimental system
- 3.3 Thermal imprint of non-photosensitive SBC-PI
- 3.4 Thermal imprint /UV hybrid imprint of
photosensitive SBC-PI
- 3.5 Summary

3.1 Soluble block copolymer polyimide (SBC-PI)

Polyimides are highly reliable interlayer insulating polymers with outstanding properties such as excellent mechanical, thermal, and electrical properties. These PIs are not soluble in solvents because of its outstanding chemical stability. In semiconductor and packaging industry, Polyamic acid (PAA, PI precursor) has been used to fabricate PI patterns. However, shrinkage of PI patterns during thermal imidization of PAA is inevitable. This shrinkage problem of PI patterns prohibits application of PI to an interposer with fine patterns used in packaging industry. Soluble block copolymer polyimides (SBC-PI) are developed to avoid this shrinkage problem. These SBC-PIs are soluble in a solvent, although it is generally difficult to dissolve imidized PIs in solvents. Figure 3-1 shows schematic chemical structure of the SBC-PI. The SBC-PI consists of two block polymer parts such as imidized polyimide block and soluble polymer block. The soluble polymer block enable imidized polyimide block to be dissolved in solvents such as imide, ester and ether.

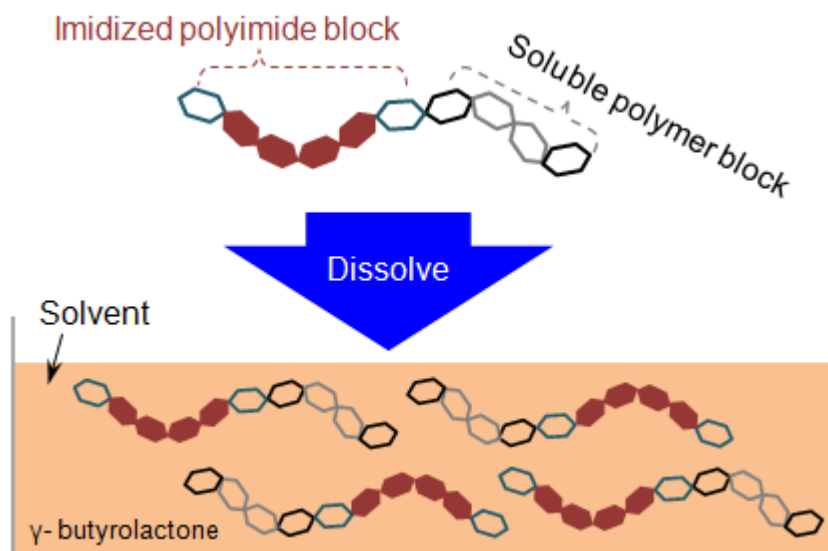


Figure 3-1. Soluble block copolymer polyimide (SBC-PI)

In the case of PI film fabricated using SBC-PI resin, shrinkage of PI film doesn't occur as shown in Figure 3-2, because SBC-PI is already imidized. SBC-PI is dissolved in a solvent. It is an ink-like liquid. In addition, the curing temperature for SBC-PI resin is relatively low compared to thermal imidization temperature of PAA.

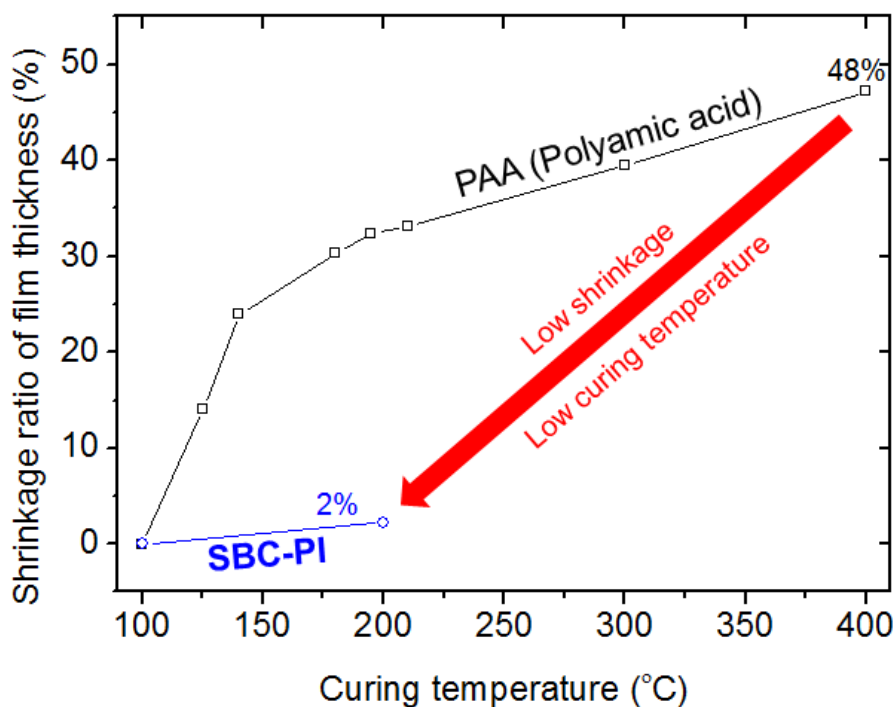


Figure 3-2. Film thickness shrinkage ratio of PAA and SBC-PI

The Young's modulus of the SBC-PI film is tested by nonindention (ELIONIX INC, ENT-2100) as shown in Figure 3-3. The fabricated SBC-PI film with 28 μm thickness was used for the measurement under the load of 1000 μN and 30 $^{\circ}\text{C}$ measuring temperature. The calculated Young's modulus using 0.34 poisson's ratio of general PI film was 2.65 GPa. Young's modulus of fabricated SBC-PI film was almost the same with general PI (DupontTM, Kapton). The Kapton film have the Young's modulus of 2.5 GPa.

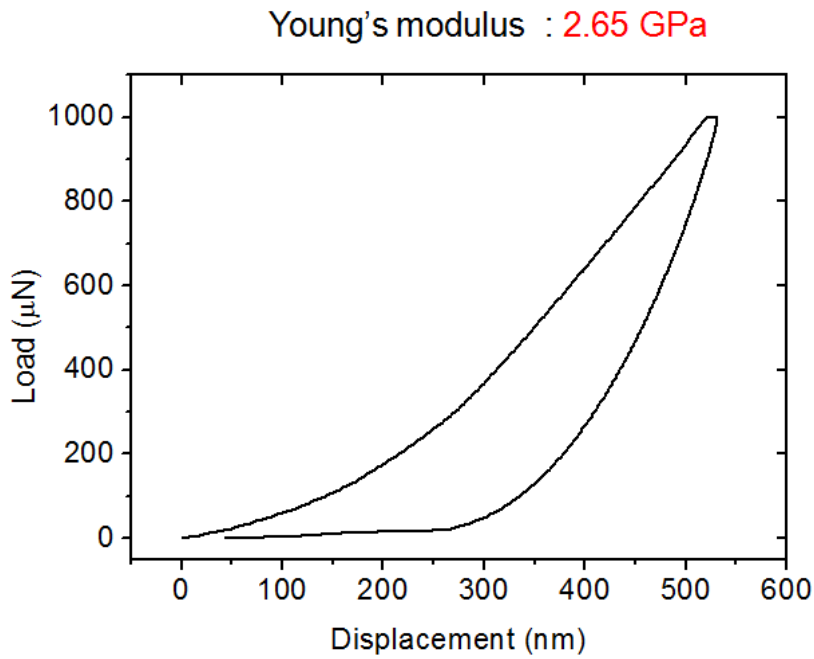


Figure 3-3. Load and displacement graph of SBC-PI by nanoindentation and calculated Young's modulus

The SBC-PI is patterned by lithography process to examine the formability of fine patterns as shown in Figure 3-4. Photosensitive agent is added to SBC-PI to simplify the patterning process.

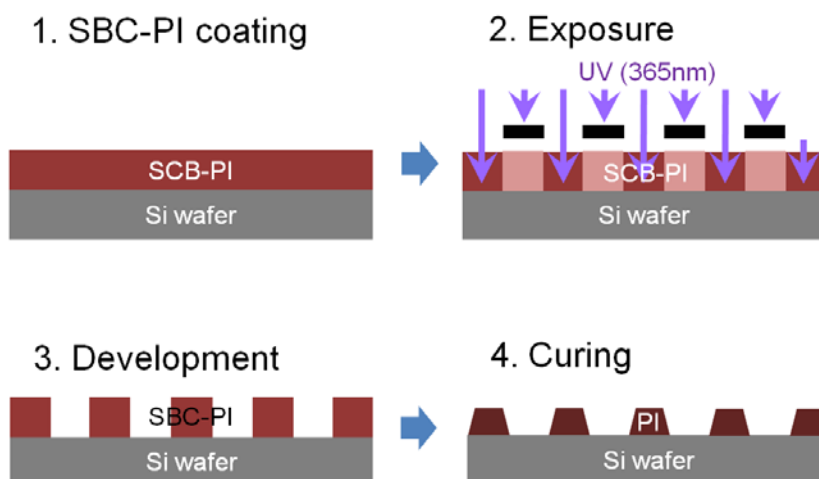
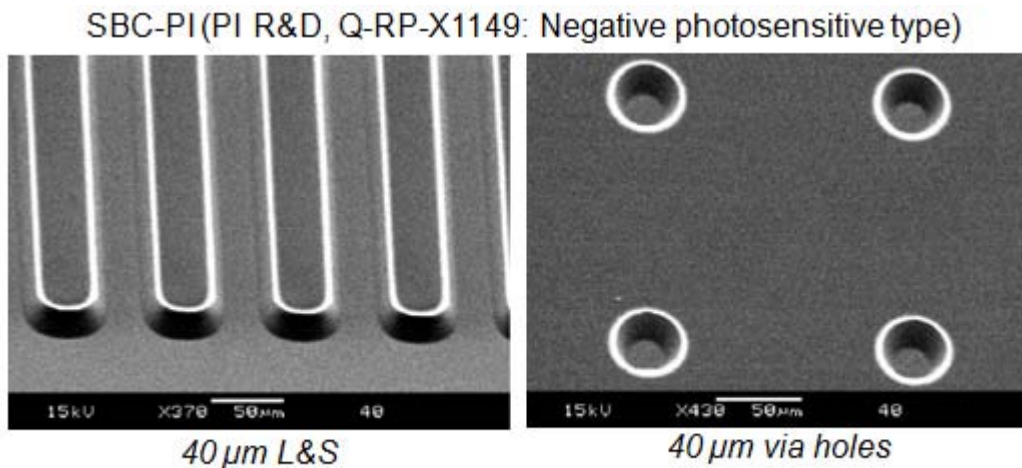


Figure 3-4. Commercial SBC-PI patterning process using photolithography

The SEM images of SBC-PI patterns fabricated by lithography process are shown in Figure 3-5. The PI patterns with 40 μm pattern size were fabricated. It is difficult to fabricate PI patterns less than 40 μm size because of poor patterning resolution of SBC-PI.



Ref.) SEM data were provided by PI R&D Co. Ltd.

Figure 3-5. SBC-PI patterns by photolithography process

3.2 Experimental system

In this study, nanoimprint technology is used as a fine PI patterning process because it has ability to form fine patterns independently on the resolution of photolithography. .

The imprint system (Eitre®8, Obducat AB) used in this study is shown in [Figure 3-6](#). The imprint system enables to perform thermal and UV imprint at the same time or UV exposure after thermal imprint. [Table. 3-1](#) shows specification of this imprint system. Maximum imprint area is 8 inch square. Maximum imprint temperature is 200 °C. Uniform imprint pressure up to 5 MPa is applied by compressed air. UV with 365nm wavelength is irradiated.

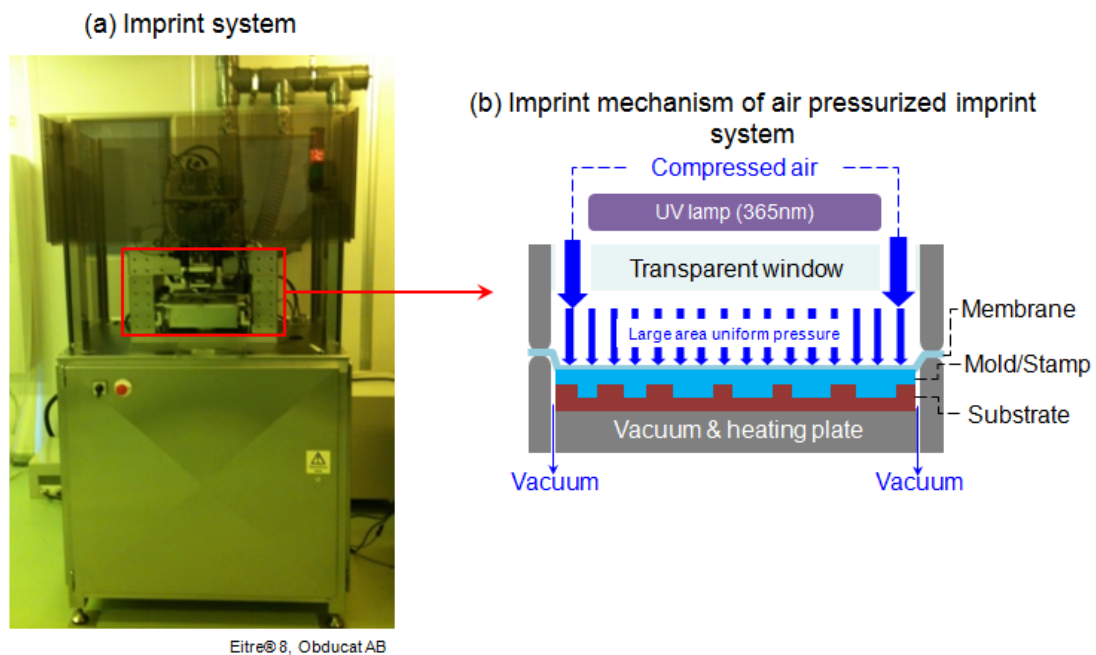


Figure 3-6. Imprint system and mechanism

Table 3-1. Specification of Imprint system

| Items | Contents |
|-----------------------------------|-------------------|
| Imprint area | Max. 8inch square |
| Imprint temperature | Max. 200°C |
| Imprint load using compressed air | Max 5MPa |
| UV wavelength | 365nm |
| Thermal imprint | Possible |
| UV imprint | Possible |
| Water cooling | Possible |

(1) Fabrication of Si master mold

Figure 3-7 shows the fabrication process of Si master mold. Hexamethyldisilazane (HMDS) is famous chemical pretreatment for increasing photoresist adhesion to oxides, nitrides, polysilicon, glass, quartz and other difficult surface. First of all, HMDS primer was coated on Si wafer to improve photoresist adhesion to Si wafer. Then Positive photoresist (MicropositTM S1830, Shipley Company) layer with 2.1 μm thickness was coated by spin coater with 4000 rpm for 30s. The coated photoresist was baked in oven of 90 °C for 20min. The baked photoresist was exposed by aligner system (PEM-800, Union Optical Co., Ltd.). Then, the exposed photoresist was developed by a developer (Microposit[®] MF[®]-319, Shipley Company). Then Si wafer is etched by Si deep etching system (MUC-21, Sumitomo precision products Co., Ltd.) using the photoresist pattern as an etching mask. Bosch process, one of the deep reactive ion etching (DRIE) technologies, was used. This bosch process is a well known anisotropic etch process to fabricate the high aspect ratio structures with nearly

vertical sidewall. Finally, remaining photoresist was removed by reactive ion etching system (RIE-10NRS, Samco. Inc.) using O₂ plasma ashing technology. Fabricated Si master mold is shown in Figure 3-8.

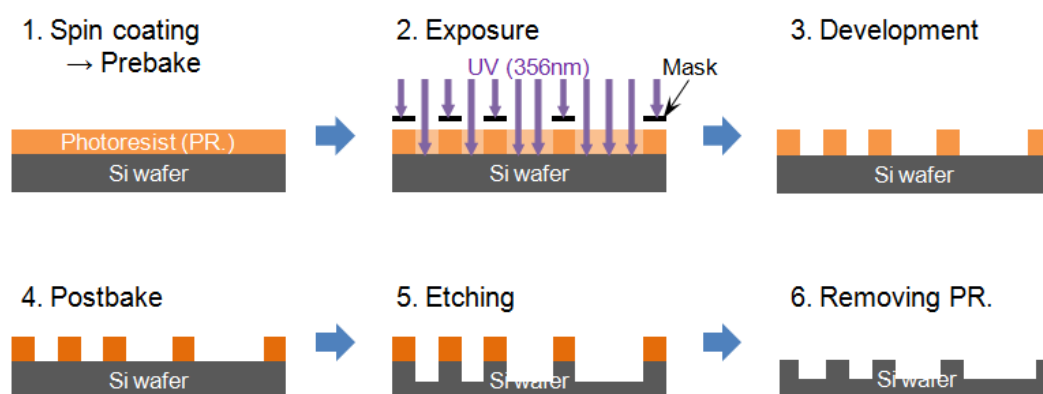


Figure 3-7. Fabrication process of Si mask mold

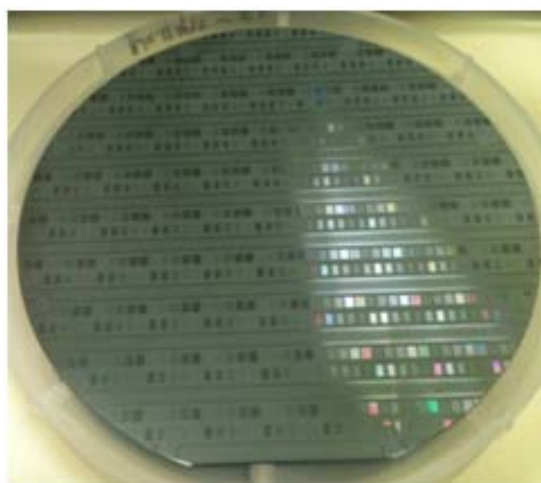


Figure 3-8. Fabricated Si mask mold

(2) Flexible polymer stamp

Flexible polymer stamp is fabricated by thermal imprint process as shown in Figure 3-9. Polymer film with 150 °C glass transition temperature (T_g) was used for duplication of patterns from Si master mold fabricated by lithography process.

Flexible polymer stamp was imprinted at 150 °C imprint temperature and 4 MPa imprint pressure.

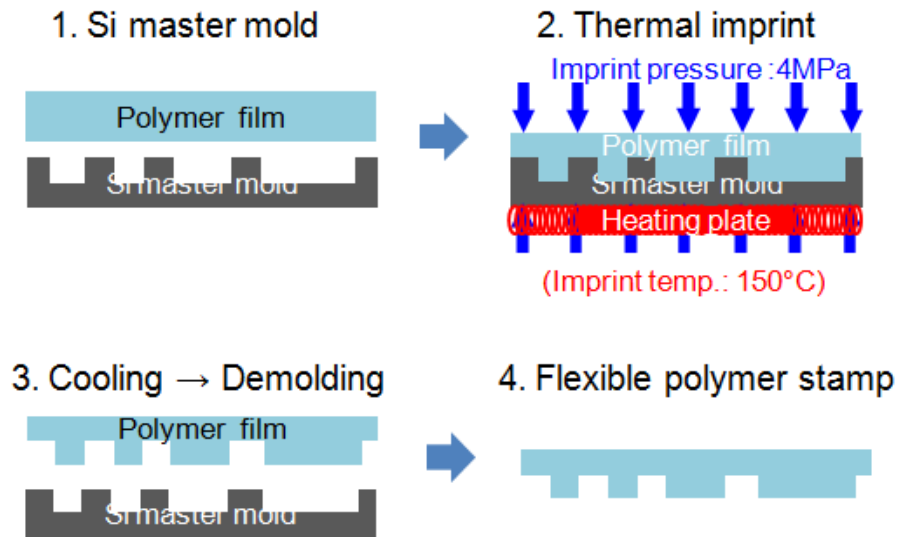


Figure 3-9. Fabrication process of flexible polymer mold

A flexible polymer stamp duplicated from a Si master is shown in Figure 3-10. The flexible polymer stamp mold had low surface energy. Contact angle of wafer is approximately 90°.

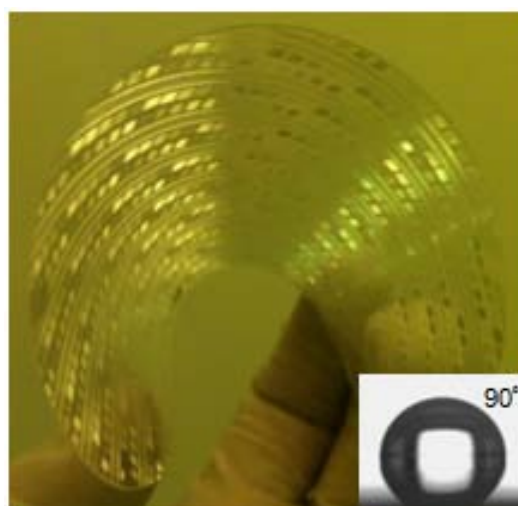


Figure 3-10. Duplicated flexible polymer stamp

Profiles of 50 μm line and space patterns of Si master mold and flexible polymerstamp is analyzed as shown Figure 3-11. Pattern depth of 4.721 μm is measured in Si master mold. In flexible polymer stamp, pattern with 4.653 μm depth is measured. To evaluate the replication fidelity, the surface profile of the imprinted feature in the polymer stamp was compared with that of the master structure in the Si mold, as shown in Fig. 3-11. The height of the imprinted feature was 1.6% smaller than that of the Si master mold structure for 50- μm -wide pattern. This dimensional difference between the master mold and the imprinted polymer stamp seems to result from the recovery of the polymer. In summary pattern profile in duplicated flexible polymer stamp is approximately identical to pattern profile in Si master mold.

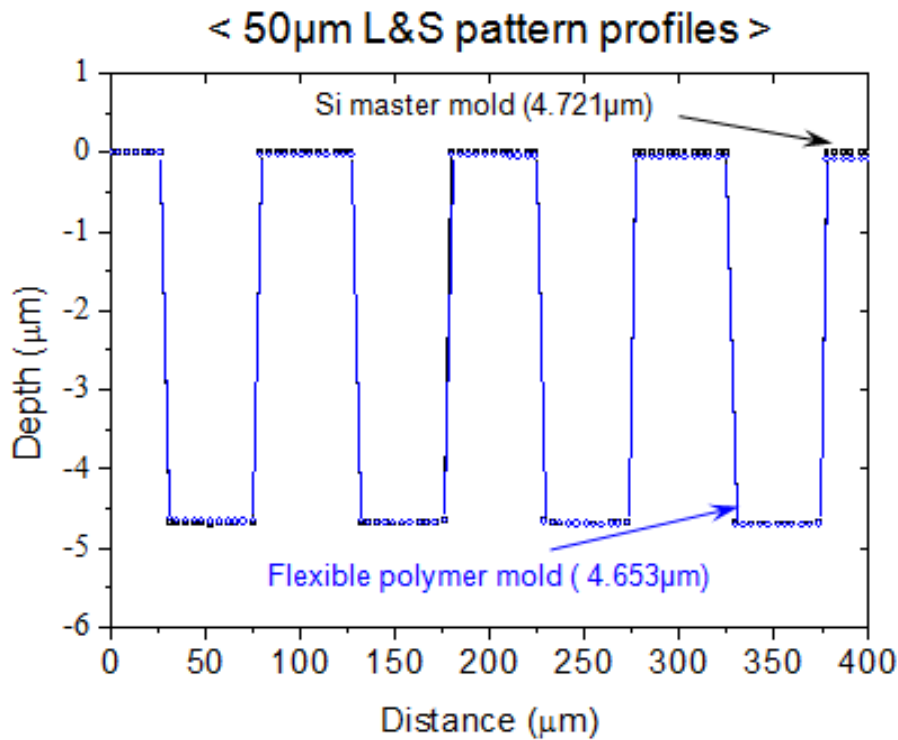


Figure 3-11. Pattern profiles of Si master mold and flexible polymer stamp

3.3 Thermal imprint of non-photosensitive SBC-PI

Non-photosensitive SBC-PI resin was **first** considered as PI film material. As shown in [Figure 3-12](#), PI pattern was fabricated by thermal imprint process. A non-photosensitive SBC-PI film with 28 μm thickness was coated on a Si wafer. SBC-PI patterns were fabricated at low imprint temperature of 120 $^{\circ}\text{C}$. Then, imprinted SBC-PI patterns were cured on hot plate. The hot plate was steadily heated from room temperature to 200 $^{\circ}\text{C}$ with heating ratio of 5 $^{\circ}\text{C}/\text{min}$.

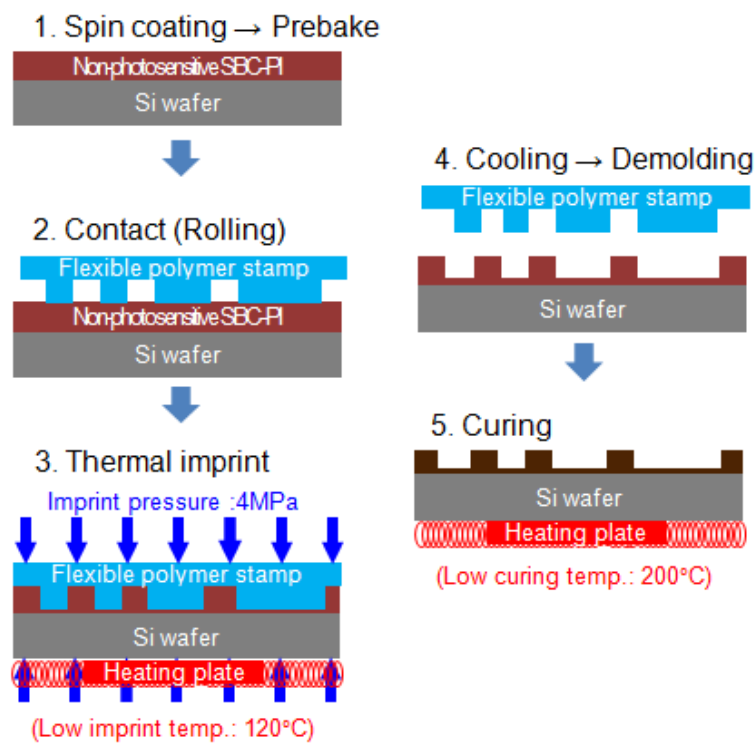


Figure 3-12. Thermal imprint process using non-photosensitive SBC-PI

[Figure 3-13](#) shows the profile of 50 μm line and space pattern after thermal imprint and curing process. Pattern height shrunk largely after curing process. The shrinkage ratio of pattern height was 60.7%. The shrinkage occurred during curing process due to thermal reflow of SBC-PI.

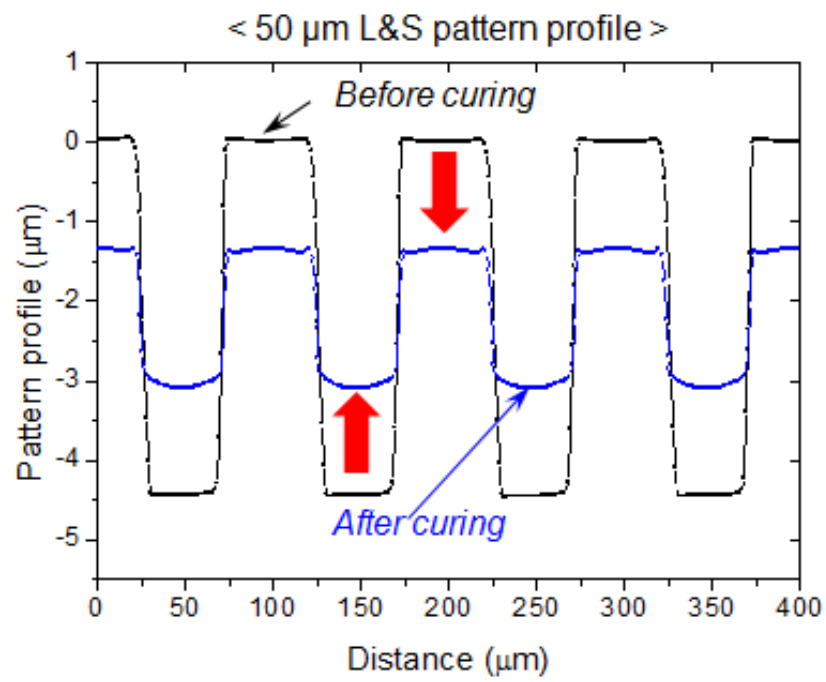


Figure 3-13. Pattern profiles before and after curing

3.4 Thermal/UV hybrid imprint of photosensitive SBC-PI

Photosensitive SBC-PI resin was used as a material of substrate film because photopolymerization of photosensitizers may decrease the thermal reflow during curing process. So, UV exposure step is added to thermal imprint process. A new type imprint process, Thermal/UV Hybrid Imprint (TUHI), was proposed. The proposed TUHI is shown in Figure 3-14. A photosensitive SBC-PI film with 28 μm thickness was coated on a Si wafer. The SBC-PI patterns were fabricated at low imprint temperature of 100 $^{\circ}\text{C}$ with a flexible polymer stamp, and the stamp was removed from SBC-PI substrate after cooling down to room temperature. As added step of TUSI process, imprinted photosensitive SBC-PI film was exposed by UV with a 365 nm wavelength. Imprinted SBC-PI patterns were cured on hot plate. The hot plate was steadily heated from room temperature to 200 $^{\circ}\text{C}$ with heating ratio of 5 $^{\circ}\text{C}/\text{min}$.

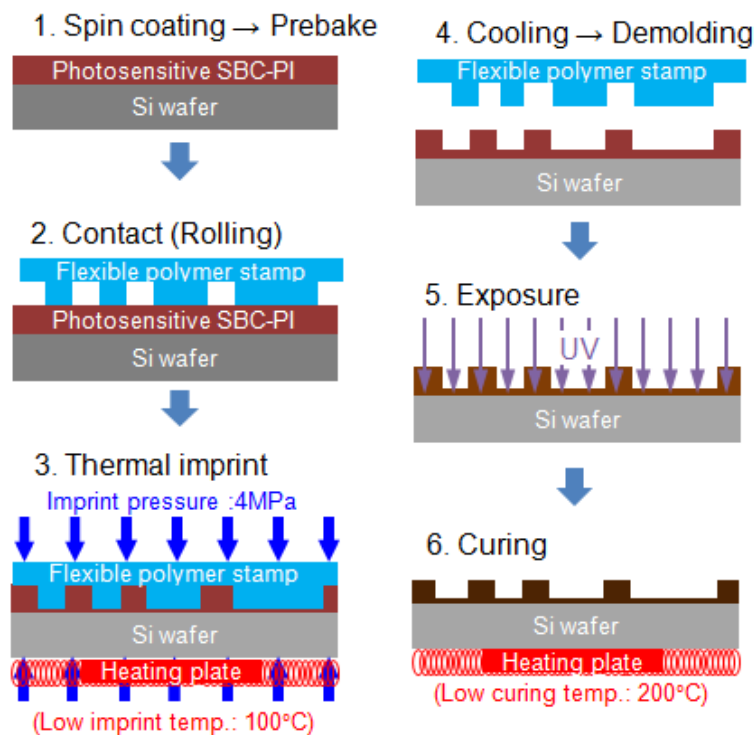


Figure 3-14. Thermal/UV hybrid imprint process using photosensitive SBC-PI

The height shrinkage of PI patterns fabricated by proposed TUHI process is smaller than that fabricated by thermal imprint as shown in Figure 3-15. Figure 3-15(a) shows the relationship between the shrinkage ratio of the pattern height and the curing temperature of non-photosensitive SBC-PI. The shrinkage ratio of the pattern height increased from 140 °C and reached 60.7% at 200 °C. On the other hand, as shown in Figure 3-15(b), in the case of photosensitive SBC-PI, pattern height shrinkage ratio decreased down to 4% after tuning of process parameters. Among the several factors (e.g., imprint temperature, UV dose and curing conditions) which affect the height shrinkage of photosensitive SBC-PI, the curing conditions (e.g., heating profile and heating rate) are the most important parameters as described in following.

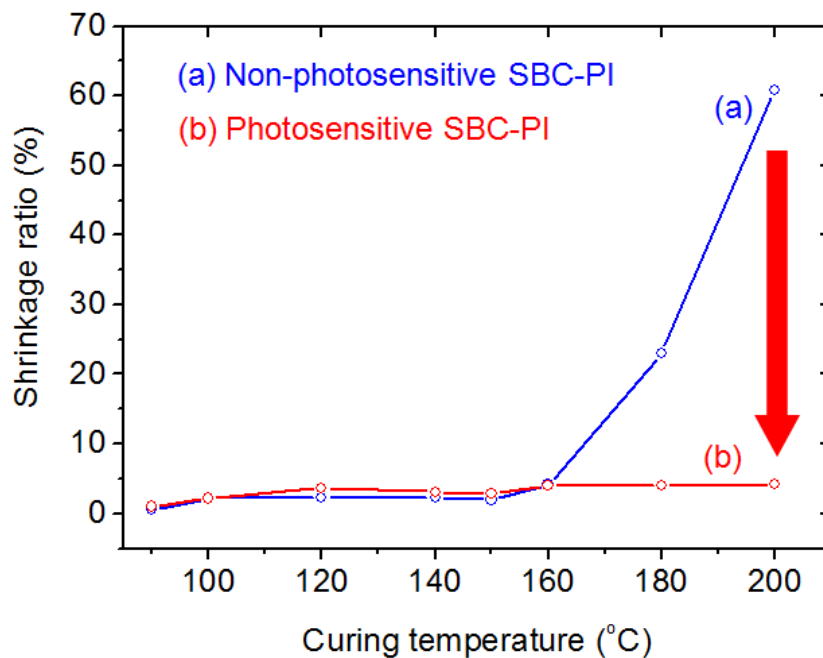


Figure 3-15. Shrinkage ratio of pattern height of non-photosensitive and photosensitive SBC-PI

Influence of UV dose on pattern height shrinkage was investigated to optimize the UV dose of proposed TUHI process. The imprinted PI patterns were exposed by UV with 0, 600, 1200 and 2400 mJ/cm² dose. As a result, pattern height shrinkage ratio decreased from 80.8 % to 48.5 % with increasing UV dose as shown in Fig. 5-16. Pattern height shrinkage was slowdown from 1200 mJ/cm² UV dose. The UV dose of 1200 mJ/cm² was used as the optimized UV dose in this study.

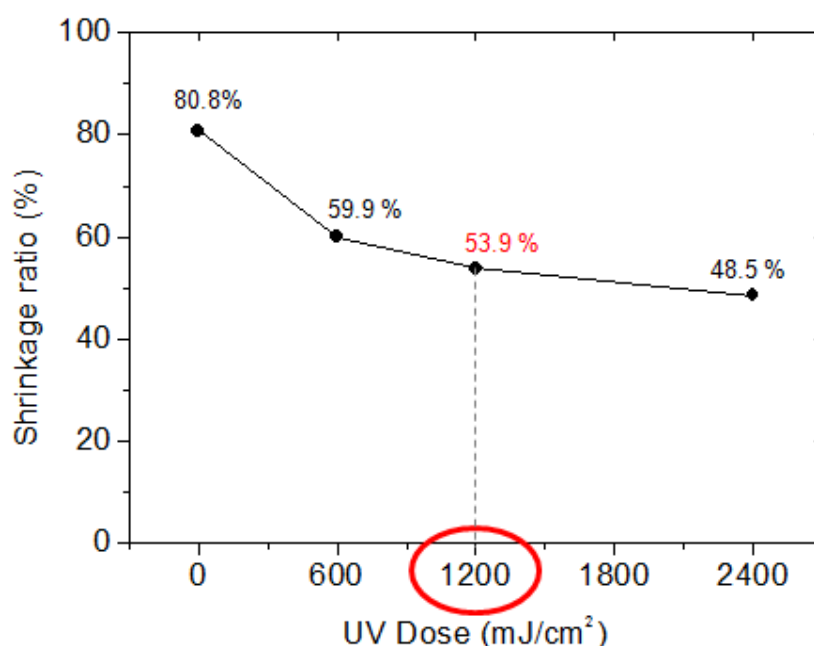


Figure 3-16. Influence of UV dose on pattern height shrinkage of photosensitive SBC-PI

Next, curing temperature conditions were investigated to optimize the proposed TUHI process for SBC-PI. All samples were heated from room temperature to 200 °C curing temperature and the final goal temperature of 200 ° was kept for about 10 min. [Figure 3-17](#) shows the temperature profile of various curing conditions. [Figure 3-17](#) (1) is curing condition with sharp temperature gradient of 20 °C/min and [Figure 3-17](#) (2) is curing condition with slow temperature gradient of 5 °C/min. [Figure 3-17](#) (3) is

curing condition of slow temperature gradient with 5 °C/min included holding step at 100 °C for 10 min which simulates post exposure bake (PEB) of the SBC-PI used as a photoresist.

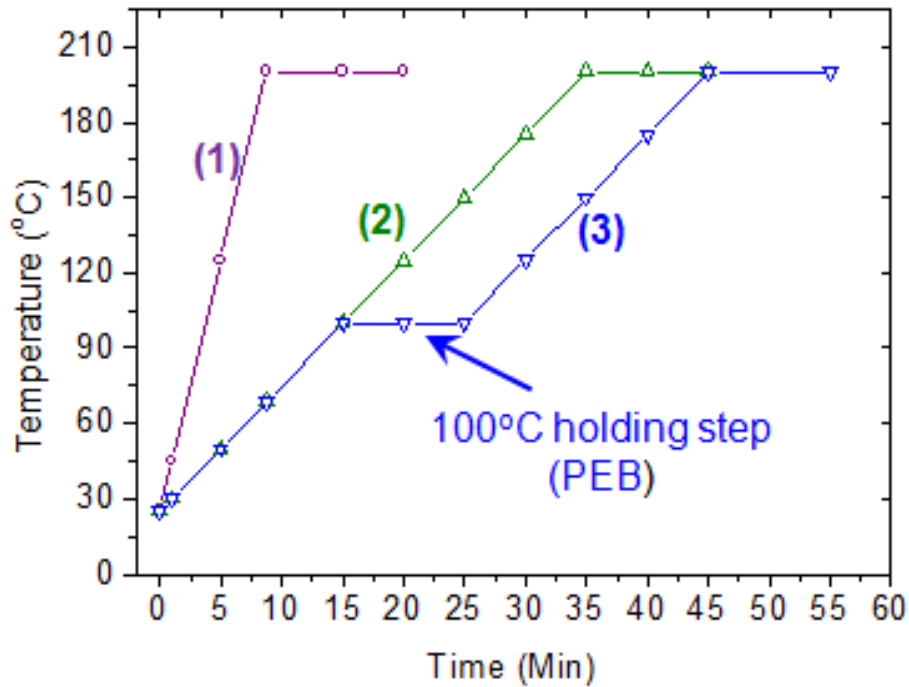


Figure 3-17. Various conditions of curing temperature

Figure 3-18 shows the shrinkage ratio of pattern height cured under various curing conditions. In the case of the sharp temperature gradient, the shrinkage ratio was 70%. The pattern shrinkage of sample cured at slow temperature gradient of 5 °C/min was 56%. Pattern shrinkage of 12% was observed at the sample of curing condition of Figure 3-17 (3)

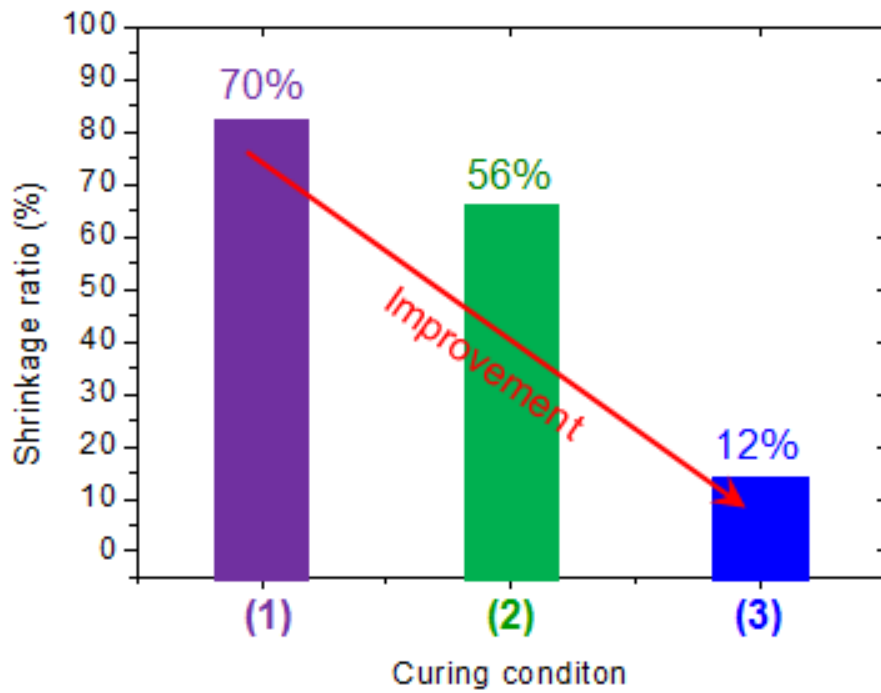


Figure 3-18. Shrinkage ratio of pattern height after various curing conditions

Figure 3-19 shows schematic diagram of photo sensitizer chemical reaction after UV exposure and PEB. The photo sensitizer reacted by UV exposure and heating. This reaction was called as cross-linking. First photo sensitizer was weakly linked by UV exposure. Then the weakly cross linked photo sensitizer was hardly linked by PEB. As a result, the cross linking reaction prevented the pattern height shrinkage caused by thermal reflow.

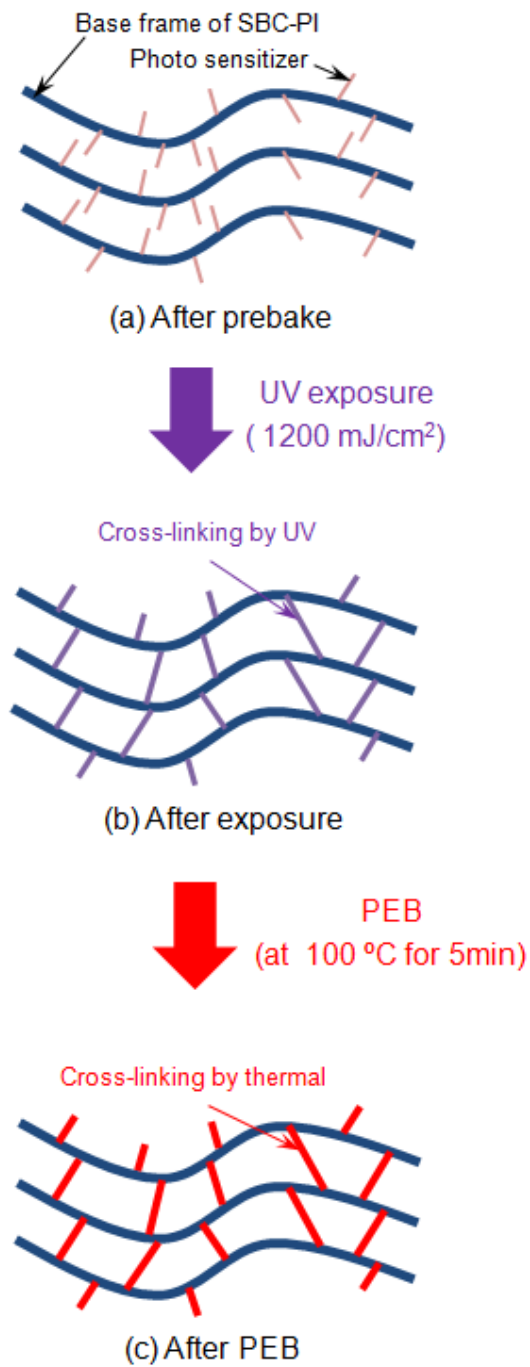


Figure 3-19. Schematic diagram of photo sensitizer chemical reaction by UV exposure and PEB

In order to study influence of photo sensitizer cross inking reaction on SBC-PI film properties, SBC-PI films at each process step were prepared and their mechanical

properties were measured by nanoindentation. Figure 3-20 shows relation of the displacement and load . The displacement of SBC-PI film after prebake was largest and after PEB was smallest. The results mean that the SBC-PI became harder by UV exposure and PEB process.

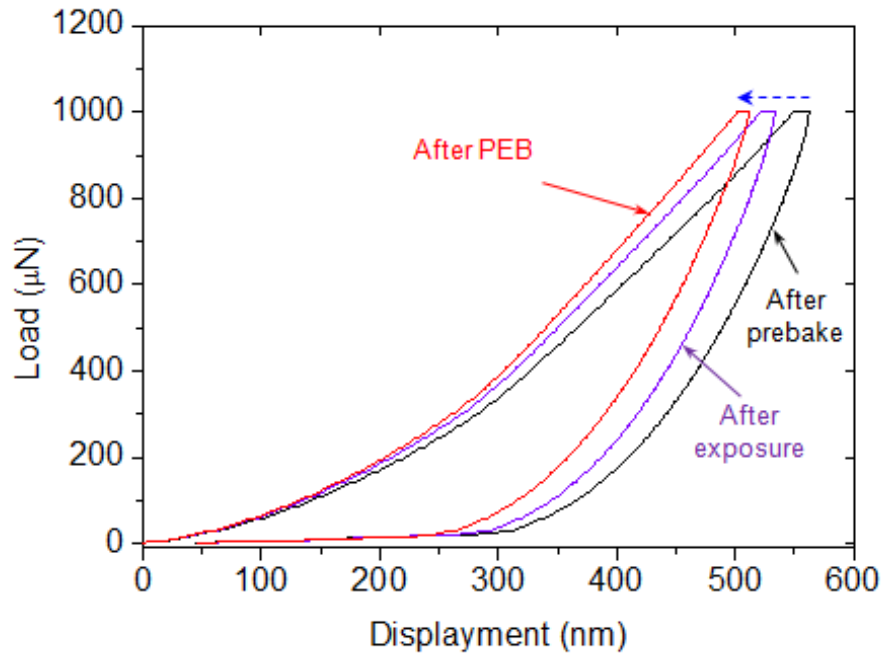


Figure 3-20. Displacement and load graph of SBC-PI film after prebake, exposure, and PEB

Figure 3-21 shows the hardness of SBC-PI after prebake, exposure and PEB. The measured hardness after prebake, exposure, PEB was 197.5 MPa, 236.1 MPa and 253.3 MPa respectively. The hardness of SBC-PI film increased after exposure and PEB. The hardness increase is estimated to be caused by cross linking reaction of photo sensitizer contained in SBC-PI resin. The increase of hardness means that cross linking reaction prevented pattern height shrinkage caused by thermal reflow.

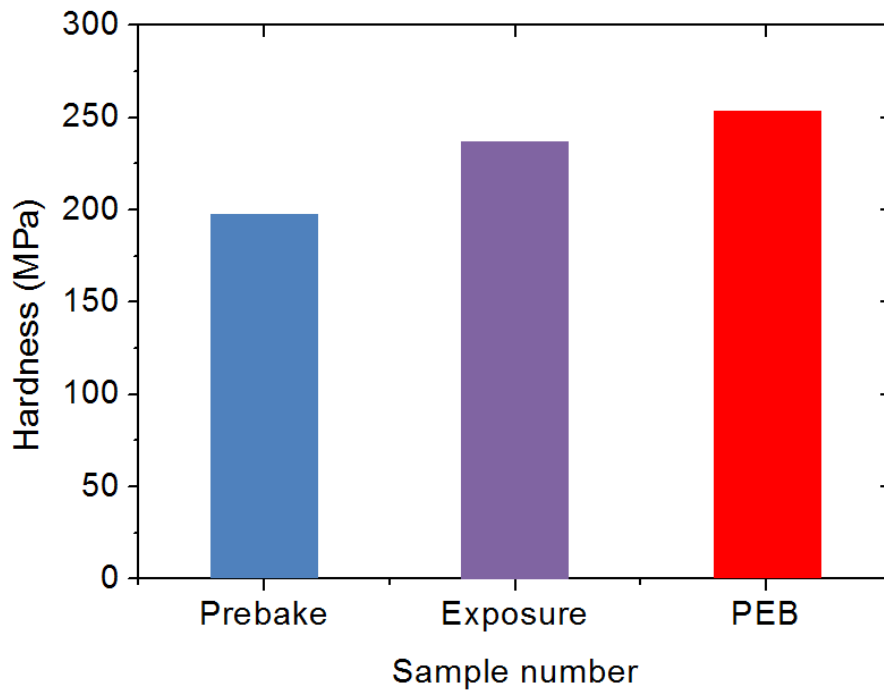


Figure 3-21. Hardness of SBC-PI after prebake, exposure and PEB

Figure 3-22 shows the Young's modulus of SBC-PI after prebake, exposure and PEB. The measured Young's modulus after prebake, exposure, PEB was 2.61 GPa, 2.80 GPa and 2.83 GPa respectively. The Young's modulus of SBC-PI film increased slightly after exposure and PEB. The properties of SBC-PI were analyzed and cross linking reaction of photo sensitizer contained in SBC-PI resin were considered. As a result of hardness and Young's modulus of SBC-PI after prebake, exposure and PEB, it is considered that the cross linking reaction prevents pattern height shrinkage of SBC-PI.

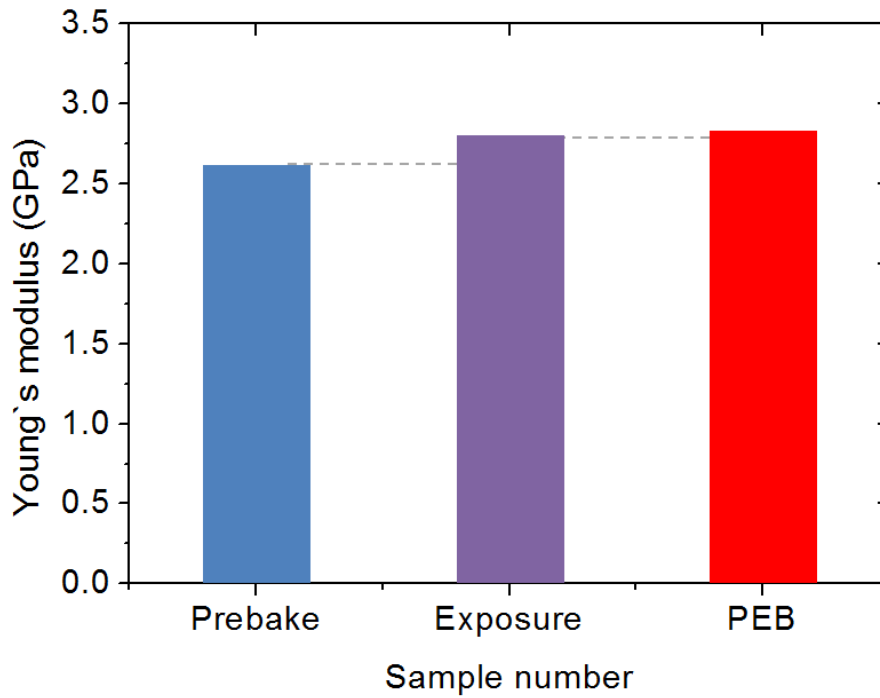


Figure 3-22. Young's modulus of SBC-PI after prebake, exposure and PEB

Figure 3-23(1) shows the heating temperature profile of curing process with heating ratio of 5 °C/min. In this case, curing time was about 1 hour. In order to reduce curing time, starting curing process from 100 °C was proposed as shown Figure 3-23(2). The heating ratio was also 5 °C/min. The entire curing time became approximately half.

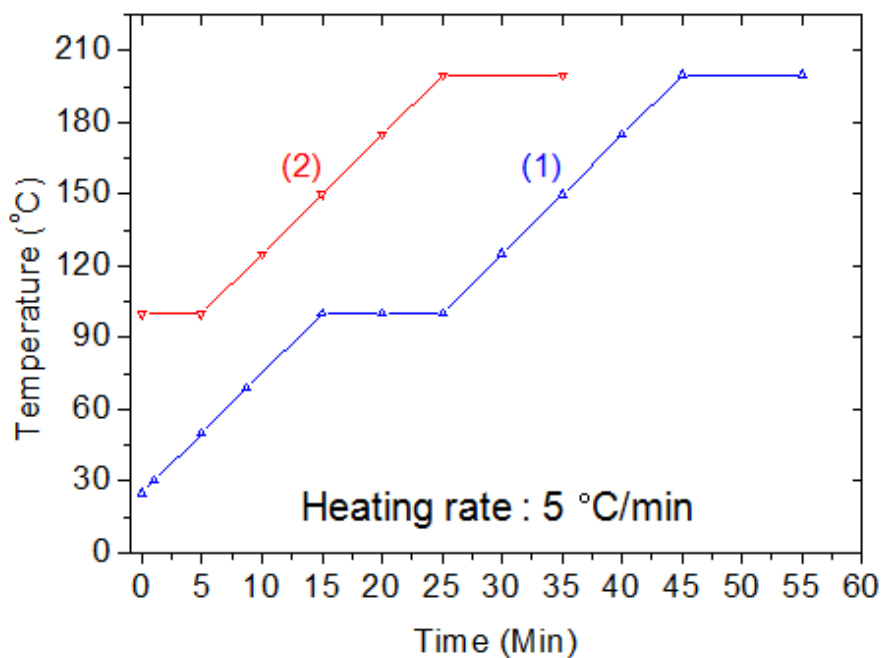


Figure 3-23. Curing temperature profile for economical process

Figure 3-24(1), (2) show the pattern height using the curing conditions of starting temperature at 25 °C and 100 °C respectively. The pattern height decreased only 23 nm in case of starting temperature of 100 °C. The decrease of pattern height showed miniscule amounts about 0.5% of total pattern height. Comparing starting curing temperature 25 °C with 100 °C, the pattern height was almost unchanged. As a result, the curing time was shorted and curing process throughput was enhanced.

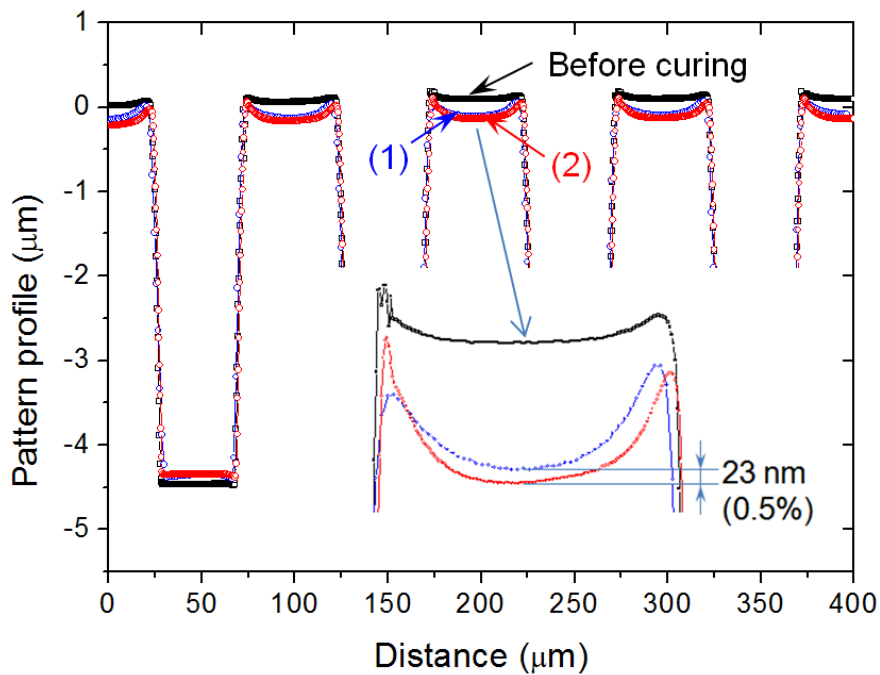


Figure 3-24. Pattern height after curing conditions of starting temperature at 25 °C and 100 °C

Finally the influences of imprint conditions were examined. Among the various imprint conditions such as imprint pressure and time, imprint temperature was considered as a major parameter for enhancing pattern shrinkage. Two type samples were fabricated at imprint temperature of 100 °C and 120 °C. Then the samples was cured at same condition of slow temperature gradient with 5 °C/min included holding step at 100 °C for 10 min. The shrinkage ratios of two samples according to curing temperatures are shown in Figure 3-25. The final shrinkage ratio of two type samples decreased from 12% to 4% by increasing imprint temperature from 100 °C to 120 °C..

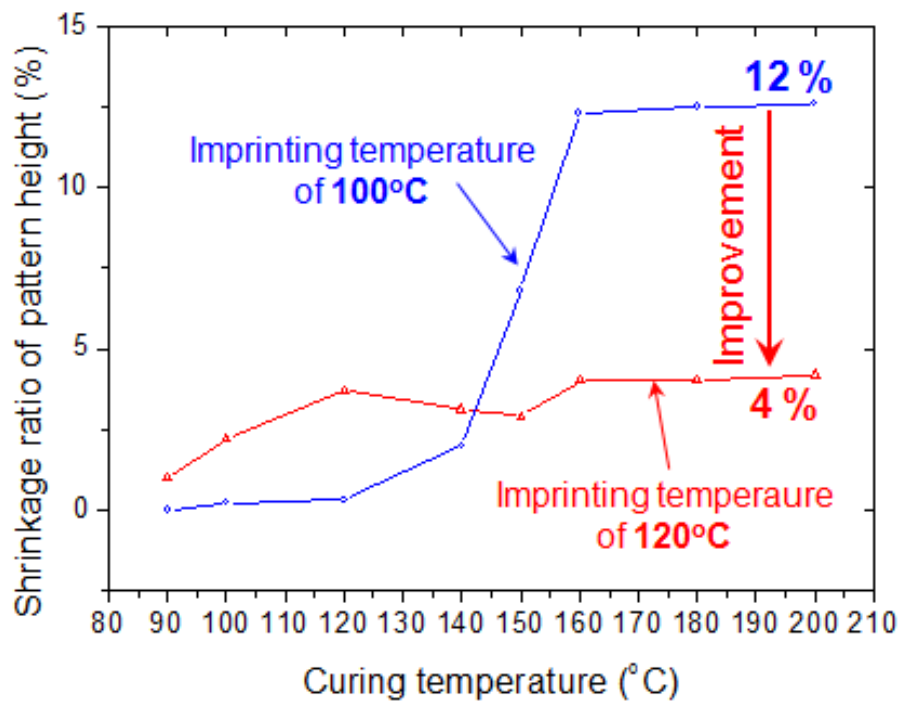


Figure 3-25. Shrinkage ratio–curing temperature curves of SBC-PI samples imprinted at 100 °C and 120 °C

In Figure 3-26, the surface profiles of 50 μm wide pattern structures imprinted at 100 °C and 120 °C. The surface profile of the mold is also shown. The height of the pattern structures was reduced by 4% in case of imprint temperature of 120 °C.

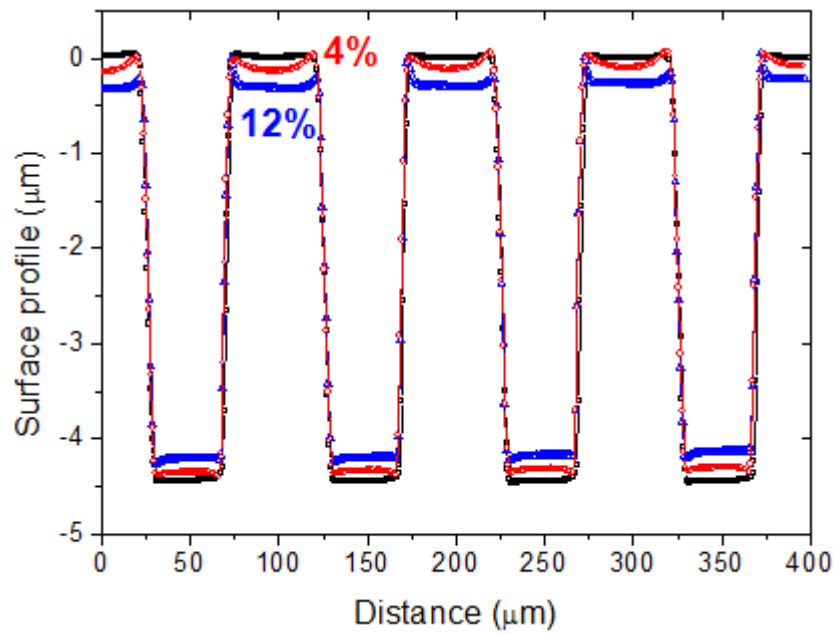


Figure 3-26. Pattern profiles of mold and SBC-PI samples imprinted at different temperatures (blue: 100 °C, and red: 120 °C) after curing at the same condition.

To examine the thermal resistance, the fabricated SBC-PI patterns were heated on hotplate at 225 °C and 260 °C for 10 min. 260 °C is typical reflow soldering temperature. In [Figure 3-26](#), the surface profiles of 10 μm line and space pattern are compared. The height of the pattern structures was reduced by 200nm after heat on hotplate of 260 °C for 10min. The shrinkage ratio of pattern height was only 4 %. This result demonstrates applicability of used SBC-PI to the reflow soldering.

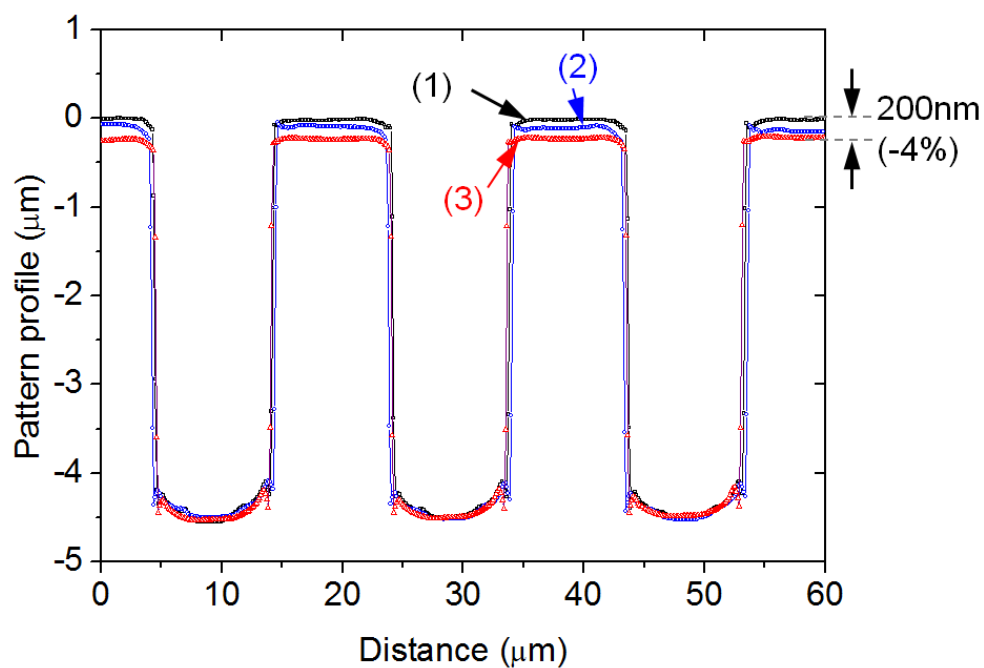


Figure 3-27. Pattern profiles of SBC-PI after heat treatment on hotplate of (1) 200 °C, (2) 225 °C and (3) 260 °C for 10min

Figures 3-27 show scanning electron microscopy (SEM) images of the imprinted SBC-PI sample surfaces. As observed in Figs. 3-27, pattern structures with a rectangular cross section and clear line edge were successfully fabricated.

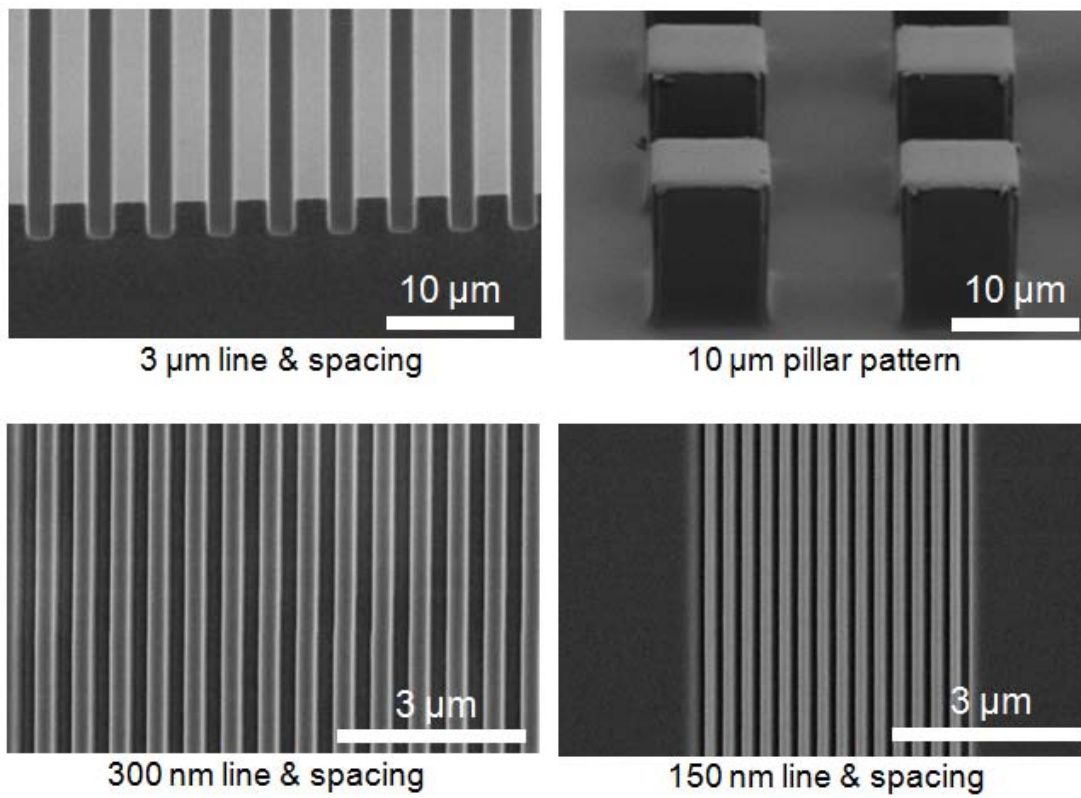


Figure 3-28. SEM images of fabricated polyimide pattern

3.5 Summary

Thermal/UV Hybrid imprint (TUHI) using photosensitive SBC-PI was developed for high precision and low temperature patterning process.

1) Thermal reflow of SBC-PI pattern was prevented by cross linking reaction of photosensitive agent. The shrinkage ratio of pattern height decreased from 60% to 4% by using photosensitive SBC-PI and TUHI.

2) Influence of curing temperature profile on shrinkage ratio of pattern height was analyzed. Shrinkage ratio of 70% decreased to 12% by keeping at 100 °C for more than 2 min in the curing process. 100 °C corresponds to the PEB temperature of photosensitive SBC-PI in case that it is patterned by photolithography. It means the cross linking plays important role to prevent pattern reflow.

3) Shrinkage ratio of pattern height decreased from 12% to 4% by increasing imprint temperature from 100°C to 120°C. It is supposed imprint process at higher temperatures also enhance crosslinking reaction.

4) 3 μm line and spacing patterns with rectangular cross section and clear line edge were fabricated. The minimum line-width of patterns realized was 150 nm. The fabricated pattern size is less than 1/100 of that fabricated by photolithography.

Chapter 4

Adhesion enhancement by VUV irradiation surface modification

- 4.1 VUV irradiation surface modification
 - 4.1.1 Adhesion problem between Cu and SBC-PI
 - 4.1.2 Surface modification system
 - 4.1.3 Modified SBC-PI surface properties
- 4.2 Electroless Cu plating using UV irradiation surface modification
- 4.3 Adhesion between Cu and modified SBC-PI
- 4.4 Analysis of modified SBC-PI surface
- 4.5 Summary

4.1 VUV irradiation surface modification

The surface modification using VUV irradiation changes surface properties from hydrophobic to hydrophilic. This process is effective for surface modification without surface roughness increase. Ozone gas generated by 185 nm VUV breaks multiple carbon and carbon bond on organic substrate. Then oxygen double bond replaces the carbon and carbon bond by active oxygen gas generated by decomposing ozone gas. The oxygen double bond forms the hydrophilic groups such as carboxyl and hydroxyl group. Therefore, hydrophobic surface of a organic substrate is modified to hydrophilic surface without increase of surface roughness.

In this study, effects of VUV irradiation conditions on topological and chemical properties of SBC-PI were investigated. The SBC-PI films were irradiated with the different VUV exposure dose by varying the exposure time. Then, properties of modified PI surface were analyzed by water droplets test, DFM and XPS. In addition, VUV irradiation surface modification was applied to an electroless Cu plating to evaluate the adhesion between Cu layer and modified SBC-PI surface.

4.1.1 Adhesion problem between Cu and SBC-PI

SBC-PI is synthesized by polyimide block and methyl hydrogen siloxane block. As shown in Figure 4-1, the methyl hydrogen siloxane block is supplemented to improve solubility and bending properties of conventional PIs.

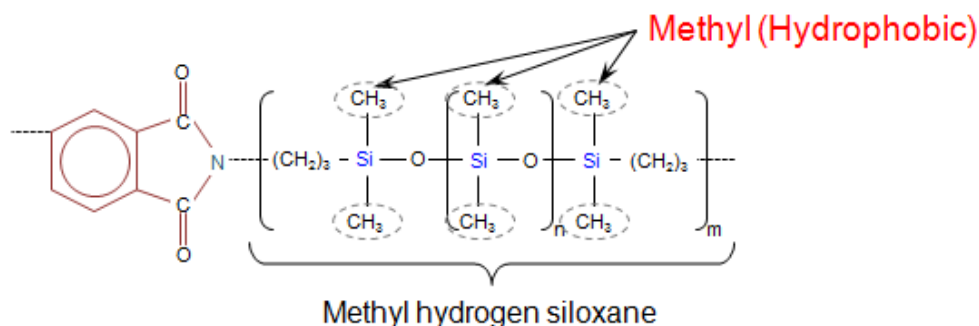


Figure 4-1. Chemical structure of SBC-PI

Because of the methyl hydrogen siloxane block, the synthesized SBC-PI has hydrophobic properties such as high contact angle and low water absorption as shown in Figure 4-2(a). These hydrophobic properties of SBC-PI are merits and demerits. Especially, adhesion to Cu layer formed by electroless plating is poor. Figure 4-2(b) shows the poor adhesion between Cu and SBC-PI. Therefore, surface treatment for adhesion enhancement is one of the important technologies in electroless Cu plating onto SBC-PI. The VUV irradiation surface treatment without increase of surface roughness is the most promising among various surface treatment technologies for electroless Cu plating.

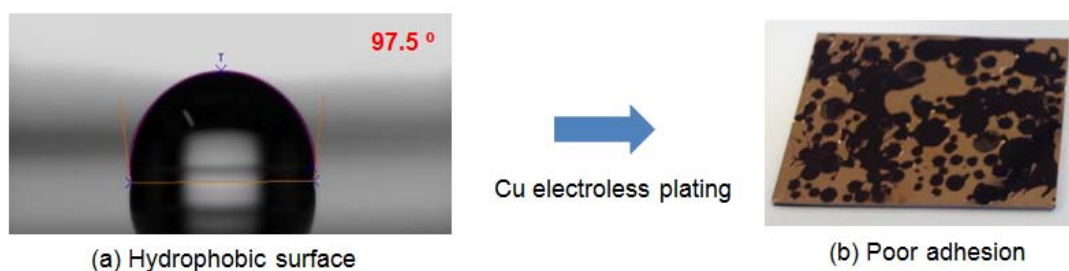


Figure 4-2. Contact angle of SBC-PI surface and poor adhesion between electroless-plated Cu and SBC-PI

4.1.2 Surface modification system

The SBC-PI films were irradiated with the different VUV exposure dose by varying the exposure time by VUV irradiation system (PL16-110, Sen engineering Co., Ltd). The VUV irradiation system is shown in Figure 4-3. A low-pressure mercury lamp (LP Hg lamp, EUV200WS-60L, Sen lights Co., Ltd) was used in the VUV irradiation system. The lamp emits VUV lights of 254 nm and 185 nm wavelength.



(SenEngineering Co., LTD)

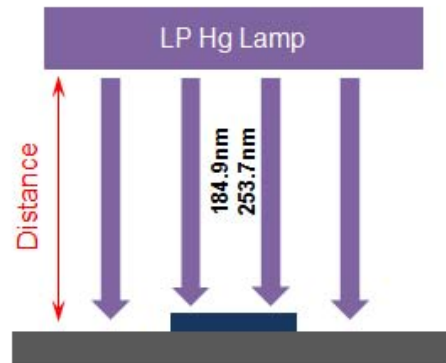


Figure 4-3. VUV irradiation system

As shown in Figure 4-3, VUV light power density at each distance from 1cm to 13cm was measured by VUV illumination meters (UVC-254 and UVC-185, Lutron electronic enterprise Co., Ltd) to explore the relationship between dose of VUV light and distance from lamp. Measured VUV light power density is shown in Figure 4-4. Power density of 254nm and 185nm wavelength of UV measured at 10 cm distant from the LP Hg lamp was about 20 mW/cm^2 and 2.5 mW/cm^2 respectively.

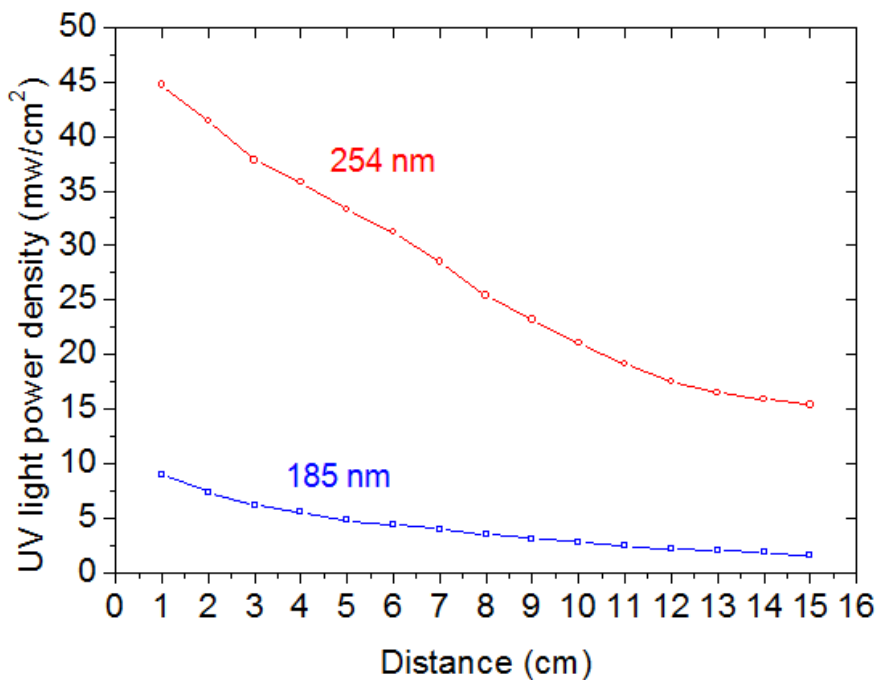


Figure 4-4. VUV light power density according to distances from LP Hg lamp

4.1.3 Modified SBC-PI surface properties

The effects of VUV dose on topological and chemical properties of SBC-PI surface were investigated. PI films with 28 μm thickness were prepared by spin coating and curing process of photosensitive SBC-PI varnish. Negative photosensitive soluble block copolymer polyimide (SBC-PI, Q-RP-X1149, PI R&D Co., Ltd) was used. Then SBC-PI films are placed on a stage in the VUV irradiation system. Distance between the stage and the LP Hg lamp was 10 cm. The dose is given by equation (4.1).

$$Dose (mJ/cm^2) = LPD (mW/cm^2) \times T(s) \dots\dots\dots (4.1)$$

Where, LPD is light power density and T is irradiation time.

Each sample was irradiated for 5 to 900 seconds at an atmospheric condition. According to irradiation times, the doses of VUV irradiation were calculated by the given equation (4.1) and are shown in Table 4.

Table 4-1. VUV dose at 10 cm distance

| Irradiation time (s) | 0s | 5s | 60s | 120s | 300s | 600s | 900s |
|---|----|------|------|------|------|-------|-------|
| Dose of 254 nm wavelength (mJ/cm ²) | 0 | 100 | 1200 | 2400 | 6000 | 12000 | 18000 |
| Dose of 185 nm wavelength (mJ/cm ²) | 0 | 12.5 | 150 | 300 | 750 | 1500 | 2250 |

Then the effects of VUV irradiation on polyimide surfaces were evaluated by a potable contact angle meter (PCA-1, Kyowa Co., Ltd) and DFM. Contact angle and surface roughness of modified SBC-PI surface are shown in Figure 4-5. As VUV dose increased, the contact angles of SBC-PI surface decreased consistently. However, the surface roughness of modified SBC-PI showed no remarkable change according to increase of VUV dose.

The reduction of contact angle means that SBC-PI surface is modified from hydrophobic to hydrophilic. The changes of contact angles were measured by water droplets test as a function of VUV dose. The contact angle of bare SBC-PI surface was 97.5°, indicating that it has a hydrophobic nature (i.e., low surface energy). As VUV dose increases, contact angle of SBC-PI surface decreased gradually. When the VUV dose was 6750 mJ/cm², the measured contact angle was 11°. These results indicate that wettability of SBC-PI can be switched from hydrophobic to hydrophilic by controlling VUV does.

In addition, the DFM measurement results of SBC-PI surface before and after VUV irradiation with the dose of 6750 mJ/cm². It was confirmed that the increase of

surface roughness was not remarkable. The ten-point mean roughness (Rz) was increased from 2.352 nm to 3.412 nm. These results indicate that the surface properties of irradiated PI film can be modified from hydrophobic to hydrophilic surface without remarkable increase of surface roughness.

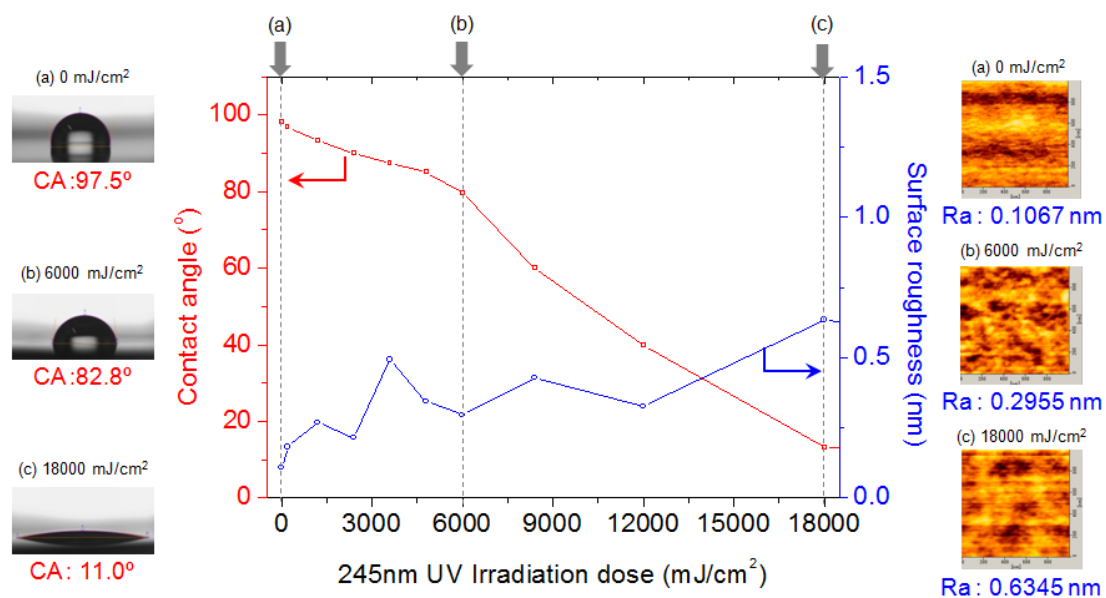


Figure 4-5. Modified SBC-PI surface properties by VUV irradiation

4.2 Electroless Cu plating using VUV irradiation surface modification

Copper layer was formed on modified SBC-PI samples by electroless plating. Figure 4-6 shows the electroless Cu plating process used. Before Cu electroless plating, the surface of SBC-PI was modified by VUV irradiation technology. Then Cu layer was deposited on modified SBC-PI surface by electroless Cu plating.

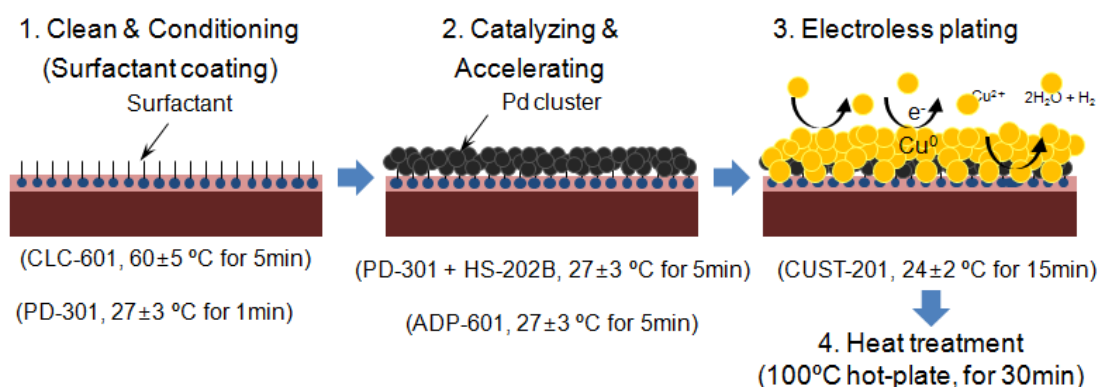
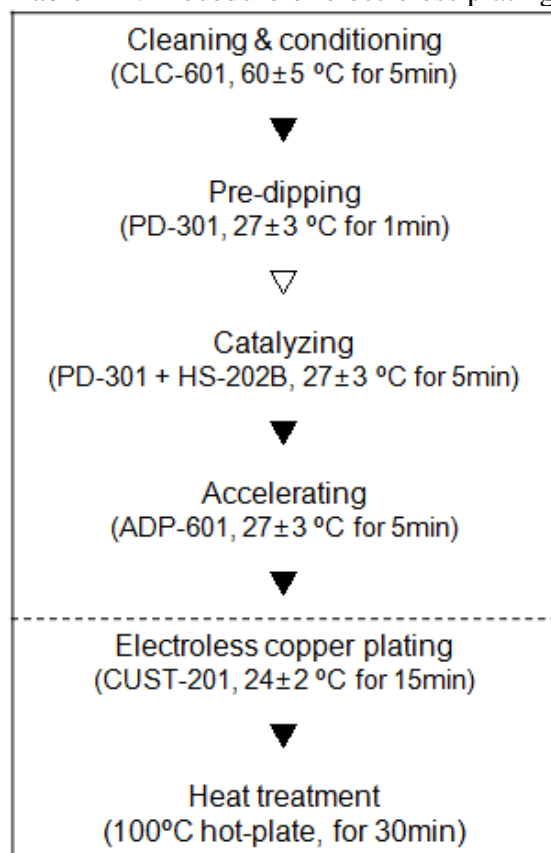


Figure 4-6. Procedure of pre-treatment and electroless copper plating

Cu layer was deposited as shown in Table 4-2. The modified PI substrates were immersed in cleaning & conditioning (CLC-601), pre-dipping (PD-301), catalyzing (PD-301 and HS-202B) and accelerating solutions (ADP-601). All of chemical solutions used in pretreatment process and electroless Cu bath were purchased from Hitachi Chemical Co., Ltd.

Table 4-2. Procedure of electroless plating



▼ : Water rinsing at room temperature for 2 min (X 2)

The composition of electroless Cu plating bath is shown in [Table 4-3](#). Three types of solutions were branded to make the electroless Cu plating bath. The plating solutions were also purchased from Hitachi Chemical Co., Ltd.

Table 4-3. Composition of electroless Cu plating bath

| Composition | | | Concentration |
|------------------|--|---------------|---------------------|
| CUST-A | CuSO ₄ ·5H ₂ O | 10~15 % | 100 ml/L |
| | HCHO | 5~10 % | |
| CUST-B | (HOCHCOO) ₂ KNa·4H ₂ O | 15~25 % | 100 ml/L |
| | NaOH | 5~10 % | |
| | NaCN | 0.01 ~ 0.02 % | |
| CUST-C | (HOCHCOO) ₂ KNa·4H ₂ O | 0.5 ~ 1.5 % | 100 ml/L |
| | NaOH | 0.02 ~0.06 % | |
| | HCHO | 1~3 % | |
| Bath pH. | | | 12.5 |
| Agitation | | | Mechanical stirring |

(Hitachi chemical Co., Ltd)

The electroless plating bath has a pH of around 12.5. Cu layer with 300nm thickness was plated at 24 °C bath temperature for 15 min as shown in Figure 4-7. In addition, the smooth interface between Cu and SBC-PI substrate was observed by the cross section image.

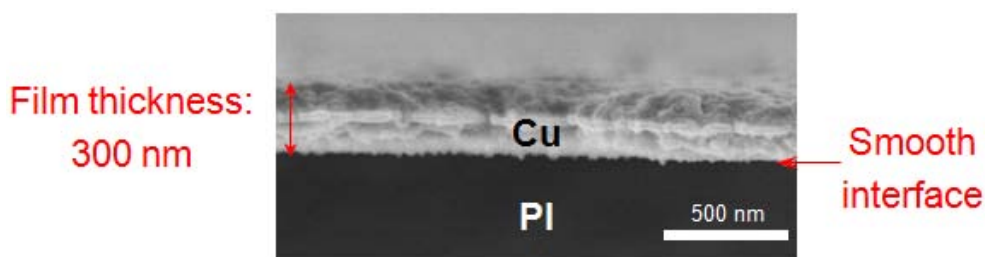
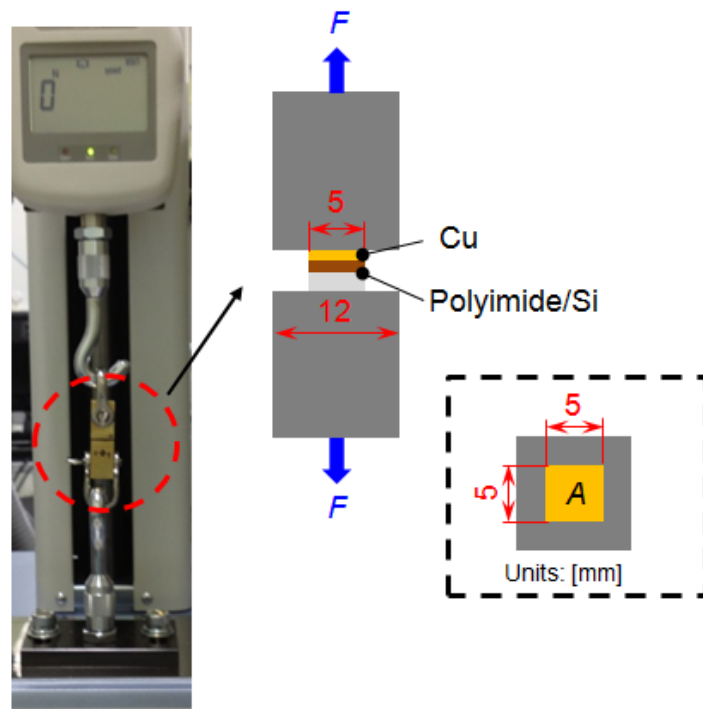


Figure 4-7. Cross-section SEM image of Cu/polyimide

4.3 Adhesion between Cu and modified SBC-PI

The effects of the VUV irradiation surface modification on the adhesion between plated Cu and PI surface were evaluated. The adhesion force was measured by a tensile tester (MX-110, IMADA, Inc) as shown in Figure 4-8. 5 mm square samples were prepared and glued to tensile tester fixture.



Evaluation system for adhesion strength

Figure 4-8. Schematic diagram of adhesion strength test

The adhesion strengths were calculated from following equation.

$$\sigma \text{ (MPa)} = F \text{ (N)} / A \text{ (m}^2\text{)} \dots\dots\dots (4.2)$$

where σ is adhesion strength (MPa), F is tensile force (N) and A is area (m²).

Figure 4-9 shows the adhesion strengths between Cu and PI surface as a function of VUV irradiation dose. Adhesion strength increased after VUV irradiation. This adhesion strength shows a peak at 2400mJ/cm² of VUV dose. With increase of VUV dose, the adhesion strength increased until 2400 mJ/cm² and then decreased. Comparing adhesion strength and surface properties of PI film such as contact angle and roughness, the adhesion strength shows difference trends.

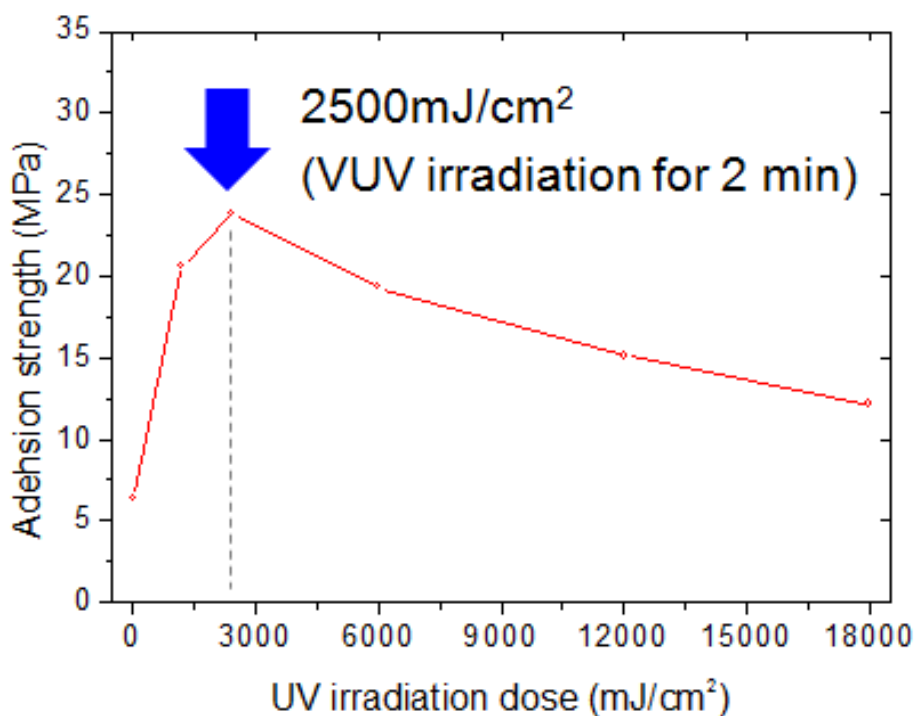
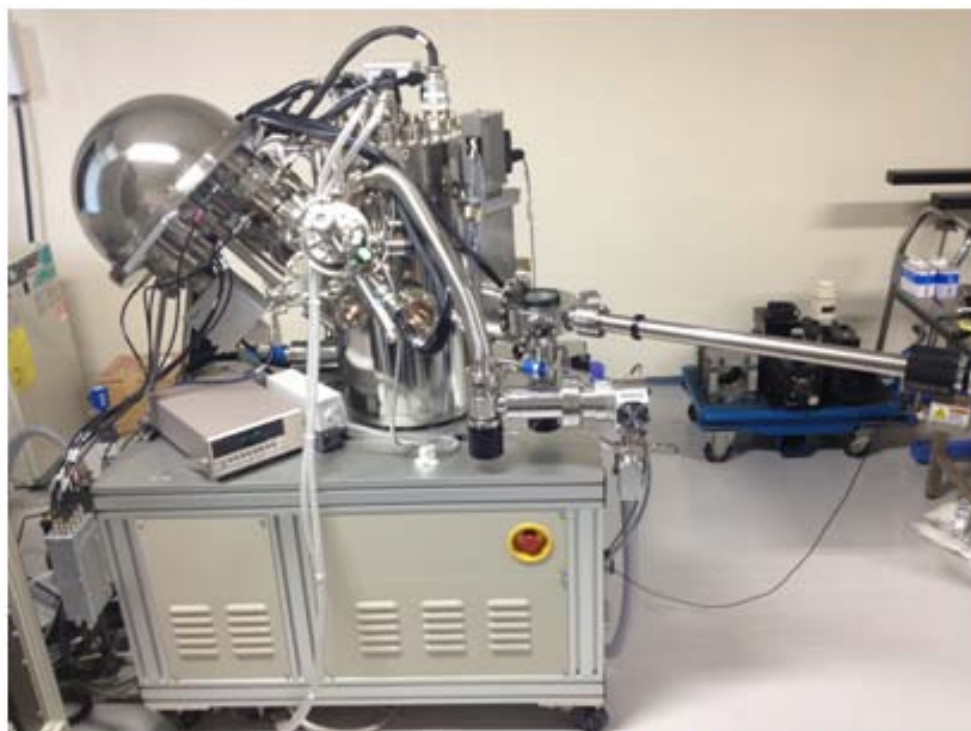


Figure 4-9. Measured adhesion strength Between Cu and SBC-PI

4.4 Analysis of modified SBC-PI surface

The relationship between the chemical state of SBC-PI surfaces and VUV dose conditions was analyzed using a XPS (PHI-5000 VersaProbe™, Physical Electronics, Inc.) shown in [Figure 4-10](#).



PHI 5000 (ULVAC-PHI, Inc.)

Figure 4-10. X-ray photoelectron spectroscopy (XPS) system

[Figure 4-11](#) shows the change of C 1s spectra of the SBC-PI surface in accordance with VUV dose. In all cases, carbon-carbon bond (C-C, binding energy: 284.0-286.0 eV), hydroxyl group (-C-OH, binding energy: 286.4-286.7 eV) and carboxyl group (O=C-OH, binding energy: 288.0-289.4 eV) were detected. With the increase of VUV dose, the photoemission intensity of the C-C bond decreased whereas that of the hydroxyl group and carboxyl group increased. From this result, it could be found that wettability switching of SBC-PI from hydrophobic to hydrophilic is resulted from the

increase of hydrophilic groups (e.g., hydroxyl and carboxyl groups) by VUV irradiation.

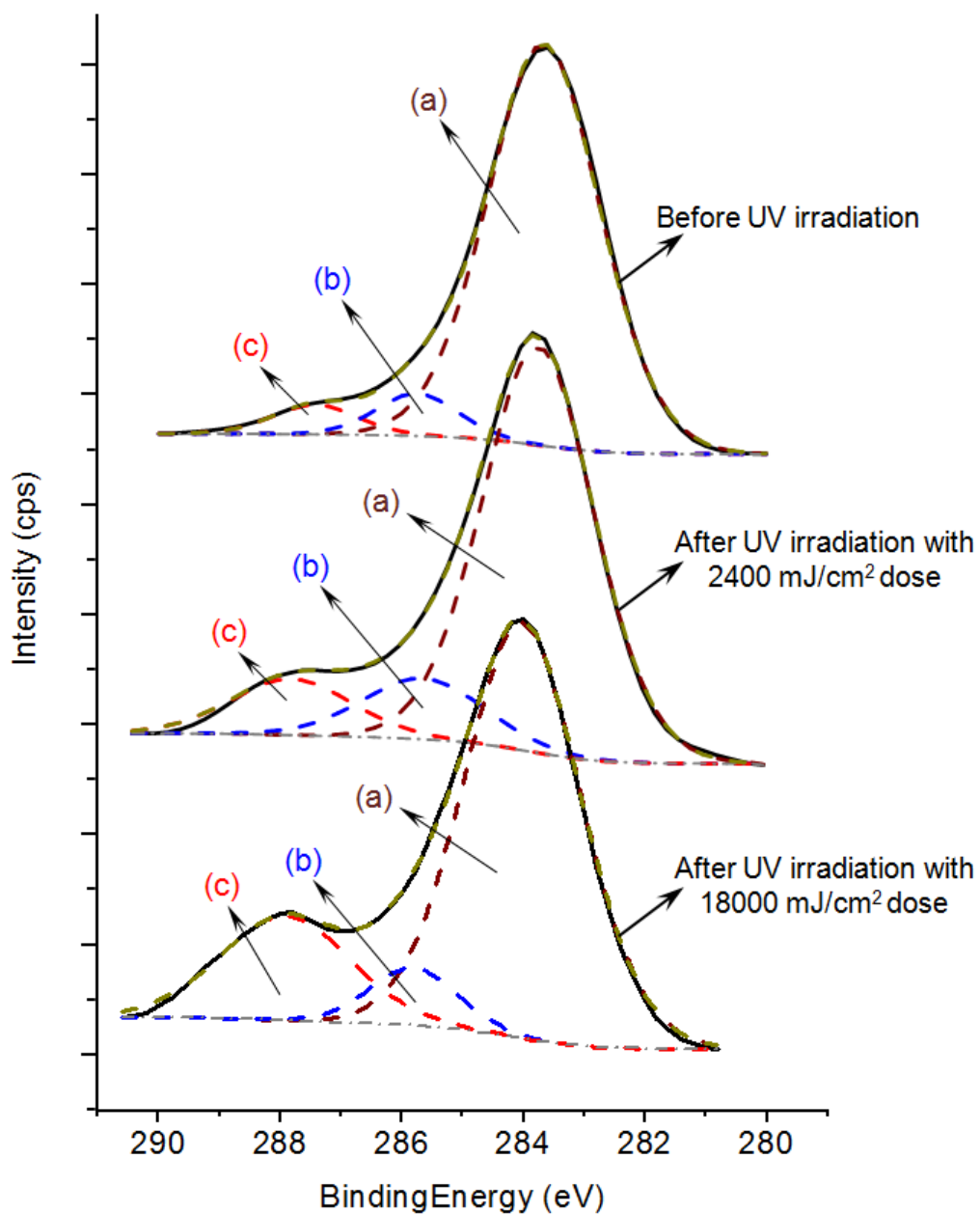


Figure 4-11. XPS spectra graphs of SBC-PI surface

Table 4-4. Binding energy of each bond groups

| Bond Group | Binding Energy (eV) |
|------------|---------------------|
| C-C (sp1) | 284.0 – 286.0 |
| Hydroxyl | 286.4 - 286.7 |
| Carboxyl | 288.0 - 289.4 |

Figure 4-12 summarizes wide scan XPS spectra which evaluate the composition of C, O, Si, and N. The detection of Si 2p seems to be resulted from an inclusion of Si particles generated during cutting SBC-PI/Si substrate. With increasing UV dose, the atomic concentration of O 1s increased gradually, whereas the atomic concentration of C 1s decreased. The increase of atomic concentration of O 1s indicates that C-C bond was replaced by oxygen double bond as a result from ozonolysis reaction of ozone (O₃) or active-oxygen (O*) generated by UV-irradiation. The N 1s and Si 2p did not change regardless of the increase of UV irradiation dose.

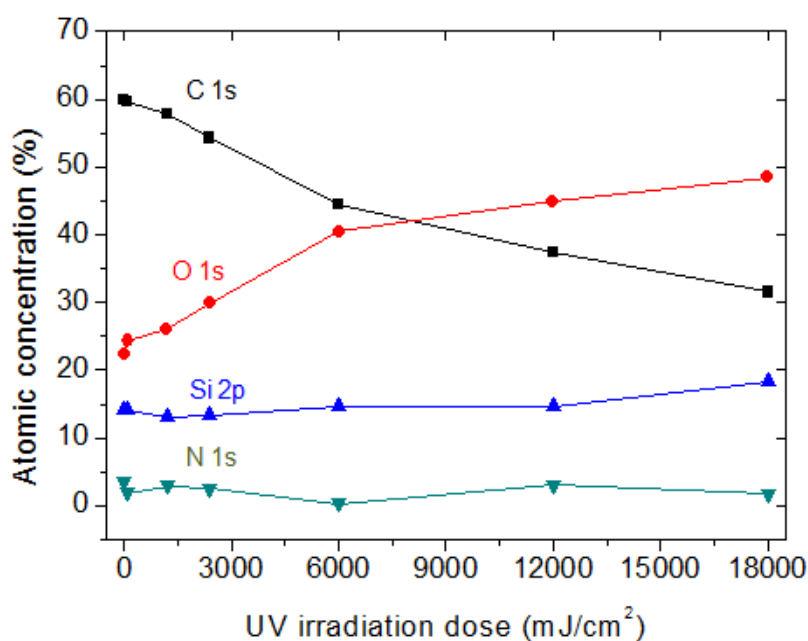


Figure 4-12. Atomic concentrations of modified PI surface

Figure 4-13 shows the chemical structure of SBC before and after VUV irradiation. Methyl group in methyl hydrogen siloxane block was modified to hydroxyl or carboxyl group by VUV and active oxygen generated by ozone decomposition caused by VUV irradiation. From this result, it could be found that modification of PI surface from hydrophobic to hydrophilic are resulted from the increase of hydrophilic groups such as hydroxyl and carboxyl groups by UV irradiation.

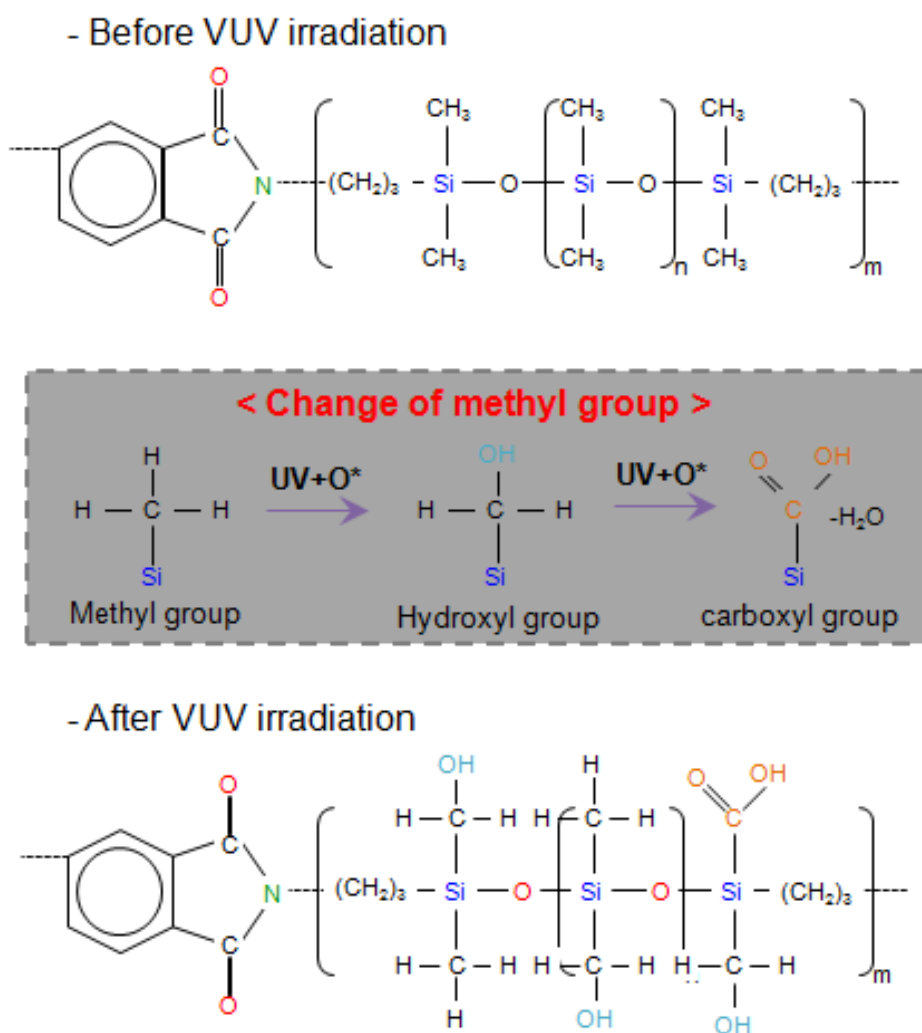


Figure 4-13. Chemical structure of PI surface

Figure 4-14 shows concentration of the carboxyl and hydroxyl group as a function of VUV irradiation dose. In case of carboxyl group, concentration increased along with increase of VUV irradiation dose. However, concentration of hydroxyl group increased until 2400 mJ/cm² of VUV irradiation dose and decreased by more VUV irradiation dose. The concentration of hydroxyl group shows significantly similar trends with the adhesion strength. These similar trends of hydroxyl group concentration and adhesion strength suggest that the hydroxyl groups play an important role in enhancing adhesion strength between plated Cu and PI surface

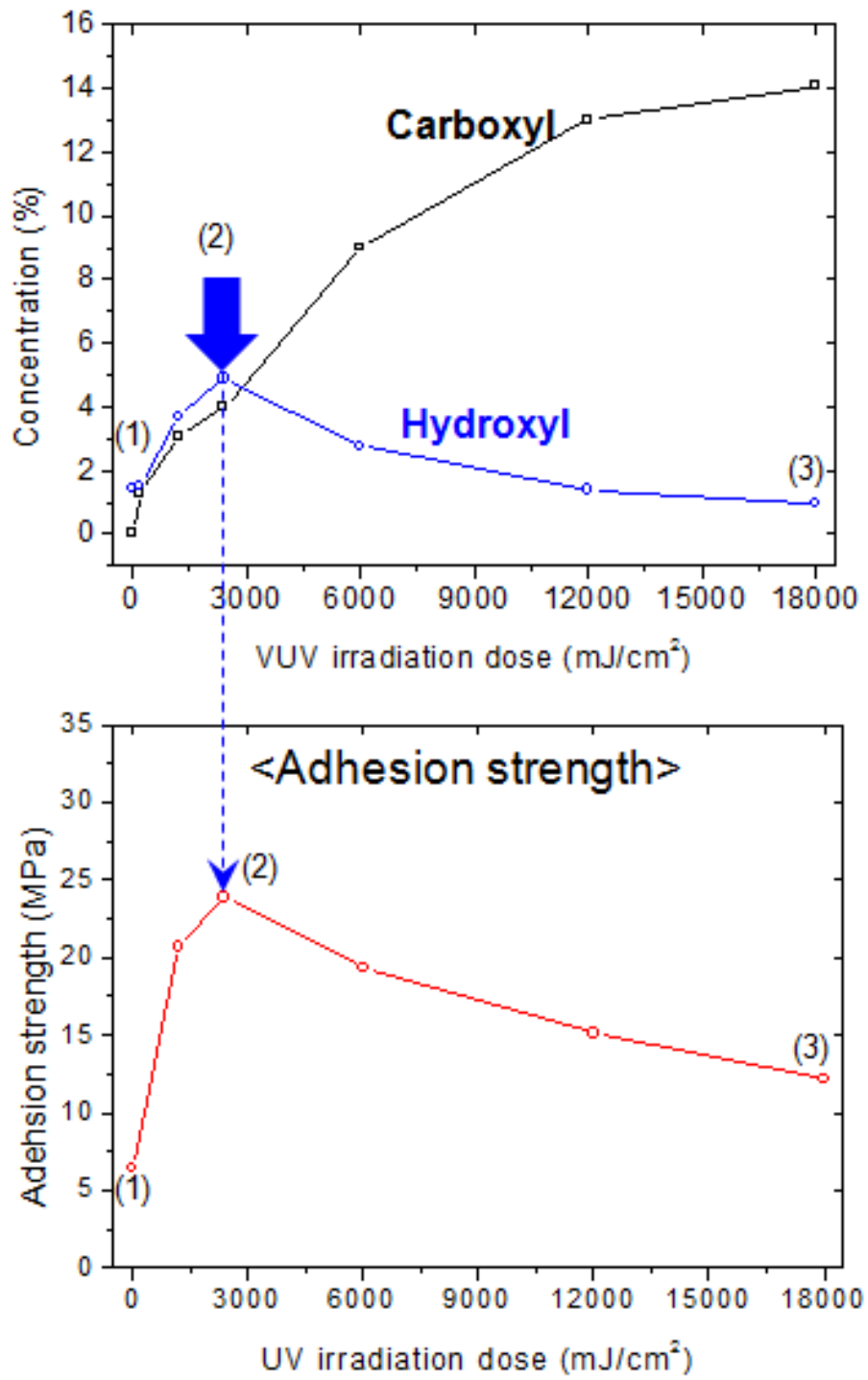


Figure 4-14. Concentration of Carboxyl and hydroxyl group and its relation with the Cu-PI adhesion strength.

Figure 4-15 schematically shows concentration change of the carboxyl and hydroxyl groups with increase of VUV irradiation. The concentration of carboxyl group was increased with increase of VUV irradiation dose. However, the concentration of hydroxyl group just increased until 2400 mJ/cm² VUV irradiation dose and decreased by the dose over 2400 mJ/cm².

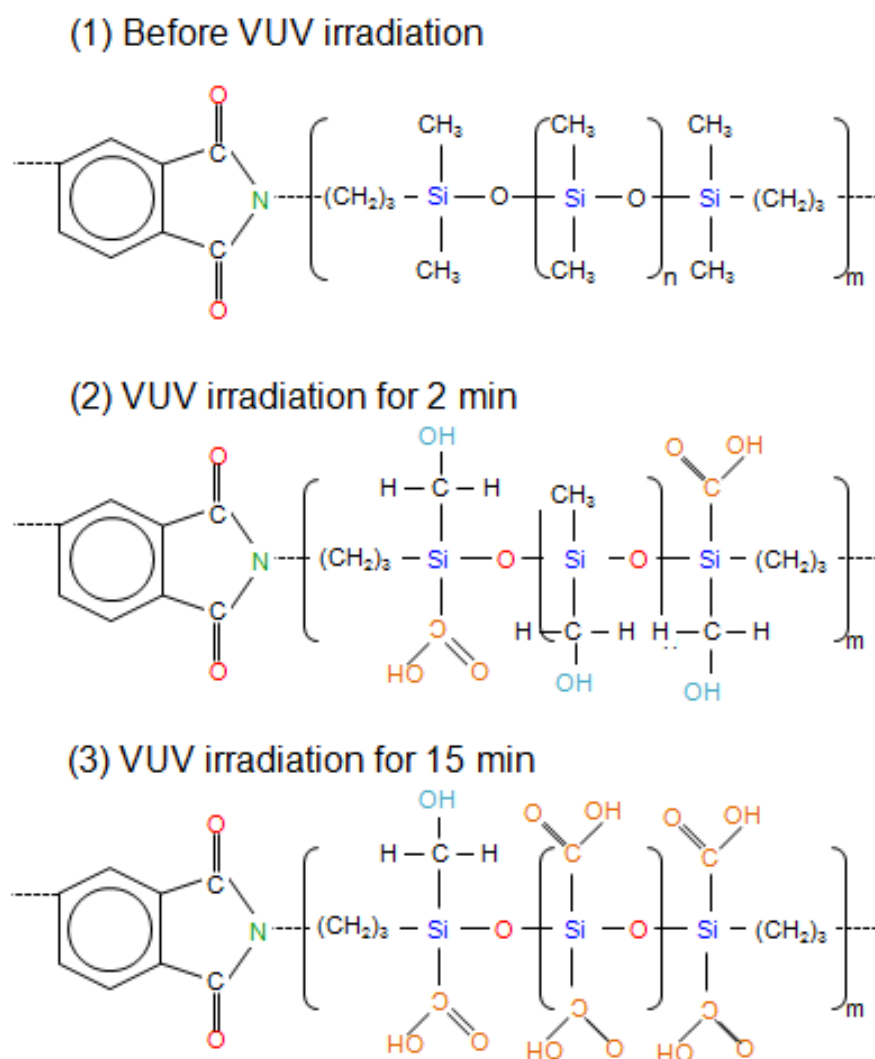


Figure 4-15. Chemical structure of SBC-PI surface

4.5 Summary

The changes of topological and chemical properties of SBC-PI by UV irradiation were investigated.

- XPS analysis revealed that the chemical properties of SBC-PI surface showed strong dependence on UV dose. With the increase of UV dose, wettability of SBC-PI surface switched from hydrophobic to hydrophilic as a result from the increase of hydrophilic groups by ozonolysis reaction.

- Contrarily, DFM measurement showed that roughening effect by the UV irradiation was negligible.

- Adhesion between Cu and PI on modified SBC-PI film was enhanced. The adhesion strength had peak value at the VUV dose of 2400 mJ/cm^2 . From this result and XPS analysis, it is supposed that hydroxyl groups on the PI surface play an important role in enhancement of adhesion strength

Chapter 5

Selective electroless Cu plating by VUV Induced Surfactant Masking (VISM)

- 5.1 Application of *Honma method* to selective fabrication of Cu interconnection on SBC-PI
- 5.2 Selective electroless Cu plating by VISM
 - 5.2.1 Mechanism of organic removal by VUV
 - 5.2.2 Application of VISM to electroless Cu plating
 - 5.2.3 Electric resistivity of fabricated interconnection
- 5.3 Selective electroless Cu plating in imprinted PI pattern
 - 5.3.1 Application of THUI and VSIM to fabrication process of Cu/PI interconnection
 - 5.3.2 Fabricated Cu interconnection in PI pattern
- 5.4 Summary

5.1 Application of the *Honma method* to selective fabrication of Cu interconnection on SBC-PI

Application of selective electroless Cu plating process described in section 2.2.3 (the Honma method) to SBC-PI surface is shown in Figure 5-1. The electroless Cu plating was carried out using the selectively modified SBC-PI film by VUV irradiation. The fabricated stencil mask was put on the cured SCB-PI film, and VUV light was irradiated at distance 10 cm from LP Hg lamp for 15 min (6750 mJ/cm² dose). Then pre-treatment processes were performed. Commercially available solutions described in section 4.2 (purchased from Hitachi chemical Co., Ltd.) were used for pre-treatment and electroless Cu plating. The pre-treatment process for electroless Cu plating consisted of four sub-processes including a) cleaning and conditioning, b) pre-dipping, c) catalyzing, and d) accelerating. Electroless Cu plating experiments were performed using a pre-treated SCB-PI film in electroless Cu plating bath for 15 min. After electroless Cu plating, the sample was heated using a hot-plate at 100°C for 30 min.

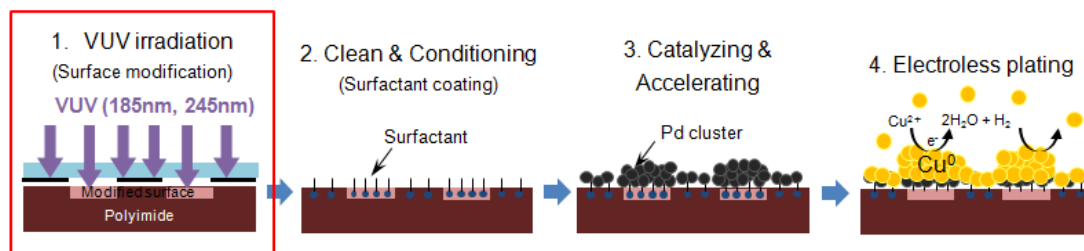


Figure 5-1. Selective electroless copper plating process on SBC-PI surface by the Honma method

In order to irradiate UV light to selective area of SCB-PI film, a five-inch sized Ni stencil mask that having the line and square patterns with different sizes (from 10 to

1000 μm) was fabricated as shown in Figure 5-2. The fabrication process of Ni stencil mask is as follows. After photolithography of resist on stainless steel substrate, 10 μm thick Ni layer was deposited on the developed photoresist by Ni electroplating. After attaching supports, the plated Ni layer (Ni stencil mask) was removed from stainless steel substrate.

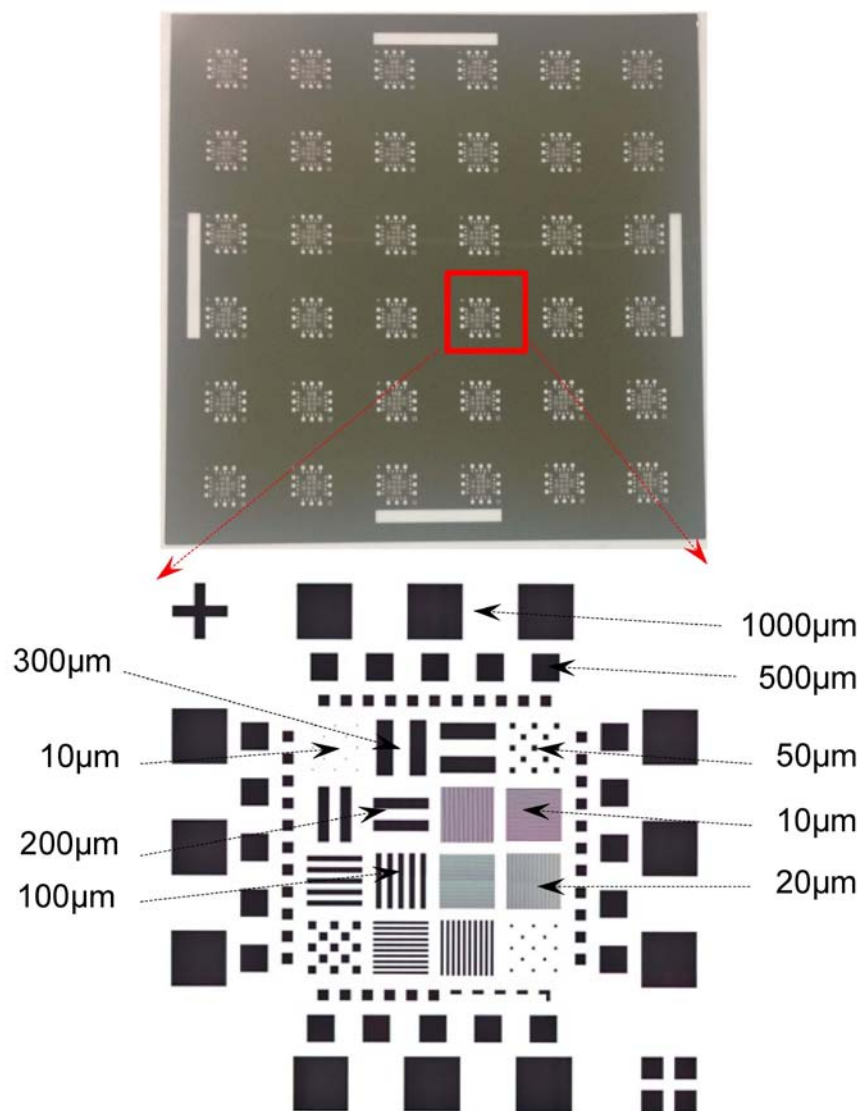


Figure 5-2. Ni stencil mask

Figure 5-3 shows the results of fabricated Cu layer on SBC-PI by the Honma method. The surfaces of achieved Cu layers were evaluated using a DFM. The electroless Cu plating experiments were carried out using the selectively modified SBC-PI film to evaluate the possibility of application of selective surface modification to selective electroless Cu plating. Figure 5-3 shows the photograph and DFM topological measurement data of Cu patterns (50 μ m line and spacing) plated on selectively modified SBC-PI surface. Electroless Cu plating was performed for 15 min with the Cu deposition rate of 20 nm/min. It was observed that a thicker Cu was deposited on the SBC-PI surface modified by UV-irradiation as compared with an un-irradiated PI surface. Cu deposited on the modified SBC-PI was thicker. It is supposed that more reducing agent (i.e. Pd) was absorbed to modified SBC-PI hydrophilic surface during pre-treatment for Cu plating. However, selectivity was not enough in case of SBC-PI by the Honma method electroless plating.

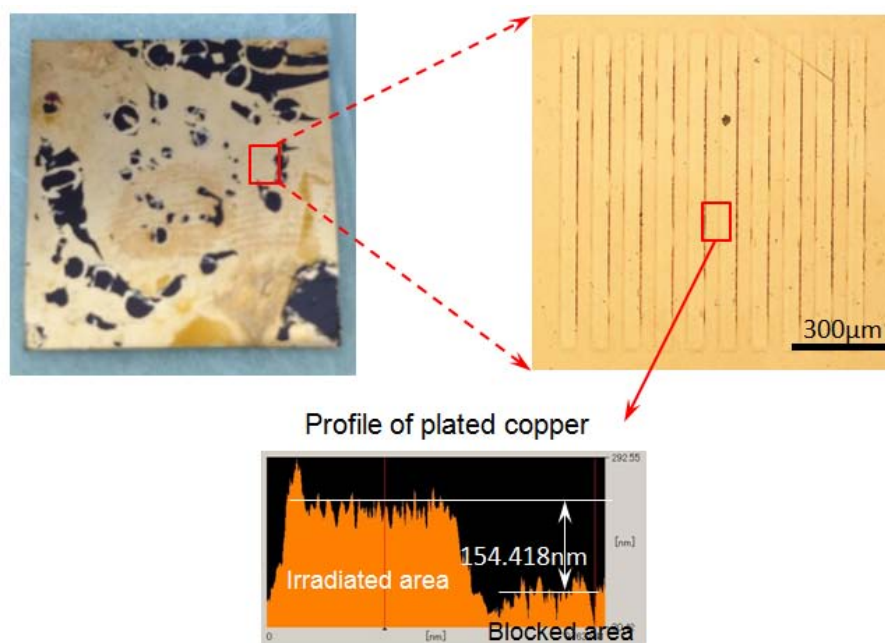


Figure 5-3. Fabricated copper layer on SBC-PI surface by the Honma method

5.2 Selective electroless Cu plating by VISM

5.2.1 Mechanism of organic removal by VUV induced

The mechanism of organic removal by VUV irradiation is shown in Figure 5-4. The organic removal technology by VUV irradiation has been used to clean glass in fabrication process of liquid crystal display (LCD). Ozone is generated by 185nm wavelength VUV light. Then generated ozone gas is decomposed into oxygen and active oxygen atom by 254nm wavelength VUV light. Finally, the active oxygen atoms oxidize organics on substrate to form CO₂ or H₂O.

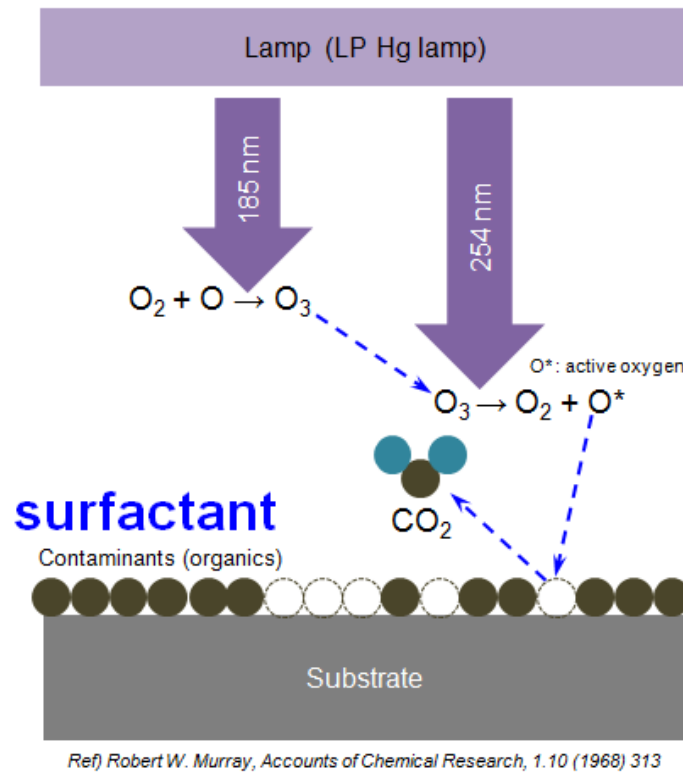


Figure 5-4. Mechanism of VUV induced organics removal

In order to fabricate photomask mask, VUV transmittance of a soda-lime glass with 0.5 mm thickness and quartz glass with 0.5mm and 1mm thickness was evaluated. Figure 5-5 shows the UV transmittance results. The soda-lime glass blocked the all UV light with 184.9 nm and 253.7 nm wavelength. However, both 184.9 nm and 253.7nm VUV light passed the Quartz glass with 0.5 mm and 1 mm thickness. According to this transmittance results, The Cr/glass mask was fabricated using quartz glass with 1 mm thickness.

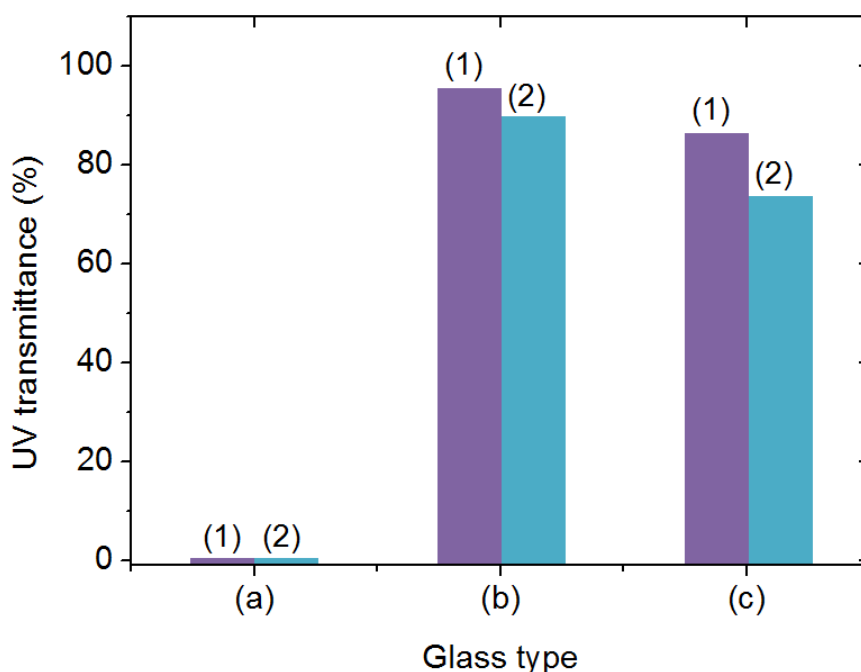


Figure 5-5. Transmittance of VUV light with wavelength of (1) 184.9 nm and (2) 253.7 nm through soda-lime glass (a) and quartz glass with 0.5 mm (b) and 1 mm (c) thickness

Surface contact angles were measured after surfactant absorption on modified SBC-PI surface under various VUV dose as described in Chapter 4. The PI film modified to hydrophilic surface (in Figure 5-6(a)) was changed to hydrophobic

surface as shown in Figure 5-6(b). The surfactant consists of head of hydrophilic and tail part of hydrophobic. The head part of surfactant is absorbed on hydrophilic surface of PI film (in Figure 5-6(2)) and the hydrophobic tail part of surfactant forms the new surface (in Figure 5-6(3)). Especially, the contact angle of PI surface coated by surfactant was not changed remarkably with VUV irradiation dose of more than 2400 mJ/cm². Therefore, measured contact angle is property of new surface formed by tail part of surfactant. Additionally, it means that PI surface was fully coated by the surfactant with VUV irradiation dose more than 2400 mJ/cm².

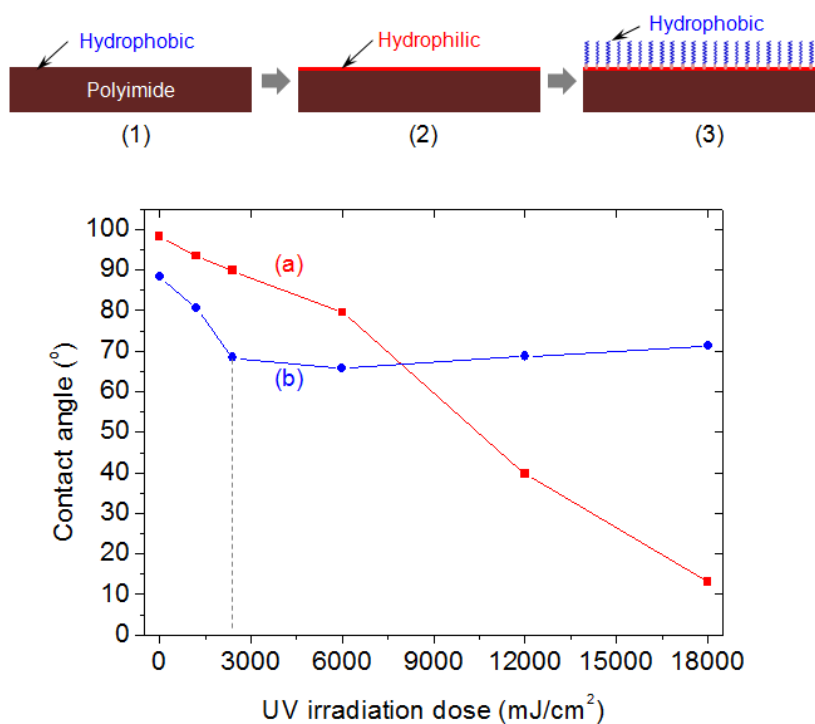


Figure 5-6. Surface contact angle of SBC-PI film with increase of UV irradiation dose; (a) just after VUV surface modification and (b) after surfactant absorption on the VUV modified surface, and schematic diagram of surface state of (1) original PI film, (2) modified PI film and (3) absorbed surfactant

The fully coated surfactant was removed by UV/Ozone treatment. For evaluating surfactant removal by UV/Ozone treatment, quartz glass with 1 mm thickness was put on the PI film coated by surfactant and then UV/Ozone treatment was performed.

Figure 5-7 shows the changes of contact angle after UV/Ozone treatment. . A peak of contact angle was observed at UV/Ozone treatment time of 10 min. The contact angle increased for first 10 min of UV/Ozone treatment as shown in Figure 5-7(a). It was supposed that surfactant layer was removed by UV/Ozone treatment for 10 min. The contact angle decreased by UV/Ozone treatment more than 10 min as shown in Figure 5-7(b). It means that the surfactant layer was completely removed and modification of PI surface was started by VUV irradiation as shown in Figure 5-8.

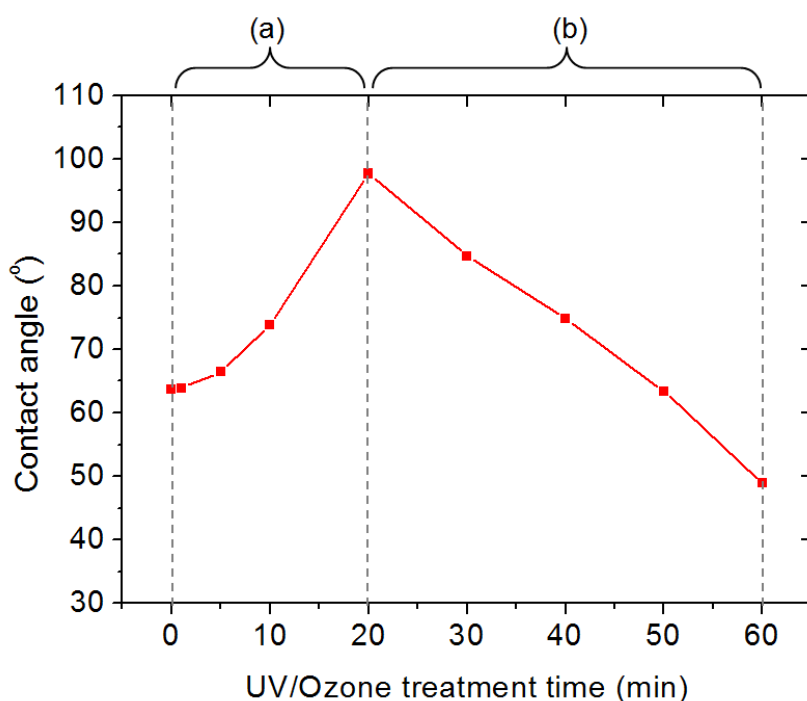


Figure 5-7. Surface contact angle of surfactant absorbed SBC-PI with increase of UV/Ozone treatment time; (a) removing section of surfactant and (b) surface modification section of PI substrate

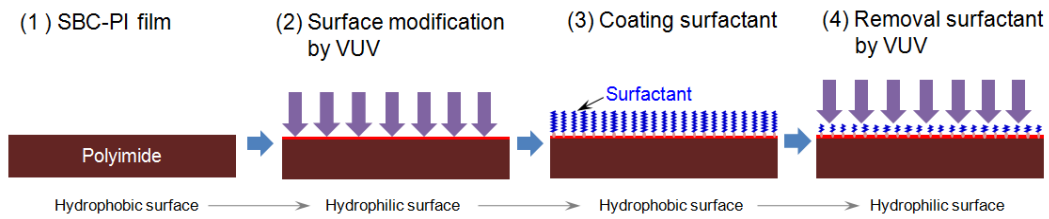


Figure 5-8. Schematics diagram of Surfactant coating and removal

5.2.2 Application of VISM to electroless Cu plating

The VUV induced Surfactant Masking (VISM) process was proposed to simplify copper metallization using electroless copper plating as shown in Figure 5-9. First, fabricated SBC-PI substrates were modified by VUV irradiation of 2400 mJ/cm^2 dose. Surfactant was absorbed on the modified PI samples by immersion in the conditioning & cleaning solution of $60 \text{ }^\circ\text{C}$ for 5min. Then Ni stencil mask was put on the PI samples with absorbed surfactant in surface modification system. The Ni stencil mask and PI substrate was below 10 cm from LP Hg lamp. The absorbed surfactant layer on PI substrate was selectively removed by UV/Ozone treatment where VUV light passed through Ni stencil mask. During the treatment, the ozone level of approximately 15 ppm was measured in surface modification system by ozone sensor (A-21ZX, KWJ Engineering Inc.). Then Pd was stuck on the surfactants of unremoved site as a reducer for Cu ions in plating bath by the catalyzing and accelerating treatment process. Finally, Cu was deposited on the partially stuck Pd layer in the electroless plating bath of $24 \text{ }^\circ\text{C}$ with pH 12.5 for 15 min.

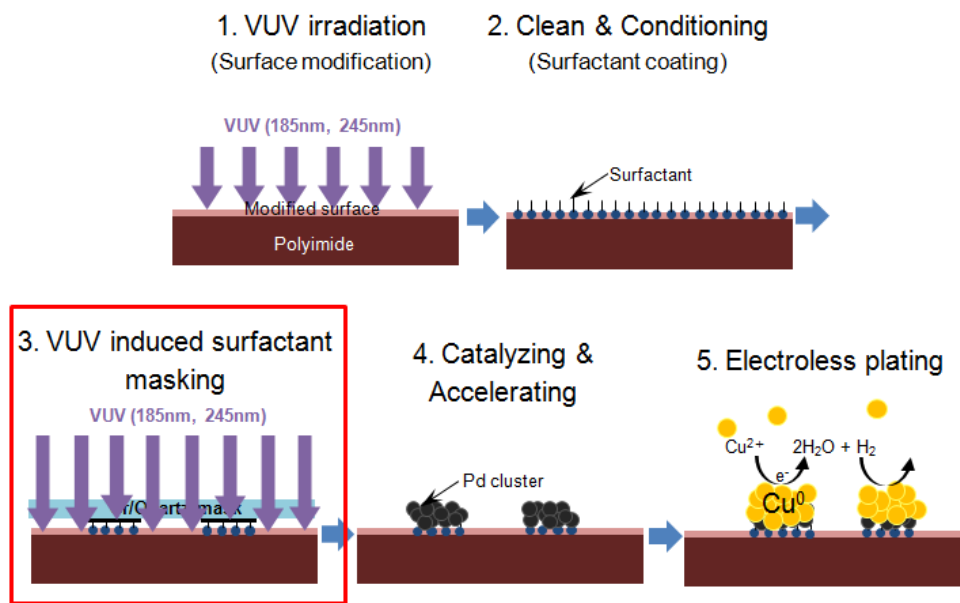


Figure 5-9. Selective electroless Cu plating process using VUV induced surfactant masking

Figure 5-10 shows the fabricated Cu/PI patterns by proposed new selective electroless Cu plating using VISM. Surfactant was selectively removed by VUV irradiation. The 5 μm line and space Cu patterns were simply fabricated on PI film by proposed VUV induced surfactant masking process.

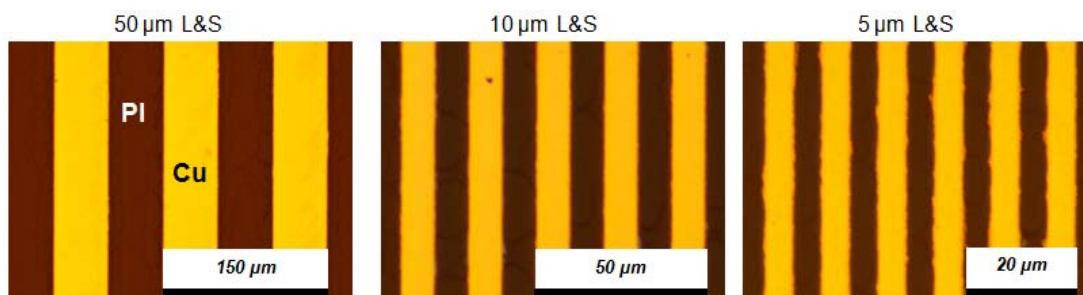


Figure 5-10. Selectively deposited Cu/PI patterns

5.2.3 Electric resistivity of fabricated interconnection

Electrical property of fabricated Cu interconnections was evaluated by four probe method using semiconductor parameter analyzer (Agilent 4155c, Agilent technologies, Inc.) as shown in [Figure 5-11](#).

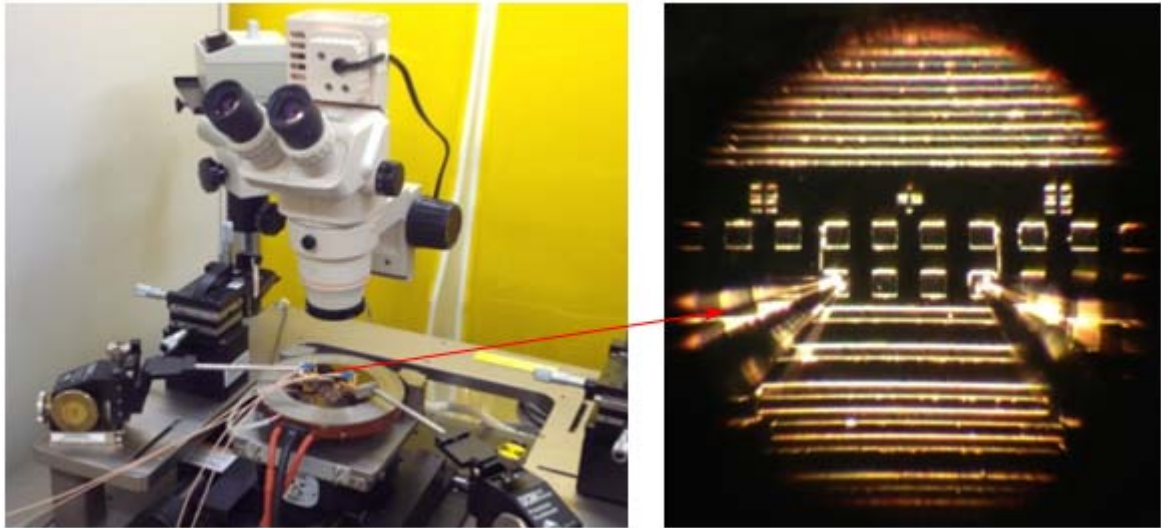


Figure 5-11. Electric resistance measuring system

For analyzing the electric properties of fabricated Cu/PI interconnection, the Cu/PI interconnections with $50\ \mu\text{m}$ line width and 1.2 mm, 3.6mm, 6.0 mm, 8.4 mm and 10.8 mm lengths were fabricated as shown in [Figure 5-12](#). The fabricated Cu/PI interconnection was observed without disconnection or short-circuit.

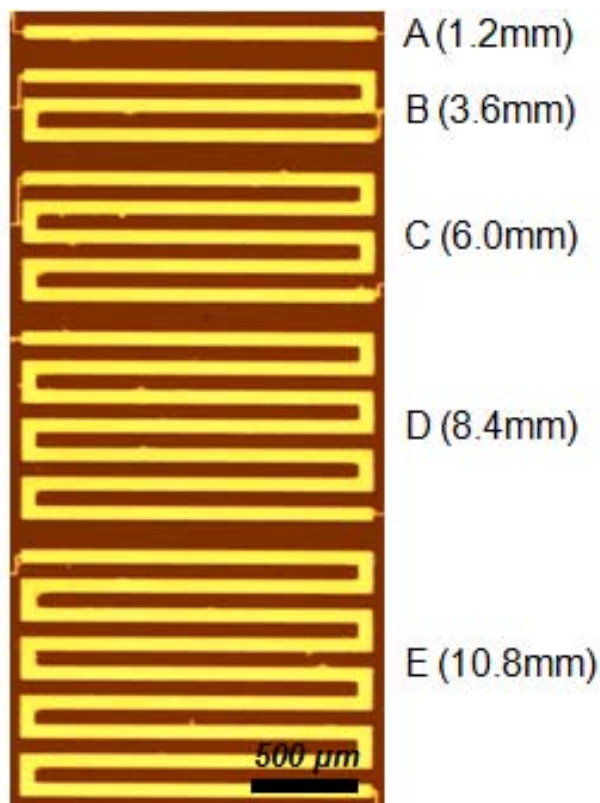


Figure 5-12. Selectively fabricated Cu/PI interconnection using VUV induced surfactant masking

The electric resistance of the fabricated Cu interconnections with 300 nm thickness was measured without disconnection defect as shown in [Figure 5-8](#). The resistance increased linearly with increase of interconnection length. The resistivity of the fabricated Cu interconnections was calculated to $2.00 \times 10^{-8} \Omega \cdot \text{m}$. Comparing with pure Cu with resistivity of $1.68 \times 10^{-8} \Omega \cdot \text{m}$, Cu interconnections with satisfactory resistivity was fabricated by proposed selective electroless Cu plating using UV/Ozone treatment.

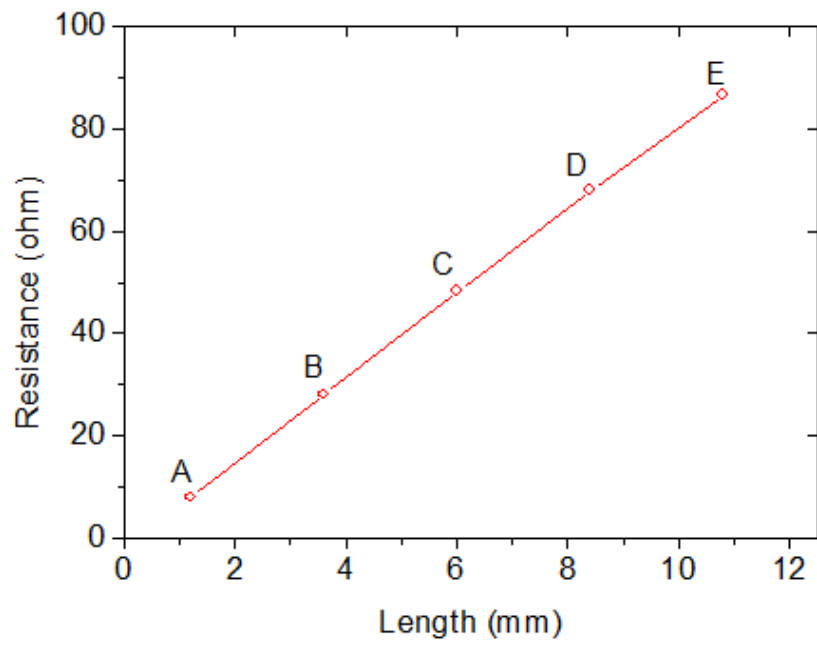


Figure 5-13. Measured electric resistance

5.3 Selective electroless Cu plating in imprinted PI pattern

5.3.1 Application of THUI and VSIM to fabrication process of Cu/PI interconnection

Figure 5-14 shows the pretreatment processes and the selective Cu plating process using UV/Ozone treatment in imprinted PI patterns. In order to modify the fabricated PI substrate with fine patterns, the fabricated PI substrates were irradiated below 10 cm distance from LP Hg lamp for a range of 60 to 900 sec. The surfactant layer was absorbed in cleaning & conditioning process. The absorbed surfactant on PI substrate was selectively removed by UV/Ozone treatment using Cr/quartz mask. Then Pd was absorbed on the unremoved surfactant layers as a reducer for Cu ions in plating bath by immersing in the pre-dipping, catalyzing and accelerating solutions. Finally, Cu was deposited on the partially absorbed Pd layer in the electroless plating bath of 24 °C with pH 12.5 for 15 min.

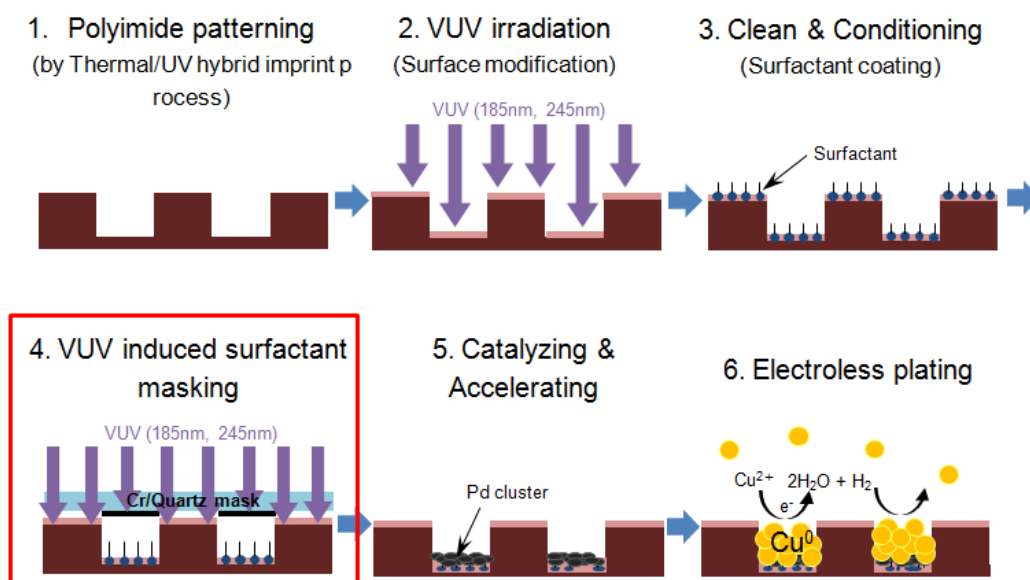


Figure 5-14. Selectively fabricated Cu interconnection in imprinted PI patterns

5.3.2 Fabricated Cu interconnection in PI pattern

Selective electroless Cu plating using UV/Ozone treatment was performed as shown in [Figure 5-15](#). The line and space patterns with ranging from 5 μm to 50 μm width and 300 nm thickness were simply fabricated without photoresist patterning process. The microscope images of fabricated Cu patterns are in [Figure 5-15](#).

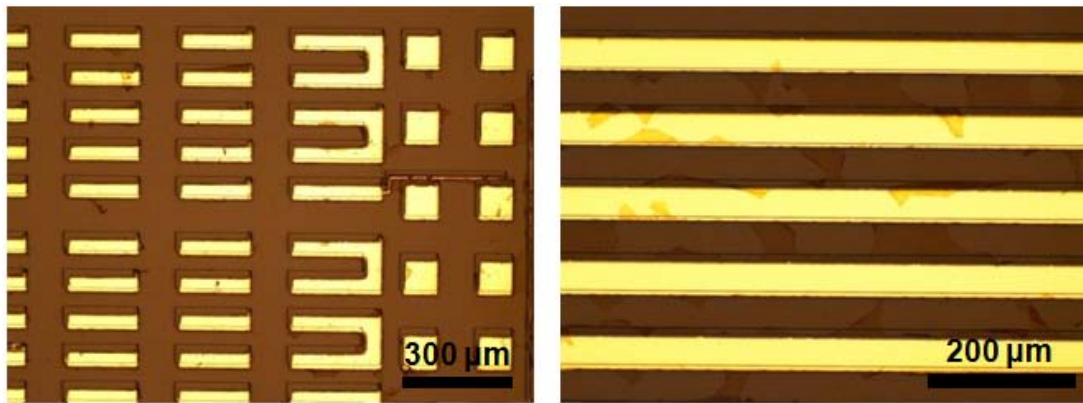


Figure 5-15. Selectively fabricated Cu interconnection in imprinted PI patterns

5.4 Summary

VUV induced Surfactant Masking (VISM) process was proposed to simplify copper metallization using electroless copper plating.

- Surfactant for Cu electroless plating was selectively patterned by VUV irradiation masking technology.

- 5 μm line and space Cu patterns were simply fabricated by the developed selective electroless plating method.

- Cu interconnections with good resistivity of $2.00 \times 10^{-8} \Omega \cdot \text{m}$ were fabricated.

- Cu interconnections were selectively plated in imprinted fine PI patterns.

- Fabrication of Cu/PI interconnection was demonstrated by Thermal/UV Hybrid Imprint (TUHI) and VUV Induced Surfactant Masking (VISM).

Chapter 6

Conclusion

This thesis proposed thermal/ultraviolet (UV) hybrid imprint and selective electroless copper plating using vacuum ultraviolet (VUV) induced surfactant masking concepts to simplify fabrication process of high density interconnection (HDI) interposer.

1) Thermal/UV Hybrid imprint (TUHI) using SBC-PI was developed for high precision and low temperature patterning process for PI.

- Thermal reflow of imprinted SBC-PI pattern was prevented by optimizing process parameters such as imprint temperature, UV dose, and temperature profile of curing including holding at 100 °C for several minutes, which corresponds to pose exposure bake for photosensitive SBC-PI. Pattern height shrinkage ratio of 70% decreased to 4%. These experimental results demonstrates that cross linking reaction of photosensitive agent plays an important role to prevent thermal reflow of SBC-PI and achieve precise imprint replication.

- 3 μm line and spacing patterns with accurate rectangular cross section profile and clear line edge were successfully fabricated by the developed process. The minimum patterns of 150 nm line-width were also realized.

2) Adhesion between Cu and SBC-PI was enhanced by VUV irradiation surface modification.

- Hydrophobic surface of PI was modified to hydrophilic without increase of surface roughness by VUV irradiation. The good surface roughness is favorable to achieve interconnections with good electric properties.

- Generating hydrophilic group such as hydroxyl and carboxyl group was confirmed by XPS data analysis.

- Concentration of hydroxyl group and adhesion strength show similar trends. It demonstrates that hydroxyl groups on the surface play an important role in adhesion between electroless plated Cu and SBC-PI substrate.
- 3) Selective electroless Cu plating using VISM was proposed. It enables a simple interconnections formation process without photoresist patterning steps.
- A surfactant layer absorbed on modified hydrophilic PI surface was selectively removed by VISM using Ni stencil mask or Cr/quartz mask.
 - Cu patterns with line and space from 5 μm to 50 μm were successfully fabricated by proposed selective electroless Cu plating using VISM.
 - The electric resistance of the fabricated Cu interconnections with line width of 50 μm was measured. The resistivity was calculated to $2.00 \times 10^{-8} \Omega \cdot \text{m}$. The resistivity is similar to that of pure copper.
 - Feasibility of proposed selective Cu plating using VISM was verified by fabricating Cu interconnection in PI patterns prepared by TUHI.

Reference

1. D. J. Liaw, K. L. Wang, Y. C. Huang, K. R. Lee, J. Y. Lai, C. S. Ha, *Polym. Sci.*, 37 (2012) 907
2. J. LaDou., *Int. J. Hyg. Environ Health*, 209 (2006) 211
3. V. Beyer, F. Kuchenmeister, M. Bottcher, and E. Meusel: *Adhe. Coat. Tech. Electro. Manufac. Confer. Proc* (1998) 28
4. C. K. Hu, B. Lutter, F. B. Kaufman, J. Hummel, C. Uzoh, D. J. Pearson, *Thin solid films* 262 (1995) 84
5. J. J. Miniet and F. L. Fla: U.S. Patent 4677528 (1987).
6. J. Engel, J. Chen, and C. Liu: *J. Micromech. Microeng.* 13 (2003) 359.
7. M. B. Pisani, C. Hibert, D. Bouvet, P. Beaud, and A. M. Ionescu: *Microelectron. Eng.* 73 (2004) 359.
8. K. N. Tu: *J. Appl. Phys.* 94 (2003) 5451.
9. V. Beyer, F. Kuchenmeister, M. Bottcher, and E. Meusel: *Adhe. Coat. Tech. Electro. Manufac. Confer. Proc* (1998) 28.
10. P. C. Andricacos: *Electrochem. Soc. Interface* (1999) 32.
11. R. B. Booth, R. H. Gephard, B. S. Gremban, J. E. Poetzinger, and D. T. Shen: U.S. Patent 5404044 (1995).
12. P. Ramm, A. Klumpp, R. Merkel, J. Weber, R. Wieland, A. B. Frazier, and M. G. Allen: *Mater. Res. Soc. Symp. Proc.* 776 (2003) E5.6.1.
13. Khandros, Igor Y., and Thomas H. DiStefano. "Semiconductor chip assemblies having interposer and flexible lead." U.S. Patent No. 5,148,266. 15 Sep. 1992.
14. Liang, Louis, Sang S. Lee, and Young I. Kwon. "Integrated circuit package having an interposer." U.S. Patent No. 5,332,864. 26 Jul. 1994.
15. T. C. Chai, X. Zhang, J. H. Lau, C. S. Selvanayagam, and etc., *J. Trans. Compon. Packag. Manufac. Tech.* 1 (2011) 660-672
16. G. Kumar, T. Bandyopdhyay, V. Sukumaran, V. Sundaram, S. K. Lim and R. Tummala, *Proceeding, Electro. Compon. Tech. Conference.* (2011) 217-223
20. Pasch, Nicholas F. "Process for interconnecting conductive substrates using an interposer having conductive plastic filled vias." U.S. Patent No. 5,468,681. 21 Nov. 1995.
21. J. H. Brannon and J. R. Lankard: U.S. Patent 4508749 (1985).
22. Y. W. Wang, C. T. Yen, and W. C. Chen: *Polymer* 46 (2005) 6959.

23. A. B. Frazier and M. G. Allen: *J. Microelectomech. Syst.* (1992) 87.
24. P. C. Andricacos, A. B. Frazier, and M. G. Allen: *IBM J. Res. Dev.* 42 (1998) 567.
25. V. Beyer, F. Kuchenmeister, M. Bottcher, and E. Meusel: *Adhe. Coat. Tech. Electro. Manufac. Confer. Proc* (1998) 28
26. C. K. Hu, B. Lutter, F. B. Kaufman, J. Hummel, C. Uzoh, D. J. Pearson, *Thin solid films* 262 (1995) 84
27. J. R. Haller: U.S. Patent 3502762 (1970).
28. T. Nishino, M. Kotera, N. Inayoshi, N. Miki, and K. Nakamae: *Polymer* 41 (2000) 6913.
29. S. H. Lee and Y. C. Bae: *Macromol. Theory Simul.* 9 (2000) 281.
30. U. Kang and K. D. Wise: *IEEE Trans. Electron Devices* 47 (2000) 702.
31. H. Matsutani, T. Hattori, M. Ohe, T. Ueno, R. L. Hubbard, and Z. Fathi: *J. Photopolym. Sci. Technol.* 18 (2005) 327.
32. J. H. Jou and P. T. Huang: *Macromolecules* 24 (1991) 3796.
33. M. Hasegawa, H. Arai, I. Mita, and R. Yokota: *Polym. J.* 22 (1990) 875.
34. R. Pfaendner, U.S. Patent 5116920 (1992)
35. M. S. Win, T. Goshima, E. Kyo, S. Nakajima, N. Hayahsi, T. Kashiwagi, K. Miyazaki, K. Yamada, N. Yamabayashi, S. Nakagama, H. Okuyama, F. Kasabo, and I. Tanaka: U.S. Patent 0127077 (2011)
36. S. C. Park, S. W. Youn, H. Hiroshima, H. Takagi, R. Maeda, T. Kato, *Jap. J. Appl. Phys.*, to be accepted for the publication (2013)
37. P. R. Young, J. R. J. Davis, A. C. Chang, and J. N. Richardson: *J. Polym. Sci., Part A* 28 (1990) 3107.
38. R. Pfaendner: U.S. Patent 5116920 (1992).
40. M. S. Win, T. Goshima, E. Kyo, S. Nakajima, N. Hayashi, T. Kashiwagi, K. Miyazaki, K. Yamada, N. Yamabayashi, S. Nakagama, H. Okuyama, F. Kasabo, and I. Tanaka: U.S. Patent 0127077 (2011).
41. H. Hou, J. Jiang, M. Ding, *Eur. Ploym. J.*, 35 (1999) 1993
42. H. Seino, O. Haba, M. Ueda, A. Mochizuki, *Polymer*, 40 (1999) 551
43. J. R. Haller, U.S. Patent 3502762 (1970)
44. Y. W. Wang, C. T. Yen, W. C. Chen, *polymer* 46(2005) 6959
45. L. Li, L. Qinghua, Y. Jie, Q. Xuefeng, W. Wenkai, Z. Zikang, and W. Zongguang: *Mater. Chem. Phys* 74 (2002) 210.

46. M. Angelopolus, E. D. Perfecto, and P. J. Wilkens: U.S. Patent 5300403 (1994).
47. J. A. Bride, S. Baskaran, N. Taylor, J. W. Halloran, W. H. Juan, S. W. Pang, and M. O'Donnell: *Appl. Phys. Lett.* 63 (1993) 3379.
48. H. Hou, J. Jiang, M. Ding, *Eur. Polym. J.*, 35 (1999) 1993
49. H. Seino, O. Haba, M. Ueda, A. Mochizuki, *Polymer*, 40 (1999) 551
50. S. W. Youn, T. Noguchi, M. Takahashi, and R. Maeda: *J. Micromech. Microeng.* 18 (2008) 045025.
51. M. Tormen, R. Malueanu, R. H. Pedersen, L. Lorenzen, K. H. Rasmussen, C. J. Luscher, A. Kristensen, and O. Hansen: *Microelectron. Eng.* 85 (2008) 1229.
52. B. Cui, Y. Cortot, and T. Veres: *Microelectron. Eng.* 83 (2006) 906.
53. C. Y. Chiu and Y. C. Lee: *J. Micromech. Microeng.* 19 (2009) 105001.
54. S. Hayase, K. Takano, Y. Mikogami, and Y. Nakano: *J. Electrochem. Soc.* 138 (1991) 3625.
55. S. S Yoon, D. O. Kim, S.C. Park, Y. K. Lee, H. Y. Chae, S. B. Jungm J. D. Nam, *Microelect. Engg.*, 85(2008) 136
56. M. B. Pisani, C. Hibert, D. Bouvet, P. Beaud, A. M. Ionescu, *Micoelectron. Engg.*, 73-74 (2004) 447
57. J. H. G. Ng, M. P. Y. Demulliez, K. A. Prior, D. P. Hand, *Micro&nano letters.*, 3 (2008) 82
58. S. S Yoon, D. O. Kim, S.C. Park, Y. K. Lee, H. Y. Chae, S. B. Jungm J. D. Nam, *Microelect. Engg.*, 85(2008) 136
59. M. B. Pisani, C. Hibert, D. Bouvet, P. Beaud, A. M. Ionescu, *Micoelectron. Engg.*, 73-74 (2004) 447
60. J. H. G. Ng, M. P. Y. Demulliez, K. A. Prior, D. P. Hand, *Micro&nano letters.*, 3 (2008) 82
61. M.J. Rich, L. T. Drzal, *Process. SPE Auto. Comp. Confe. Expo. Troy, MI. CD-ROM* (2008)
62. J. H. Kim, H. W. Kim, S. M. Park, N. E. Lee, *J. Kore. Phys. Soci.*, 52 (2008) 318
63. H. Kaxzmarek, J. Kowalonek, A. Szalla, A. Sionkowska, *Surf. Scie.*, 507 (2002) 883
64. K. Inoue, K. Matusi, M. Watanabe, H. Honma, *J. Surf. Finish. Soc. Jap.*, 59 (2008) 47
65. T. Sugiyama, Y. Iimori, K. Baba, M. Watanabe, H. Honma, *J. Electrochem. Soc.*, (2009) D360

Research achievement

Journal papers

1. [S.C.Park](#), S.W.Youn,, H. Hiroshima, H. Takagi, R. Maeda and T. Kato, “Simplified Cu/polyimide damascene approach based on imprint process of soluble polyimide block copolymer”, Jpn. J. Appl. Phys, 52(2013), 10MD03.
2. [S.C.Park](#), S.W.Youn, H.Takagi, H.Hiroshima, R. Maeda and T. Kato, “A Study on Surface Modification of Soluble Block Copolymer Polyimide by UV Irradiation and Its Application to Electroless Plating”, JOURNAL OF PHOTOPOLYMER SCIENCE AND TECHNOLOGY, 2013
3. S.W.Youn, [S.C.Park](#), K.Suzuki, Q.Wang, H.Hiroshima, “A Fabrication Process of Quartz Multitier Mold Based on Electron Beam Lithography and Grayscale Laser Beam Lithography”, JAPANESE JOURNAL OF APPLIED PHYSICS, 2011
4. S.W.Youn, [S.C.Park](#), Q.Wang, K.Suzuki, H.Hiroshima, “A Study on Quartz Multitier Mold Fabrication Using Gray Scale Laser Beam Lithography”, JAPANESE JOURNAL OF APPLIED PHYSICS, 2011
5. S.W.Youn, H.Takagi, [S.C.Park](#), M.Takahashi, R.Maeda, “Surface Patterning of Glass by Electrostatic Imprinting Using Platinum Mold”, JOURNAL OF NANOSCIENCE AND NANOTECHNOLOGY, 2010

Proceeding papers

1. S.W.Youn, H.Takagi, [S.C.Park](#), M.Takahashi, R.Maeda, “Surface Patterning of Glass by Electrostatic Imprinting Using Platinum Mold”, ENGE conference, 2010
2. Takagi Hideki, Masaharu Takahashi, Sung Won Youn, Kazuma Kurihara, [Sang-Cheon Park](#), Seiichi Yoshimi, “High efficiency integrated MEMS production technology”, ISIM, 2010
3. [S.C.Park](#), H.Takagi, M.Takahashi, R.Maeda1, D.S.Choi, T.J.Je, E.S.Lee, K.H.Whang, “Development of Tool Alignment System for Machining Roll Mold with Micro Square Pyramid Pattern”, JCK MEMSNEMS, 2010

4. S.W.Youn, [S.C.Park](#), H.T.akagi, H.Hiroshima, M.Takahashi, R.Maeda, “Simplified micro-scale Cu dual-damascene process based on imprint lithography of chemically amplified photoresist using a self-aligned two-tiered Ni mold”, JCK MEMSNEMS, 2010
5. [S.C.Park](#), M.Takahashi, R.Maeda, D.S.Choi, K.H. Whang, E.C. Jeon, T.J. JE, “A Study of Machining Technology for Micro Complex Prism Patterns with Different Formation Angles on Copper-Electroplated Roll Mold”, CIRP HPC, 2010
6. S.W.Youn, [S.C.Park](#), Q.Wang, K.Suzuki, H.Hiroshima, “Multi-tier mold fabrication by gray scale laser lithography combined with dry etching ”, NNT, 2010
7. S.W.Youn, [S.C.Park](#), H.Takagi, H.Hiroshima, M.Takahashi, R.Maeda “UV-assisted thermal imprint lithography for micro-scale Cu dual-damascene process”, ASNIL, 2010
8. S.W.Youn, [S.C.Park](#), K.Suzuki, Q.Wang, H.Hiroshima, M.Takahashi, R.Maeda, “Fabrication of Multi-tiered Quartz Nanopatterns by Grayscale Laser Beam and Electron Beam Lithography”, JCK MEMSNEMS, 2011
9. S.W.Youn, [S.C.Park](#), K.Suzuki, Q.Wang, H.Hiroshima, “A Study on Grayscale Laser Beam Lithography on Nano Patterned Quartz Substrate”, NNT, 2011
10. [S.C.Park](#), S.W.Youn, A.Sawada, H.Takagi, H.Hiroshima, M.Takahashi, R.Maeda, “Patterning process of photosensitive polyimide by UV-assisted thermal imprinting using intermediate polymer stamp”, JCK MEMSNEMS, 2011
11. S.W.Youn, [S.C.Park](#), K.Suzuki, Q.Wang, H.Hiroshima, “A Study on Fabrication Process of Capacity-equalized Mold by Electron Beam Lithography and Grayscale Laser Beam Lithography”, MNC, 2011
12. [S.C.Park](#), S.W.Youn, H.Takagi, M.Takahashi, R.Maeda, “Fabrication of Pt mold for electrostatic imprint process of a glass”, JSPE spring conference, 2011
13. [S.C.Park](#), S.W.Youn, H.Takagi, H.Hiroshima, R. Maeda and T. Kato, “A Study on Surface Modification of Soluble Block Copolymer Polyimide by UV Irradiation and Its Application to Electroless Plating”, International Conference of Photopolymer Science and Technology, 2013

14. [S.C.Park](#), J.Choi, T.Kato, S.W.Youn, H.Takagi, H.Hiroshima and R.Maeda, "Selective Electroless Copper Plating on Polyimide Substrate by UV/Ozone treatment", International Conference on Advanced Eelctromaterials, 2013

15. [S.C.Park](#), J.Choi, T.Kato, S.W.Youn, H.Takagi, H.Hiroshima and R.Maeda, "Direct Formation of Copper Pattern on Polyimide Surface Modified by UV/Ozone Treatment", Nanoimprint and Nanoprint Technology, 2013